

Identification and characterisation of novel human dendritic cell progenitors

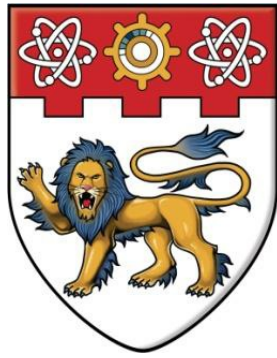
See, Peter Chi Ee

2016

See, P. C. E. (2016). Identification and characterisation of novel human dendritic cell progenitors. Doctoral thesis, Nanyang Technological University, Singapore.

<https://hdl.handle.net/10356/67316>

<https://doi.org/10.32657/10356/67316>



NANYANG
TECHNOLOGICAL
UNIVERSITY

**IDENTIFICATION AND CHARACTERISATION OF NOVEL
HUMAN DENDRITIC CELL PROGENITORS**

SEE CHI EE PETER
SCHOOL OF BIOLOGICAL SCIENCES
2016

**IDENTIFICATION AND CHARACTERISATION OF NOVEL
HUMAN DENDRITIC CELL PROGENITORS**

SEE CHI EE PETER

SCHOOL OF BIOLOGICAL SCIENCES

A thesis submitted to the Nanyang Technological
University
in partial fulfillment of the requirement for the degree of
Doctor of Philosophy

2016

ACKNOWLEDGEMENT

I would like to thank Dr Florent Ginhoux for the opportunity to undertake my PhD in his laboratory, and also for his constant guidance and encouragement. I am greatly appreciative of the various opportunities that he has given me over the past few years. His zeal for research has always been a great motivation and inspiration to me.

I would also like to thank my Thesis Advisory Committee (TAC) Members Dr Laurent Renia and Associate Professor Christiane Ruedl for their invaluable suggestions during each TAC meeting.

Next, I would like to thank all my ex- and current colleagues in the FG laboratory for their invaluable guidance and help in the course of this work. Particularly, I would like to thank Dr Pearline Teo for her guidance and training as a “butcher” and sharing her get-rich schemes during the long and monotonous mass organ/tissue harvest; Ms Ooi Poi Ling as my lunch companion and also her contributions of quick-get-rich schemes; Dr Muzlifah Haniffa for advice and suggestions whenever I am stuck in the projects; Ms Amanda Shin for practicing Korean with me so that I will not forget the language; Dr Naomi McGovern, Dr Shawn Lim, Dr Svetoslav Chakarov and Ms Gillian Low for entertainment in the laboratory.

I would also want to thank Dr Ng Lai Guan and the NLG lab members particularly Dr Chong Shuzhen, Ms Goh Chi Ching and Mr Maximilien Evrard for reagents, mice, entertainment at SAH4 and in the laboratory, and most importantly, in believing in me and my abilities. Not forgetting the ladies in Mouse Core, Ms Cindy Phua, Ms Florida Toh and Ms Yap Tian Tian for providing mice for my experiments; Dr Evans Newell, Ms Karen Teng and Mr Hermi for guiding me on how to run CyTOF and analysing the complex data, as well as the Flow girls in the Flow Team, Ms Ivy Low, Ms Nurhidaya and Ms Seri for their assistance in sorting and training to be a part-time Flow boy! Also, I would also like to thank my lunchtime kaki Ms

Lee Hui Yin for the lunch companionship, advice and simply just being there.

My fellow PhD batch mates based at SlgN: Sin Wei Xiang, Daniela Cerny, Zuzana Hruskova, Sharrada Subramaniam, Poh Chek Meng, Gun Sin Yee, Teo Teck Hui and Joey Xu. We survived!

I would also like to thank my external collaborators, Dr Esther Wong and Lois Sim from IMB for generation of Upk1b-Cre; Dr Jerry Chan, Ms Bei En and Dr Chen Qingfeng for cord blood samples and humanized mice.

Dear Mickey, Minnie and the anonymous sample donors, this work would not be possible without you. Also, I would like to thank A*GA for providing financial support during these 4 years.

On a personal note, there are several people that I want to acknowledge. DK Fu, it wasn't so long ago when I was cheering you on for your M. Arch. Now, it is your turn to pay in forward. 我们会得到幸福的! Puay Ling thanks for being my listening ears over these years. Hammer Low, Loo Chin and Shufen, thanks for being my guarantors. You are now a free man/woman!

爸妈，哥哥和弟弟，感激你们默默地在我背后自持我。

TABLE OF CONTENTS

TABLE OF CONTENTS	i
LIST OF FIGURES	iv
LIST OF TABLES	v
ABBREVIATIONS	vi
ABSTRACT	ix
1. INTRODUCTION	
1.1. General features of dendritic cells	1
1.2. Antigen processing and presentation	3
1.3. DC migration	4
1.4. DC-T cell interaction	5
1.5. Dendritic cell heterogeneity and classification	6
1.6. Conventional DC (cDC) subsets	8
1.6.1. cDC1 subset	9
1.6.2. cDC2 subset	14
1.7. Plasmacytoid DC (pDC)	18
1.8. Ontogeny of DCs	21
1.9. Aims	24
2. MATERIALS AND METHODS	
2.1. Mice	25
2.2. Bacterial strains and plasmids	25
2.3. Sample collection	25
2.4. Construction of Upk1b-cre targeting plasmid	26
2.5. Gene targeting in mouse ES cells	31
2.6. Southern blot analysis of targeted clones	32
2.7. Establishment of Upk1b-Cre knock-in mouse strain	33

2.8. Murine and human cell suspension preparation	33
2.9. Antibodies and flow cytometry	34
2.10. Immunofluorescence microscopy	35
2.11. DC assay on MS5 stromal cells	35
2.12. Stimulation with TLR ligands	35
2.13. Mixed lymphocyte reaction (MLR)	36
2.14. Microarray analysis	36
2.15. Quantitative RT-PCR	37
2.16. Statistical analysis	37
 3. RESULTS	
3.1. Generation of fate mapping model for DC ontogeny	38
3.1.1. Uroplakin (Upk) 1b is a potential candidate to map DCs derived from CDPs	38
3.1.2. Generation of knock-in Upk1b-cre mouse model	40
3.1.3. Low expression of YFP protein in DCs but not in microglia of Upk1b-cre:Rosa-YFP mice	42
3.1.4. Discussion	47
3.2. Identification and characterization of human pre-cDC	51
3.2.1. Identification of human pre-cDC in cord blood, bone marrow and peripheral blood	51
3.2.2. Identification of committed pre-cDC subsets in peripheral blood	56
3.2.3. Gene expression analysis of pre-cDC subsets	58
3.2.4. Functional analysis of pre-cDCs	63
3.2.5. Flt3L treatment of humanized mice expands DC- restricted progenitors	64
3.2.6. Pre-cDC and its involvement in pathological diseases	68
3.2.7. Discussion	69
 4. CONCLUSION AND FUTURE WORK	74
 5. REFERENCES	75

LIST OF FIGURES

<i>Figure 1. Life cycle of DCs.</i>	<i>1</i>
<i>Figure 2. Antigen presentation pathways in DCs.</i>	<i>4</i>
<i>Figure 3. T cell stimulation and polarization requires 3 signals from DCs.</i>	<i>5</i>
<i>Figure 4. DC subsets shape distinct types of immune responses.</i>	<i>7</i>
<i>Figure 5. Dendritic cell development.</i>	<i>23</i>
<i>Figure 6. Plasmid map of mini-targeting and retrieval plasmid.</i>	<i>29</i>
<i>Figure 7. Plasmid map of pBlight-Upk1b Cre.</i>	<i>32</i>
<i>Figure 8. Upk1b is a uniquely expressed in CDP and pre-cDC.</i>	<i>40</i>
<i>Figure 9. Generation of knock-in Upk1b-cre mice.</i>	<i>42</i>
<i>Figure 10. Low YFP fluorescence was detected in splenic DCs from the Upk1b-cre fate mapping model.</i>	<i>45</i>
<i>Figure 11. Low expression of YFP fluorescence in DC progenitors.</i>	<i>46</i>
<i>Figure 12. High levels of YFP fluorescence in microglia.</i>	<i>47</i>
<i>Figure 13. Identification of human pre-DCs.</i>	<i>54</i>
<i>Figure 14. Pre-cDC is able to differentiate into cDC1 and cDC2 subsets.</i>	<i>55</i>
<i>Figure 15. Comparison of pre-cDC population.</i>	<i>56</i>
<i>Figure 16. Characterisation of pDCs and pre-cDC using initial markers defining pDCs.</i>	<i>57</i>
<i>Figure 17. Identification of committed pre-cDC populations.</i>	<i>60</i>
<i>Figure 18. Microarray analysis of pre-cDC populations.</i>	<i>62</i>
<i>Figure 19. Phenotypic characterisation of pre-cDC and DC populations.</i>	<i>63</i>
<i>Figure 20. Cytokine production by pre-cDC.</i>	<i>66</i>
<i>Figure 21. Flt3L expands the pre-cDC populations.</i>	<i>67</i>
<i>Figure 22. Bulk pre-cDC showed a positive correlation with SLEDAI score.</i>	<i>68</i>

LIST OF TABLES

<i>Table 1. PCR conditions and primers used in generating Upk1b-Cre targeting plasmid.</i>	<i>28</i>
<i>Table 2. PCR conditions and primers used for ES clones and KI mice screening.</i>	<i>33</i>
<i>Table 3. PCR conditions and primers used to generate DIG-labeled probes.</i>	<i>33</i>
<i>Table 4. Primers used in qPCR.</i>	<i>38</i>

ABBREVIATIONS

4-OHT	4-hydroxytamoxifen
APC	Antigen presenting cell
BATF	Basic leucine zipper transcription factor, ATR-like
BAC	Bacterial artificial chromosome
BM	Bone marrow
bZIP	basic leucine zipper
CCL	C-C chemokine ligand
CCR	C-C chemokine receptor
cDC	Conventional dendritic cell
CDP	Common dendritic cell progenitor
CLR	C-type lectin receptor
cMOP	Common monocyte progenitor
Cre	Cre recombinase
CSF-1R	Colony stimulating factor 1 receptor
CX3CR1	CX3C chemokine receptor 1
CXCR3	CXC chemokine receptor 3
DC	Dendritic cell
DIG	Digoxigenin
<i>E. coli</i>	<i>Escherichia coli</i>
ER	Oestrogen receptor
ESAM	Endothelial cell-specific adhesion molecule
FLT	Cytokine fms-like tyrosine kinase 3 receptor
Flt3L	Cytokine fms-like tyrosine kinase 3 ligand
GFP	Green fluorescence protein
GM-CSF	Granulocyte-macrophage colony stimulating factor
GMP	Granulocyte-macrophage progenitor
HLA	Human leukocyte antigen
HSC	Haematopoietic stem cell
ID2	Inhibitor of DNA binding 2
IFN	Interferon
IRF	Interferon regulatory factor

KLF4	Kruppel-like factor 4
LC	Langerhans cell
LBD	Ligand-binding domain
LPS	Lipopolysaccharide
LT	Lymphoid tissue
LT β R	Lymphotoxin- β receptor
MC	Monocyte-derived cells
MDP	Monocyte-macrophage dendritic cell progenitor
MHC	Major histocompatibility complex
MLP	Multi-lymphoid progenitor
MLR	Mixed lymphocyte reaction
Neo	Neomycin
NFAT-AP1	Nuclear factor of activated T cells-activator protein 1
NFIL3	Nuclear factor interleukin 3 regulated
NF- κ B	Nuclear factor kappaB
NK	Natural killer
NLT	Non-lymphoid tissue
Notch2	Neurogenic locus notch homolog protein 2
pDC	Plasmacytoid dendritic cell
pre-cDC	Precursor of conventional dendritic cell
PAMP	Pattern-associated molecular patterns
PRR	Pattern recognition receptors
RALDH	Retinaldehyde dehydrogenase
Relb	Viral oncogene homolog B
RFP	Red fluorescence protein
RLR	RIG-I-like receptor
RT-qPCR	Quantitative real time polymerase chain reaction
SCF	Stem cell factor
SLE	Systemic Lupus Erythematosus
Th	T helper
TLR	Toll-like receptor
TPO	Thrombopoietin
TRAF6	TNF-associated factor 6
Treg	Regulatory T cell

Upk1b	Uroplakin 1b
YFP	Yellow Fluorescence protein
Zbtb	Zinc finger BTB domain containing transcription factor

ABSTRACT

Dendritic cells (DCs) are professional antigen presenting cells that initiate the immune response. They are heterogeneous and are broadly classified into three groups – two major subsets of conventional DCs (cDC) named cDC1 and cDC2, and plasmacytoid DC (pDC). Each subset has unique transcription factor dependency, and specialised functions. DCs are derived from a unique lineage of DC-restricted progenitors that are until now not yet fully characterised. Currently, there are limited genetic lineage fate mapping mice models available to track the development of DCs in steady state and inflammation. We have identified Uroplakin-1b (Upk1b) as uniquely expressed in DC-restricted progenitors. Surprisingly, this molecule is also expressed in microglia. We developed a fate mapping Upk1b-cre mouse, which was crossed to Rosa-YFP reporter mouse to generate Upk1b-cre:Rosa YFP. Contrary to our expectations, we observed low recombination in DC-restricted progenitors and DC subsets. However, the recombination level in the microglia was close to 80% in young adults, suggesting that it may be a useful model for microglial research. Upk1b is conserved across species and may serve as a potential marker to identify DC-restricted progenitors in humans.

Although human DC-restricted progenitors were recently identified, here, we extended and further refined the definition of the precursor of cDC (pre-cDC). We showed that they share several common phenotypic markers such as CD303, CD123 and CD45RA with pDC, thereby contaminating the pDC fraction of the peripheral blood. Hence, this might explain why pDC when stimulated with IL-3 and CD40 ligand, were found to differentiate into cells with cDC-like morphology. We also demonstrated that pre-cDC but not pDC were able to differentiate into cDC subsets in MS5 stromal culture supplemented with the cytokines Flt3L, SCF and GM-CSF. We further interrogated the bulk pre-cDC population in peripheral blood and identified three populations of pre-cDC, namely early, uncommitted pre-cDC and committed pre-cDC1 and pre-cDC2. Early, uncommitted pre-cDC

differentiated into both cDC subsets, while committed pre-cDC1 and pre-cDC2 differentiated into their respective cDC subsets. We also observed that they are responsive to Flt3L stimulation and were able to induce allogeneic naïve T cell proliferation in the absence of stimulation. Finally, we observed that pre-cDC was expanded in the blood of Systemic Lupus Erythematosus (SLE) patients, and are currently investigating the role of pre-cDC in this autoimmune disease.

1. INTRODUCTION

1.1. General features of dendritic cells

The immune system is constantly exposed to threats from both the external and internal environments. Thus, it has evolved to respond quickly by mounting protective immune responses against infections from microorganisms as well as self-antigens and tumour cells within the body. Although the immune system can generate diverse and specific responses to clear the various threats, the initiation of the immune response was not well understood until the discovery of an adherent, accessory cell in the mouse spleen in 1973. These accessory cells were structurally distinct from macrophages and possessed a stellate morphology with extended veils that resembled dendrites (Steinman and Cohn 1973). Hence, they were termed dendritic cells (DCs) by the late Nobel Laureate Ralph Steinman. In the following paragraphs, we will provide a brief overview of DCs in the context of sentinels *in vivo*, antigen processing and presentation, migration and maturation (**Figure 1**).

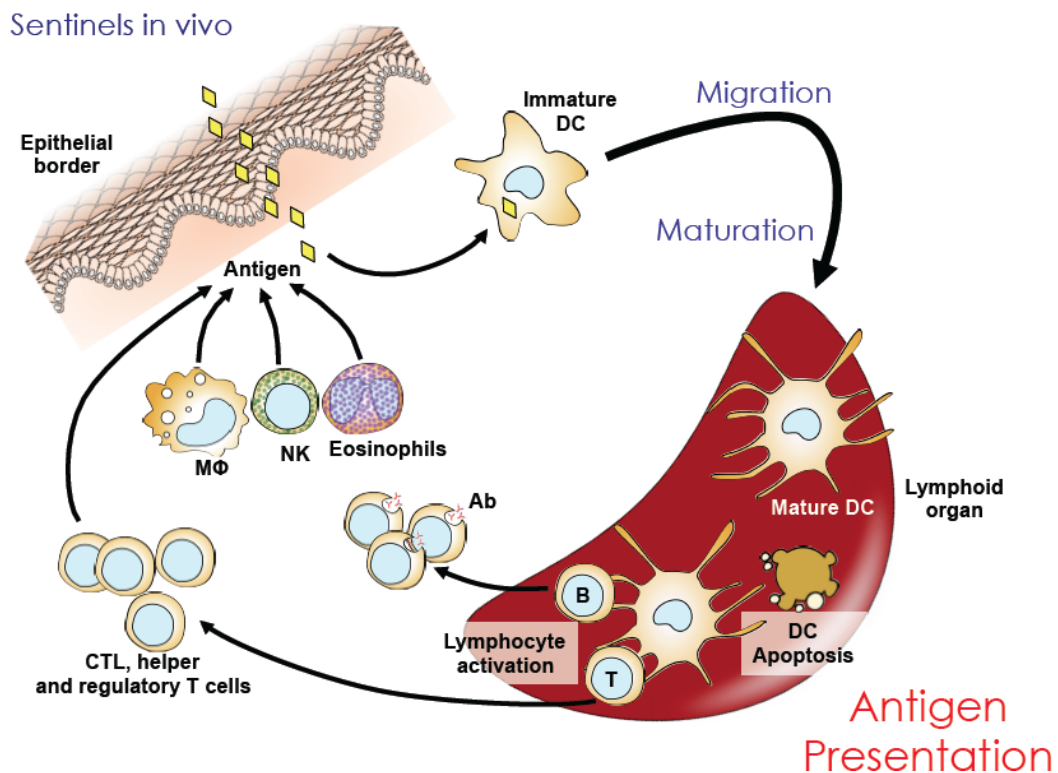


Figure 1. Life cycle of DCs.

DCs are located in interstitial tissues of major tissues and organs where they act as sentinels and sample the environment for antigens. As professional APCs, they uptake and process antigens, leading to their maturation and migration towards the lymphoid organs. At the lymphoid organs, they present the antigens to lymphocytes, thereby causing their activation, proliferation and migration towards the inflammation site to combat invading microorganisms. (Adapted from (Banchereau et al. 2000)

DCs are distributed in the interstitial tissues of major tissues and organs, with the exception of the brain where they reside in the meninges surrounding the brain and choroid plexus (Hart and Fabre 1981; Sertl et al. 1986; D'Agostino et al. 2012). They act as sentinels, constantly sampling the environment for antigens. They belong to a group of specialised cells called antigen-presenting cells (APC), which process antigens and display the peptide fragments via major histocompatibility complex (MHC) molecules on the cell surface to activate naïve T cells (Steinman 2012). B cells, macrophages and DCs are examples of APC; however, DCs are often referred to as professional APC for their superior antigen presentation ability.

DCs express both MHC class I and II molecules constitutively (Steinman and Witmer 1978; Nussenzweig and Steinman 1980), and their cell membranes are rich with T cells co-stimulatory molecules such as CD80 and CD86 (Sharpe and Freeman 2002). They also possess a repertoire of pattern-recognition receptors (PRR) such as Toll-like receptors (TLRs), RIG-I-like receptors (RLRs), C-type lectin receptors (CLRs), which recognise pattern-associated molecular patterns (PAMP) often associated with microorganisms and cellular stress, leading to their activation and release of cytokines that activate and shape the adaptive immune responses (Iwasaki and Medzhitov 2015). For instance, DCs possess a repertoire of TLRs such as TLR3, TLR4 and TLR9 which allow them to detect nucleic acids and bacterial lipopolysaccharide (LPS), leading to their activation and secretion of

inflammatory cytokines to control and eliminate the infection (Kawai and Akira 2011).

1.2. Antigen processing and presentation

DCs can present peptides derived from endogenous proteins by proteasomal degradation in the cytosol, and load them onto MHC class I molecules (Villadangos and Schnorrer 2007). They can also uptake exogenous antigens from the external environment via phagocytosis, pinocytosis or receptor-mediated endocytosis (Wilson and Villadangos 2005). Internalised antigens are directed to lysosomes where they are degraded into peptides by hydrolytic enzymes in endocytic compartments, and then loaded onto MHC class II molecules in endosomes and lysosomes (Segura and Amigorena 2015). In addition, DCs are also able to uptake exogenous antigens such as necrotic or dying apoptotic cells (Qiu et al. 2009; Desch et al. 2011), and present the degraded peptides onto MHC class I molecules in a process called cross-presentation (Joffre et al. 2012) (**Figure 2**). Hence they play important roles in anti-viral, anti-tumour immunity as well as tolerance induction. It was also demonstrated that DCs could present endogenous antigens via MHC class II molecules in a process facilitated by autophagy (Münz 2012). Autophagy mediated antigen presentation could prolong the stimulation of CD4⁺ T cells (Schmid et al. 2007; Romao et al. 2013), but could be limited to the presentation of certain pathogens (Münz 2012). Autophagy may also play a role in cross-presentation to CD8⁺ T cells, but it requires more investigation as current data remain conflicting (Mintern et al. 2015).

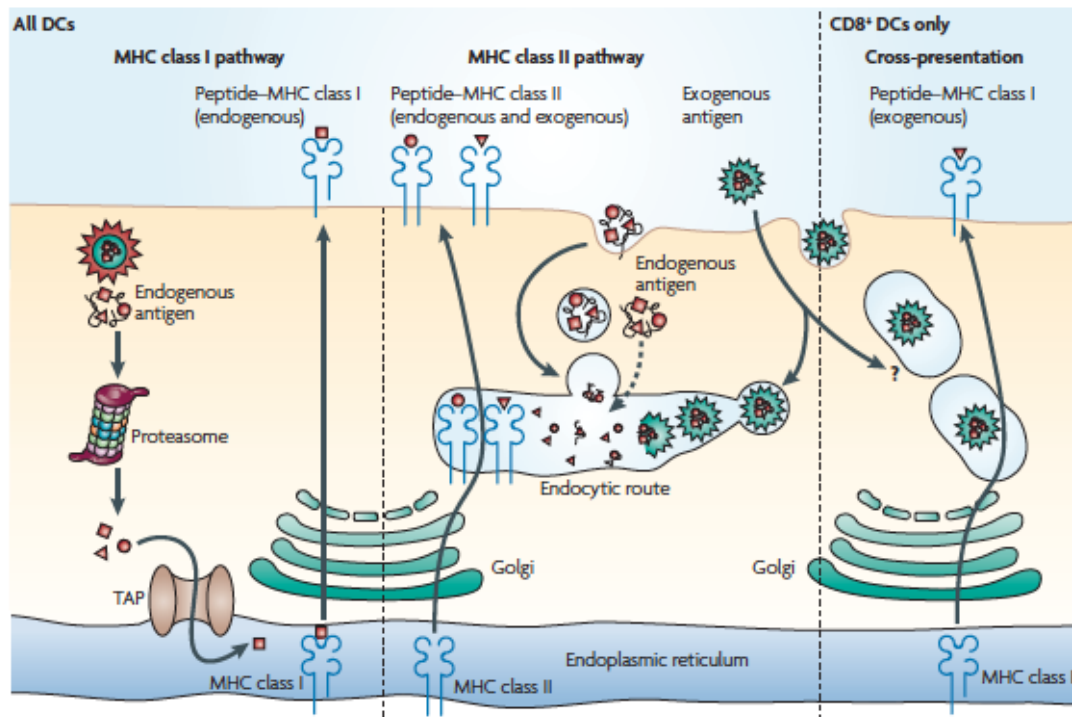


Figure 2. Antigen presentation pathways in DCs.

DCs constitutively express MHC class I and II molecules. They can present peptides derived from endogenous proteins degraded via the proteasome in the cytosol via MHC class I molecules. Both endogenous and exogenous proteins can also be degraded in the endosomal compartments and loaded onto MHC class II molecules for presentation. However, a subset of DCs – cDC1, appears to excel in the cross-presentation of exogenous peptides onto MHC class I molecules. (From (Villadangos and Schnorrer 2007).)

1.3. DC Migration

Activated DCs migrate from the peripheral tissues to the draining lymph nodes via the lymphatics in a C-C chemokine receptor type 7 (CCR7)-dependent mechanism in response to C-C chemokine ligand 21 (CCL21) produced by the lymphatics vessel (Ohl et al. 2004). Autocrine secretion of CCL19 may also direct migration towards the direction of fluid drainage. Once in the lymph nodes, DCs interact with T cells, which are located in the T cell zone, to induce T cell activation and polarization (Randolph et al. 2005). DC migration to the lymph nodes

during steady state also occurs in order to maintain peripheral tolerance (Förster et al. 2008; Desch et al. 2011).

1.4. DC-T cell interaction

DCs activate T cells through three distinct signals: (1) engagement of T cell receptor with peptide loaded MHC molecules (Signal 1); (2) co-stimulatory signalling mediated by B7 family members (Signal 2); (3) cytokines production (Signal 3). T cells that receive signal 1 only undergo anergy, while proliferation and expansion of naïve T cells requires both signal 1 and 2. However, differentiation into specific effector T cells is dependent on signal 3 (Kapsenberg 2003) (**Figure 3**).

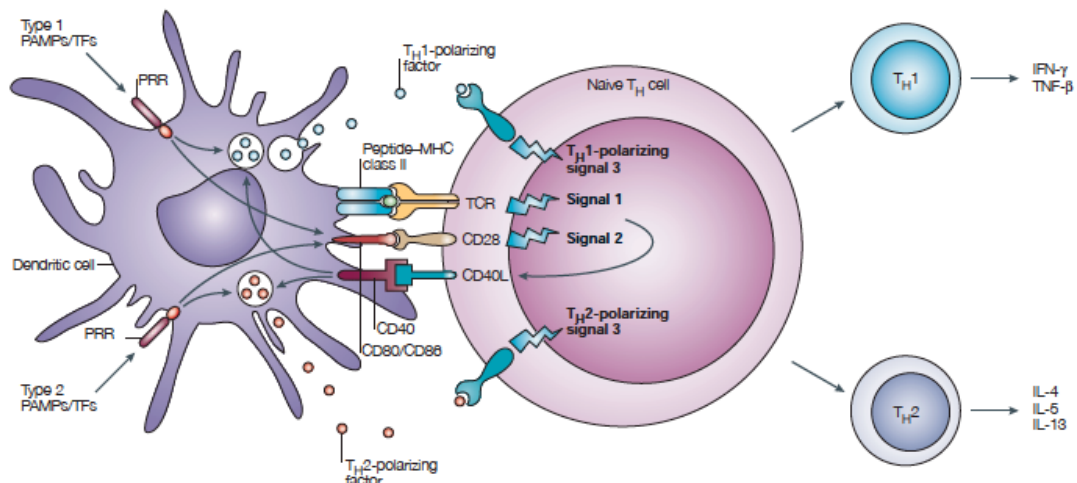


Figure 3. T cell stimulation and polarization requires 3 signals from DCs.

DCs activate T cells through 3 signals. Signal 1 refers to antigen-specific signal that is mediated through T cell receptor and peptide loaded MHC class II molecules. Signal 2 refers to the co-stimulatory signal mediated by triggering of CD28 on the T cell by CD80 and CD86 on the DCs. The last signal, signal 3, refers to the polarizing signal from soluble factors and chemokines. (From (Kapsenberg 2003).)

Naïve CD8⁺ T cells, upon contact with peptides loaded on MHC class I molecules, differentiate into cytotoxic effector T cells. In contrast, CD4⁺ T cells, upon contact with peptides loaded on MHC class II molecules,

can differentiate into various effector T helper (Th) cells such as Th1, Th2, Th17 and regulatory T (Treg) cells (Yamane and Paul 2012; Raphael et al. 2015). Each subset of T helper cells secretes unique cytokines that help to control infection and inflammation. For example, Th1 cells play an important role in clearing intracellular bacterial infection by activating macrophages, as well as to stimulate B cells to produce antibodies to clear extracellular bacteria. Th2 cells are involved in the control of parasitic infection, while Th17 cells are implicated in the clearance of fungal infections. Tregs possess a suppressive immune function to act as immunoregulators in many inflammatory and autoimmune diseases (Sallusto and Lanzavecchia 2009).

1.5. Dendritic cell heterogeneity and classification

DCs are heterogeneous and are classified into distinct subsets based on various parameters such as localisation, phenotype, ontogeny, gene expression profile and specialised functions. Often, these methods of classification make it difficult to interpret published literature as the same DC subset could be given different name. Hence, a new nomenclature based on ontogeny and extended by transcription factor dependency was recently proposed (Guilliams et al. 2014). With this scheme, DCs are broadly classified into three groups: Two major subsets of conventional DC (cDC) named cDC1 and cDC2, and plasmacytoid DC (pDC) (**Figure 4**).

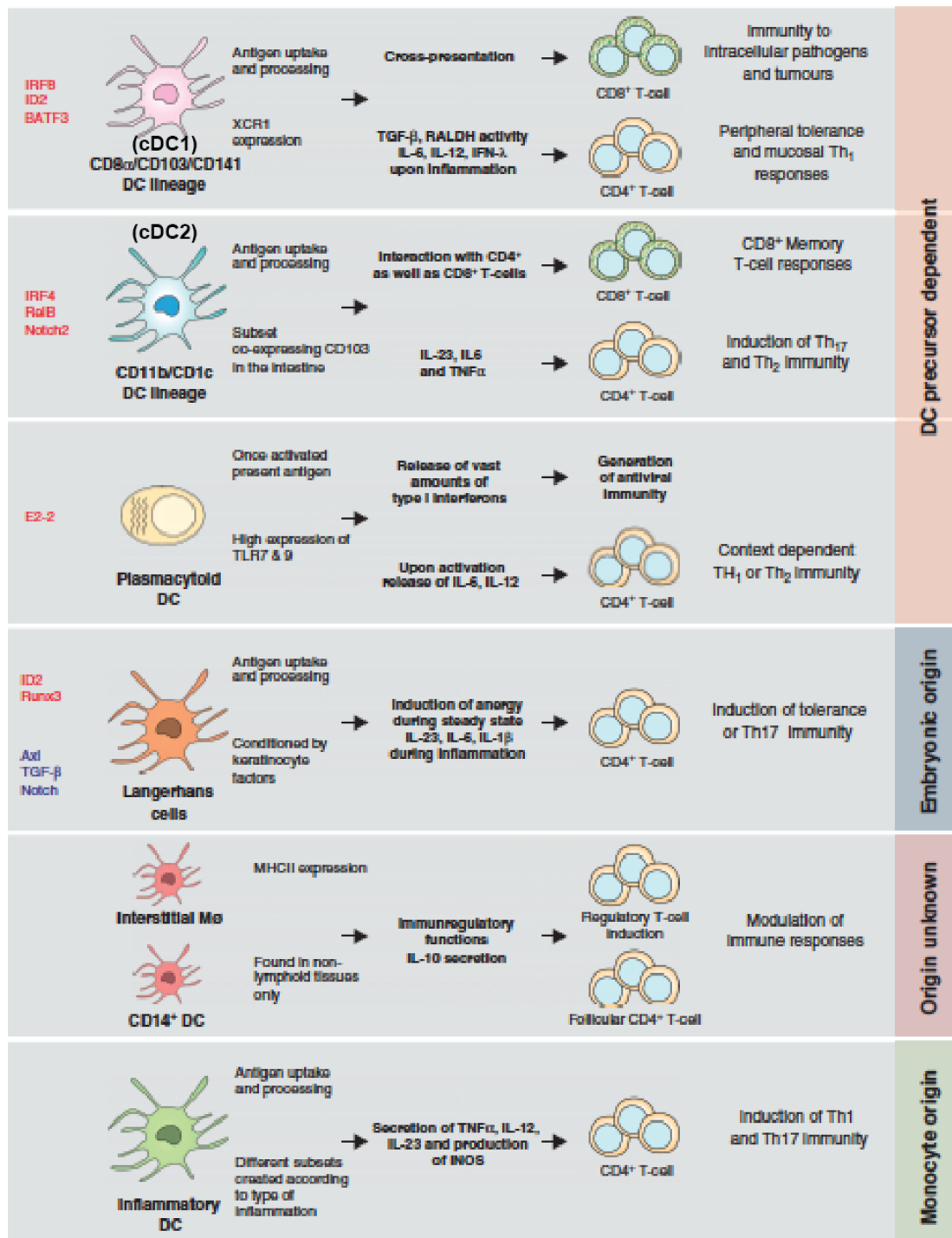


Figure 4. DC subsets shape distinct types of immune responses.

DCs can be broadly classified into 3 groups: two major subsets of conventional DCs (cDCs) – cDC1 and cDC2, and plasmacytoid DCs (pDCs). LCs and MCs, which includes interstitial macrophages, CD14 $^+$ DCs (found in human) and inflammatory DCs, share phenotypic and functional features with DCs. Each lineage has distinct transcription factors

dependency (human – blue, mouse – red), origins and functional specialisations. (From (Schlitzer and Ginhoux 2014).)

Traditionally, Langerhans cells (LC) and monocyte-derived cells (MC) are classified within the cDC denomination because of their shared features with DCs at the phenotypic and functional levels (Schlitzer et al. 2015a) .

Paul Langerhans first described LCs in 1868, which shared similar characteristics with DCs. They express DC markers such as type I transmembrane protein integrin- α X (CD11c) and MHC class II, and migrate to the draining lymph nodes in both steady-state and under inflammation (Ginhoux and Merad 2010). Unlike DC, they express high levels of C-type lectin receptor, Langerin (CD207) (Valladeau et al. 2000; Valladeau and Clair-Moninot 2002) and possess an unique embryonic ontogeny as they derive from both embryonic yolk sac macrophages and fetal monocytes, (Hoeffel et al. 2012), and not from DC-restricted progenitors present in the bone marrow (BM) that we will describe below. Hence they represent an unusual type of tissue-resident macrophage that acquires DC-like functions upon maturation (Schlitzer et al. 2015a). Monocytes can be divided into two distinct populations based on lymphocyte antigen 6 complex (Ly6C) expression (Geissmann et al. 2003). During inflammation, there is a substantial influx of monocytes into tissues which differentiate into cDCs (Mildner et al. 2013). Instead of being a *bona fide* DC subtype, MCs represent a distinct type of plastic cell that acquire a multitude of functional capabilities, some of which are commonly shared with either DCs or macrophages (Ginhoux and Jung 2014). Given their differences in ontogeny, these two groups of cells should be separated from the cDC lineage (Guilliams et al. 2014).

1.6. Conventional DC (cDC) subsets

Conventional DCs are found in lymphoid (LT) and non-lymphoid (NLT) tissues of mouse and human. In mouse, cDCs are generally identified

by the surface expression of both CD11c and MHC class II molecules. However, both markers are not specific to DCs only and their expression can be regulated in both steady state and inflammatory conditions (Merad et al. 2013). In human, cDCs are defined as human leukocyte antigen (HLA) -DR⁺ cells and the absence of lineage markers CD3, CD19/CD20, CD56 and CD14/CD16, which are commonly used to identify T cells, B cells, natural killer (NK) cells and monocytes, respectively. Heterogeneity is found within the cDCs and they can be further divided into two distinct populations cDC1 and cDC2.

1.6.1. cDC1 subset

1.6.1.1. Phenotype

cDC1 subset in murine tissues is identified by the expression of CD8 α and integrin- α E (CD103) in LT and NLT, respectively (Helft et al. 2010; Shortman and Heath 2010). Its equivalent in human blood and tissue, is defined by high expression of thrombomodulin (CD141, BDCA-3) (Dzionek et al. 2000; MacDonald et al. 2002; Haniffa et al. 2012). CD141 can be expressed by other DC subsets or type of cells in human tissues, making this marker difficult to use (Haniffa et al. 2012). However, conserved markers such as cell adhesion molecule CADM1 (NECL2), C-type lectin-like receptor CLEC9A and chemokine receptor XCR1, are shown to be specifically expressed by both mouse and human cDC1 (Dutertre et al. 2014).

1.6.1.2. Homology

Comparative studies involving transcriptomics, phenotype and functional analyses have aligned human (XCR1⁺CD141⁺ DCs) from blood and skin with mouse (CD8 α ⁺/CD103⁺ DCs) in the spleen and NLT, suggesting that both populations are homologous (Bachem et al. 2010; Crozat et al. 2010a; Haniffa et al. 2012; Poulin et al. 2012).

1.6.1.3. Cytokines Requirement

The cytokine fms-like tyrosine kinase 3 ligand (Flt3L) and its receptor (FLT3) was shown to be crucial for the development and homeostasis of both murine cDC subsets (Waskow et al. 2008; Ginhoux et al. 2009; Liu et al. 2009), as the cytokine instruct DC commitment at the level of DC progenitors (Karsunky et al. 2003). Murine cDC1 subset express high levels of FLT3, proliferate in response to Flt3L and are strongly reduced in Flt3L-deficient mice (McKenna et al. 2000; Ginhoux et al. 2009). Besides Flt3L, granulocyte-macrophage colony stimulating factor (GM-CSF) is often used in culture to promote differentiation of hematopoietic progenitors and monocytes into DCs (Inaba et al. 1992; Caux et al. 1996). Despite its importance in culture, this cytokine is not essential for CD8 α ⁺ development (Vremec et al. 1997). In contrast, it is critical for the survival of NLT CD103⁺ DC as a reduction in the number of CD103⁺ DC is observed in the intestine, dermis and lung of mice deficient in GM-CSF (Greter et al. 2012). Not much is known about the cytokine requirement of human CD141⁺ DCs. However, FLT3 signalling is likely to play a role in their development as the mRNA expression of *FLT3* is higher as compared to cDC2 subset (Haniffa et al. 2012). Moreover, humanised mice treated with Flt3L showed an increased in the numbers of both human cDC subsets (Ding et al. 2014). Lastly, Flt3L is also of paramount importance for *in vitro* generation of cDCs from either murine bone marrow or CD34⁺ HSCs obtained from human umbilical cord blood (Brasel et al. 2000; Naik et al. 2005; Poulin et al. 2010; Proietto et al. 2012; Lee et al. 2015a).

1.6.1.4. Transcription Factors

The development of cDC1 lineage has been studied extensively in mice. This subset is dependent on the following transcriptional factors: interferon regulatory factor 8 (IRF8), inhibitor of DNA binding 2 (ID2), nuclear factor interleukin 3 regulated (NFIL3)

and basic leucine zipper transcription factor, ATR-like 3 (BATF3) (Belz and Nutt 2012; Satpathy et al. 2012b). The precise mechanisms by which these transcription factors interact and control cDC1 differentiation remain to be fully characterised and will be discussed below.

IRF8 belongs to the IRF family of transcription factors and controls myeloid cell differentiation by promoting macrophage and DC differentiation and inhibiting granulocytes development (Holtschke et al. 1996; Li et al. 2011; Becker et al. 2012). Mice deficient in IRF8 lack pDCs and lymphoid tissue CD8 α ⁺ DCs (Schiavoni et al. 2002; Aliberti et al. 2003; Tsujimura et al. 2003). Interestingly, mice that carry a spontaneous mutation (R294C) of IRF8 in BXH2 mice exhibited myeloproliferation (Turcotte et al. 2005) and are deficient in cDC1 subset (Ginhoux et al. 2009), but have normal numbers of pDCs (Tailor et al. 2008). IRF8 also plays a role in CD8 α ⁺ DC maturation and the production of IL-12 (Schiavoni et al. 2002).

ID2 protein is a member of the HLH transcription factor family that acts to inhibit the binding of other HLH proteins to DNA (Murphy 2013). It is expressed by both cDC subsets with the highest expression in cDC1 subset (Ginhoux et al. 2009; Jackson et al. 2011). Mice lacking ID2 have dramatic reduction in cDC1 subset and an unaffected cDC2 subset (Hacker et al. 2003; Ginhoux et al. 2009). The basic leucine zipper (bZIP) transcription factor BATF3 competes with FOS for JUN dimerisation to repress the activity of nuclear factor of activated T cells-activator protein 1 (NFAT-AP1) complexes and is also expressed by both cDC subsets (Belz and Nutt 2012). Similar to IRF8-deficient mice, BATF3-deficient mice have a deficiency in cDC1 subset but not cDC2 subset (Hildner et al. 2008; Edelson et al. 2010). Interestingly, normal numbers of CD8 α ⁺ DCs were found in the draining lymph node (Edelson et al. 2011)

suggesting that other AP1 molecules can compensate BATF3's role (Murphy 2013). NFIL3, another bZIP transcription factor, is crucial for development of NK cells and innate lymphoid cells (Belz and Nutt 2012; Geiger et al. 2014; Seillet et al. 2014). In NK cells, NFIL3 acts downstream of the IL-15 receptor to regulate ID2 expression in a dose-dependent manner (Belz and Nutt 2012). Recently, it was shown to be involved in the development of CD8 α^+ DCs as NFIL3-deficient mice had significant reduction in spleen CD8 α^+ DCs (Kashiwada et al. 2011).

To understand the hierarchy and sequential involvement of IRF8, ID2 and BATF3 in cDC1 lineage development, a fluorescent reporter was inserted into the ID2 locus to generate ID2-GFP reporter mice (Jackson et al. 2011). The reporter mice were crossed with BATF3-deficient mice and IRF8-deficient mice, respectively. IRF8 is required for the development of ID2-expressing DC progenitors (Jackson et al. 2011), but commitment of cDC1 lineage is dependent on BATF3 as it sustains the auto-activation of IRF8 (Grajales-Reyes et al. 2015). In the absence of BATF3, IRF8 expression decays and the DC-restricted progenitors are driven into a cDC2-like lineage. Overexpression of IRF8 in BAT3-deficient mice leads to restoration of the cDC1 lineage as requirement for BATF3 for auto-activation is bypassed, indicating that IRF8 is a master regulator in cDC1 development. BATF3 is also required for the maturation of cDC1 subset (Jackson et al. 2011). NFIL3 may act upstream of BATF3 as overexpression of BATF3 bypasses the requirement for NFIL3 in CD8 α^+ DCs (Kashiwada et al. 2011). However, its involvement with IRF8 and ID2 is currently not known.

In human, BATF3 has been shown to play a role in cDC1 development. shRNA knockdown of *BATF3* in cord blood CD34 $^+$

HSCs inhibit their differentiation into cDC1 *in vitro* (Poulin et al. 2010). However, when humanized mice were reconstituted with *BATF3* knockdown cord blood CD34⁺ HSCs, a decreased in cDC1 was not detected, suggesting that other members of BATF family transcription factors may compensate *BATF3* in cDC1 development (Tussiwand et al. 2012). DCs differentiated from cord CD34⁺ HSCs in the presence of GM-CSF and IL-4 were found to up regulate *ID2* mRNA (Hacker et al. 2003). More evidence is required to ascertain the roles of *ID2* and *NFIL3* in cDC1 development in human. Existing data on the transcription factors profile of human cDC1 fits with the mouse dependency such as the requirement of *BATF3* for cDC1 development.

1.6.1.5. Functional Roles

The cDC1 subset expresses a limited number of TLRs as compared to cDC2 subset. Importantly, and in line with the capacity to fight against viruses, in both mice and human, they express TLR3 which senses for viral dsRNA but other TLRs such as TLR10, and TLR11 have also been reported (Luber et al. 2010; Hémond et al. 2013). They also express interferon (IFN)- λ when stimulated with TLR3 agonist poly I:C (Lauterbach et al. 2010). This subset has demonstrated to efficiently prime CD8⁺ T cells through cross-presentation of exogenous antigen on MHC class I molecules (Haan et al. 2000; Bedoui et al. 2009) and produce IL-12p70 to promote Th1 differentiation of naïve CD4⁺ T cells to clear intracellular pathogens (Reis e Sousa et al. 1997; Hildner et al. 2008). They can also induce Th2 response (Nakano et al. 2012; Segura et al. 2012) but as compared to cDC2 subset, they elicit a weaker response which is driven by OX40L expression (Yu et al. 2014).

Murine cDC1 subset has also been shown to be involved in the maintenance and induction of tolerance to prevent autoimmunity. At steady-state in the skin, migrating CD103⁺ DCs cross-present

keratinocyte-associated antigens to CD8⁺ T cells in the lymph node (Bedoui et al. 2009; Henri et al. 2010). Similarly, CD8α⁺ DCs in the spleen and CD103⁺ DCs in the lung were observed to uptake dying cells and promote tolerance in steady state (Qiu et al. 2009; Desch et al. 2011).

1.6.2. cDC2 subset

1.6.2.1. Phenotype

Murine cDC2 subset is defined as MHCII⁺CD11c⁺ cells that express integrin-αM (CD11b⁺) cells. In the spleen, they also express CD4 and the endothelial cell-specific adhesion molecule (ESAM) (Crowley et al. 1989; Vremec et al. 2000; Lewis et al. 2011), whereas in the NLT, they express heat stable antigen (CD24) (Schlitzer et al. 2013). Initially, NLT cDC2 were thought to be heterogeneous as they were demonstrated to derive from both bone marrow DC-restricted progenitors as well as monocytes, and were partially dependent on the cytokines Flt3 and colony stimulating factor 1 receptor (CSF-1R) (Ginhoux et al. 2009). Through the combination usage of exclusive DC (CD24) or monocyte/macrophages (CD64 or MerTK) markers, *bona fide* DCs and contaminating monocyte/macrophages within this population were better segregated in various non-lymphoid tissues (Langlet et al. 2012; Tamoutounour et al. 2012; Plantinga et al. 2013; Schlitzer et al. 2013). A CD11b⁺ DC population that co-expresses CD103 and CD11b also exists in the intestine of mice (Bogunovic et al. 2009; Varol et al. 2009).

Human CD1c⁺ DCs are characterised by the high expression of CD11c, CD1c, CD11b and SIRPα (MacDonald et al. 2002; Schlitzer et al. 2013). Similarly in the human small intestine, a CD103⁺SIRPα⁺ DC population also exists (Watchmaker et al. 2014).

1.6.2.2. Homology

Using comparative transcriptomics, human blood and skin CD1c⁺ DCs aligned closely with murine lung CD11b⁺CD24⁺ DCs and splenic CD11b⁺CD4⁺ DCs (Haniffa et al. 2012; Schlitzer et al. 2013), while intestinal CD103⁺SIRPα⁺ DCs aligned with its mouse counterpart (Watchmaker et al. 2014).

1.6.2.3. Cytokines Requirement

Similar to the cDC1 subset, murine CD11b⁺ DCs also exhibit dependency on FLT3 and GM-CSF (Ginhoux et al. 2009; Greter et al. 2012; Schlitzer et al. 2013). Although, not much is known about the cytokines requirement of human CD1c DCs, Flt3L and GM-CSF are often added to *in vitro* DC culture system to promote DC differentiation from CD34⁺ HSCs (Poulin et al. 2010; Lee et al. 2015a).

1.6.2.4. Transcription Factors

In contrast to cDC1 lineage, the requirement and hierarchy of transcription factors required for murine cDC2 lineage development is still largely unclear. However, the transcription factors IRF2, IRF4, neurogenic locus notch homolog protein 2 (Notch2) and viral oncogene homolog B (Relb) play important roles in cDC2 development and maturation (Belz and Nutt 2012; Satpathy et al. 2012b; Merad et al. 2013).

IRF2-deficient mice had reduced numbers of splenic CD4⁺ DCs (Honda et al. 2004), but their numbers were restored when type I IFN signalling was eliminated (Ichikawa et al. 2004). IRF4 plays multiple roles as it controls cDC2 development, migration and antigen presentation (Schlitzer et al. 2015a). IRF4-deficient mice displayed a severe reduction in splenic CD4⁺ DCs with a slight reduction in pDCs, but no defects in cDC1 subset (Suzuki et al. 2004; Tamura et al. 2005). Conditional knockout of *IRF4* gene in CD11c-expressing cells demonstrated that IRF4 is important for

development of CD11b⁺ DC in the lung and CD11b⁺CD103⁺ DC in large and small intestine (Persson et al. 2013; Schlitzer et al. 2013).

Canonical signalling through Notch receptor regulates the development of splenic ESAM⁺CD4⁺CD11b⁺ DCs and intestinal CD11b⁺CD103⁺ DCs as both population were ablated in conditional knockout of Notch-RBP-J or Notch2 receptor in CD11c-expressing cell (Caton et al. 2007; Lewis et al. 2011). Even though Notch2 dependent CD11b⁺ cells are dependent on FLT3 signaling, they may selectively require lymphotoxin-β receptor (LTβR) for homeostasis as mice deficient in LTβR showed reduction in ESAM⁺CD4⁺CD11b⁺ DCs (Kabashima et al. 2005; Lewis et al. 2011; Satpathy et al. 2013). Also, the transcription factors Relb and TNF-associated factor 6 (TRAF6), which are involved in nuclear factor kappaB (NF-κB) signalling pathway, mediates signalling through LTβR (Wu et al. 1998; Kobayashi et al. 2003). In mice deficient with Relb or TRAF6, reduced numbers of mature splenic CD4⁺ DC were observed but not much is known about the mechanism by which these molecules control cDC2 lineage development.

Kruppel-like factor 4 (KLF4), a downstream target of IRF8 activation, is known to regulate monocyte development (Feinberg et al. 2007; Kurotaki et al. 2013). Recently, it was implicated in the development of IRF4-expressing cDCs (Tussiwand et al. 2015). cDC2 lineage was ablated in conditional knockout of KLF4 in CD11c-expressing cells, and IRF4 expression was severely reduced at DC-restricted progenitor pre-cDC but not at mature cDCs. Thus suggesting a developmental requirement for KLF4 in the induction of IRF4 expression. However, it is not known if the impaired development is a result of reduced IRF4 expression at the pre-cDC stage or some actions modulated by KLF4.

Not much is known about the roles of these transcription factors in human cDC2 development. IRF8, a transcription factor implicated in the cDC1 lineage, may also play a role in cDC2 development. A complete loss of monocytes, pDCs, cDC1 and cDC2 was observed in the peripheral blood of patients with biallelic human IRF8 K108E mutation (Hambleton et al. 2011). However, patients with autosomal dominant IRF8 T108A mutation showed a selective loss of cDC2 subset and IL-12 production (Hambleton et al. 2011). Further studies are required to clarify these discrepancies as this is in contrast to what was observed in mice. Mice deficient in IRF8 or carrying a spontaneous mutation (R294C) were deficient in monocytes, pDCs and cDC1 subset but not cDC2 subset (Schiavoni et al. 2002; Taylor et al. 2008; Ginhoux et al. 2009). In human, IRF4 expression is higher in CD1c⁺ DCs (Schlitzer et al. 2013) suggesting that the transcription factor expression profile may fit with the mouse dependency.

1.6.2.5. Functional Roles

The functional diversity exhibited by cDC2 subset could be due to their unique innate plasticity or their yet unresolved heterogeneity. cDC2 subset expresses a broad spectrum of PRR, such as TLR 7, 9 and 13, RIG-I, as well as CLEC6a and CLEC7a, which serve as receptors for fungi recognition (Luber et al. 2010; Harman et al. 2013; Hémond et al. 2013). This enables them to sense a repertoire of PAMPs, thereby inducing either Th2 or Th17 responses in various tissues (Kumamoto et al. 2013; Plantinga et al. 2013; Satpathy et al. 2013; Zhou et al. 2014; Tussiwand et al. 2015). Human CD1c⁺ blood DCs can produce IL-12p70 only upon stimulation with TLR7/8 agonist (Schlitzer et al. 2013). Similar to its mouse counterpart, human CD1c⁺ DCs have shown to induce Th17 differentiation (Schlitzer et al. 2013), and are less efficient at cross-presentation (Haniffa et al. 2012).

cDC2 subset may also play a role in maintenance of immunity and induction of tolerance. Murine intestinal CD103⁺SIRPα⁺ DC was demonstrated to be efficient inducers of Tregs as it expressed high levels of retinaldehyde dehydrogenase (RALDH) (Coombes et al. 2007). RALDH metabolises vitamin A into retinoic acid which skewed the T cells to differentiate towards a tolerogenic phenotype (Guilliams et al. 2010). However, a recent study demonstrated that the ablation of CD103⁺CD11b⁻ DCs using Clec9A-diphtheria toxin receptor (DTR) mice exacerbated intestinal inflammation, while ablation of CD103⁺CD11b⁺ DCs with the Clec4a4-DTR mice conferred resistance in the development of dextran sulphate sodium (DSS)-induced colitis (Muzaki et al. 2015). Hence, CD103⁺CD11b⁻ DCs may play a bigger role in maintaining intestinal homeostasis through the balance between Treg and Th17 effector cells (Muzaki et al. 2015).

1.7. Plasmacytoid DC (pDC)

1.7.1. Phenotype

pDCs were first described in human peripheral blood and tonsil and their round morphology resembled that of plasma cells. However, when stimulated *in vitro* with IL-3 in the absence or presence of CD40L, they differentiated into cells with mature DC morphology (Grouard et al. 1997; Cella et al. 1999). They also produce large amounts of type I IFN such as IFN-α in response to viruses (Cella et al. 1999; Siegal et al. 1999). In mouse, they are identified using the markers CD11c, MHCII, protein tyrosin phosphatase receptor Type C (CD45R or B220), Ly6C, bone marrow stromal antigen 2 (BST2 or tetherin) and sialic acid-binding immunoglobulin-like lectin H (Siglec-H) (Reizis et al. 2011). Human pDCs are identified by expression of CD4, IL-3 receptor α-subunit (CD123), immunoglobulin-like transcript 3 (ILT3 or LILRB4), ILT7 (LILRA4), C-type lectin

transmembrane glycoprotein (CD303 or BDCA-2) and neuropilin-1 (CD304 or BDCA-4) (Dzionek et al. 2000; Swiecki and Colonna 2015). BDCA-2 participates in antigen-presentation to T cells and inhibit type I interferon production by pDCs (Dzionek et al. 2002), whereas BDCA-4 is also expressed on endothelial and tumour cells (Colonna et al. 2004). In contrast to human pDCs, murine pDCs express low levels of CD11c and do not express CD123 (Asselin-Paturel et al. 2001; Björck 2001; Nakano et al. 2001).

1.7.2. Homology

Comparative transcriptomics studies of murine and human pDCs, as well as functional properties that will be discussed below, have shown that they aligned closely together (Robbins et al. 2008; Crozat et al. 2010b).

1.7.3. Cytokine Requirement

pDCs exhibit dependency on Flt3L as mice deficient in Flt3L have reduced levels of pDCs (Waskow et al. 2008). Similar to what is observed in mice, injecting human with Flt3L also increased pDC numbers (Pulendran et al. 2000). Likewise, Flt3L is paramount for *in vitro* differentiation of pDCs from murine bone marrow and human CD34⁺ HSCs (Brasel et al. 2000; Naik et al. 2005; Lee et al. 2015a). Thrombopoietin (TPO) in combination with Flt3L also promotes the *in vitro* development of pDC from murine bone marrow and human CD34⁺ HSCs (Chen et al. 2004; Proietto et al. 2012; Onai et al. 2013). Human pDCs also require IL-3 for survival and differentiation into cells with cDC morphology (O'Doherty et al. 1994; Grouard et al. 1997; Olweus et al. 1997; Cella et al. 1999). How IL-3 exerts its effect is still unknown, but it could be mediated through IFN- α (Kadowaki et al. 2000).

1.7.4. Transcription Factors

E2-2, an essential transcription factor involved in pDC development in mouse and human, directly suppressed cDC differentiation and

controls expression of a range of pDC-associated transcription factors such as B cell lymphoma 11a (BCL-11A), IRF8 and SPI-B (Reizis et al. 2011). In patients with Pitt-Hopkins syndrome, an autosomal dominant genetic disorder due to E2-2 haploinsufficiency, reduced pDC population was observed although a population of CD45RA⁺CD123⁺ cells, which lacked BDCA-2 expression and had reduced IFN- α production when stimulated, were present in their blood (Cisse et al. 2008). In mice, deletion of E2-2 in mature pDCs resulted in the loss of pDC-associated markers, and the spontaneous generation of cDCs (Ghosh et al. 2010).

SPI-B is a transcription factor crucial for the differentiation of pDCs (Schotte et al. 2004; Sasaki et al. 2012), as it controls the survival of pDCs and their progenitors through induction of anti-apoptotic protein BCL2-A1 (Karrich et al. 2012). BCL-11A regulates the expression of E2-2, thereby maintaining a positive feedback loop for pDC development (Wu et al. 2013; Ippolito et al. 2014).

1.7.5. Functional Roles

pDCs express high levels of nucleic acid sensors TLR 7 and 9, which are involved in recognition of single-stranded RNA and DNA, respectively (Kawai and Akira 2011). Activation of these receptors results in the secretion of type I IFN by pDCs to combat viral infections (Swiecki and Colonna 2015). They can present antigens to naïve CD4⁺ T cells to induce Th1 or Th2 responses (Villadangos and Young 2008), but not as efficiently as cDCs. Virus-activated pDCs elicit a potent Th1 response mediated by type I IFN, leading to the secretion of large amounts of IFN- γ and IL-10 (Cella et al. 2000; Kadowaki et al. 2000). IL-3 induced pDC preferentially elicit Th2 response mediated by OX40L, leading to the production of IL-4, IL-5 and IL-13 (Rissoan 1999; Ito et al. 2004). pDCs are also able to efficiently cross-present antigens to naïve CD8⁺ T cells (Salio 2004; Hoeffel et al. 2007; Mouriès et al. 2008).

They also play a role in tolerance as they can induce CD4⁺CD25⁺Foxp3⁺ Tregs (Moseman et al. 2004; Ito et al. 2007). The inability to maintain tolerance to nucleic acid may result in autoimmune diseases such as Systemic Lupus Erythematosus (SLE) and Psoriasis (Swiecki and Colonna 2015).

1.8. Ontogeny of DCs

The ontogeny of DCs has been extensively studied in mouse. DC development starts at the bone marrow (BM) where BM-resident hematopoietic stem cells (HSCs) differentiate via several intermediates into the monocyte-macrophage dendritic cell progenitor (MDP), which commits exclusively to monocyte and DC lineage (Fogg et al. 2006). MDP gives rise to the common dendritic cell progenitor (CDP) (Naik et al. 2007; Onai et al. 2007)), which is committed only to cDC lineage, and the common monocyte progenitor (cMOP) that retains solely monocyte differentiation potential (Hettinger et al. 2013). The CDP is heterogeneous and is divided into two populations based on CSF-1R expression (Onai et al. 2013). CSF-1R⁻ CDPs preferentially give rise to pDCs, whereas CSF-1R⁺ CDPs differentiate into pre-cDCs that exit the BM into the circulation to seed the organs and tissues (Ginhoux et al. 2009; Liu et al. 2009) (**Figure 5**). Using two independent approaches – single cell mRNA sequencing and genetic knockout mice model, two groups showed that commitment to the two cDC lineages is decided in the bone marrow (Grajales-Reyes et al. 2015; Schlitzer et al. 2015b). Furthermore, pre-cDCs were shown to be heterogeneous and can be separated into 4 distinct populations based on Siglec-H and Ly6C expression. Siglec-H⁺Ly6C⁻ pre-DC was developmentally closer to CDP and retained pDC potential *in vivo*, while Siglec-H⁺Ly6C⁺ pre-DC differentiated exclusively to cDCs only. Siglec-H⁺Ly6C⁺ pre-DC either lost expression of Siglec-H and differentiated into cDC2 lineage or lost expression of both Siglec-H and Ly6C, while acquiring CD24 to differentiate into cDC1 lineage (Schlitzer et al. 2015b).

In humans, both multi-lymphoid progenitor (MLP) and the granulocyte-macrophage progenitor (GMP) showed DC potential (Doulatov et al. 2010). Recently, human equivalent of MDP, CDP and pre-cDCs were identified in the cord blood, bone marrow and peripheral blood based on increasingly restricted expression of cytokine receptors macrophage colony stimulating factor receptor (M-CSFR or CD115), granulocyte-macrophage colony stimulating factor receptor (GM-CSFR or CD116), c-kit (CD117) and CD45RA (Breton et al. 2015; Lee et al. 2015b). Cross-phenotyping revealed that MLP and GMP are heterogeneous groups of cells with surface markers similar to MDP and CDP, which may explain why both populations contain DC potential (Lee et al. 2015b). Further investigation is required to determine if human CDPs can be further separated into pDC-committed CDPs and cDC-committed CDPs as observed in the mouse. It is also unclear if the recently identified pre-cDCs identified can give rise to cDCs in the blood and tissues as circulating cDCs are thought to be precursors of tissue cDCs (Collin et al. 2011; Breton et al. 2015; Haniffa et al. 2015). Despite the recent gain in knowledge in DC ontogeny, much remains to be done such as resolving the contribution of CDP and monocytes into cDC in steady state and during inflammation.

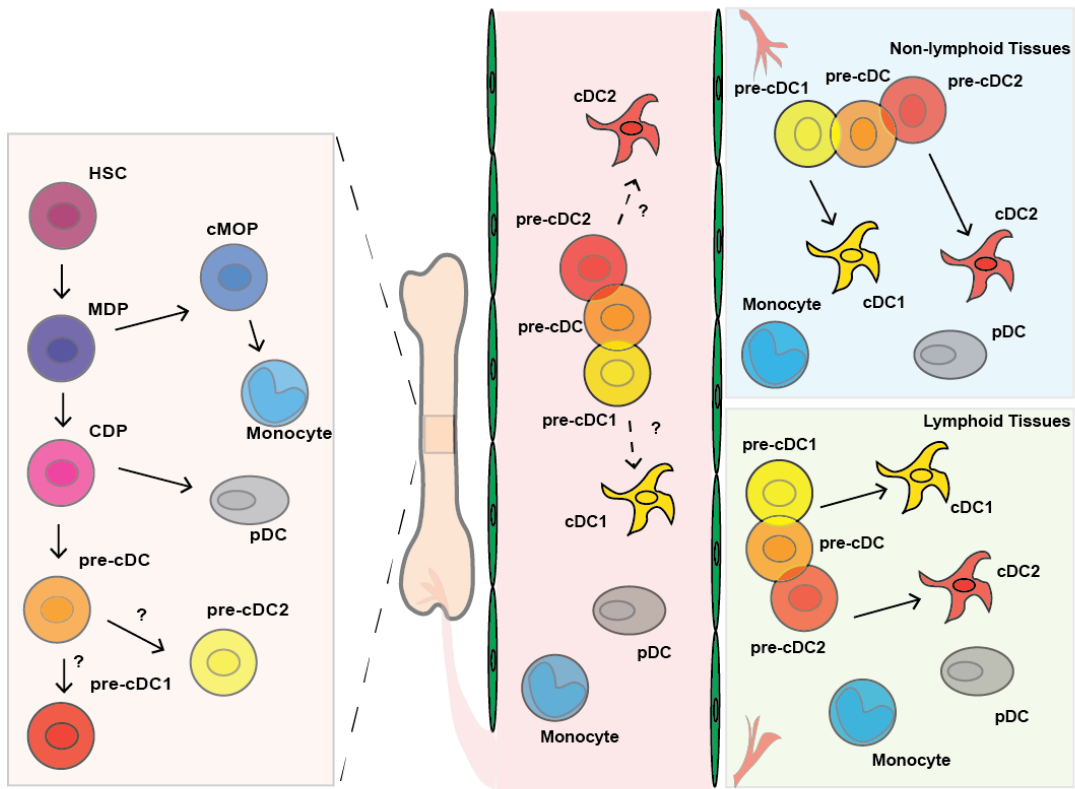


Figure 5. Dendritic cell development.

DC development starts in the bone marrow where HSCs differentiate via several intermediates into MDPs, which give rise to both monocytes and DCs through cMOP and CDPs, respectively. CDPs further differentiate into pDCs and pre-cDCs. pDCs mature and exit the bone marrow to enter the circulation to seed the tissues. In mouse, committed pre-cDC subsets have recently been identified but it is unclear if they exist in humans. Pre-cDCs enter the circulation and seed the tissues where they differentiate into cDC subsets. (HSC: hematopoietic stem cell, MDP: monocyte-macrophage dendritic cell progenitor, CDP: common dendritic cell progenitor, cMOP: common monocyte progenitor, cDC: conventional dendritic cell, pDC: plasmacytoid dendritic cell)

1.9. AIMS

Although DCs have been shown to develop from CDPs, monocytes were shown to differentiate into DCs during inflammation in various models of infection (Serbina et al. 2003; León et al. 2007; Hohl et al. 2009). During steady state, circulating murine monocytes labelled with latex particles were found in murine lungs, and Ly6C^{hi} and Ly6C^{lo} monocytes were found to preferentially differentiate into CD103⁺ and CD11b⁺ DCs, respectively (Jakubzick et al. 2008). Hence, this suggested that monocytes or its precursor cMOP might contribute to DC ontogeny. Similarly, not much is known about the identity of human equivalent DC-restricted progenitors such as CDP and pre-cDC until recently. Despite their discoveries, some questions remain unanswered such as the presence of committed pre-cDC subsets, the relationship between pre-cDCs, circulating and tissue cDCs as this could have implications in vaccine design and therapeutics

Therefore in this PhD, we seek to:

1. Understand the contribution of CDP versus monocytes in tissue DC subsets in steady state by developing a fate-mapping model where Cre recombinase gene is placed under the promoter of an identified gene of interest uniquely expressed by DC-restricted progenitors. This Cre mouse strain will be crossed to a reporter mouse strain to tag committed DC-restricted progenitors and their downstream progeny, thereby allowing us to understand better DC ontogeny.
2. Identify and characterise human DC-restricted progenitors through various approaches such as transcriptomics and functional studies, so as to understand human DC development to improve intervention and design new therapeutic strategies.

2. MATERIALS AND METHODS

2.1. Mice

C57BL/6J mice were obtained from the Biomedical Resource Centre (BRC), A*STAR, Singapore. Upk1b-RFP reporter mice were purchased from Jackson Laboratory and Rosa-LSL-YFP reporter mice were obtained from Dr Nancy Jenkins (Institute of Molecular and Cell Biology (IMCB), A*STAR, Singapore), and humanized mice generated as described in (Chen et al. 2009) were obtained from Dr Chen Qingfeng (Institute of Molecular and Cell Biology (IMCB), A*STAR, Singapore). Upk1b-cre mice were generated with the help of Dr Esther Wong (Institute of Medical Biology (IMB), A*STAR, Singapore). All mice were bred and kept under specific pathogen-free conditions in BRC according to guidelines and protocols approved by the Institutional Committee of Animal Welfare of A*STAR, Singapore.

2.2. Bacterial strains and plasmids

XL10-Gold competent *E. coli* cells were purchased from Stratagene while SW102 *E. coli* cells and pBlight plasmid were a gift from Dr Esther Wong (IMB, A*STAR, Singapore). Dr Pearline Teo constructed the plasmids pPGK-Cre-bpA and pTA-fre-neo-frt, while the BAC clone RP24-157N17 was purchased from Children's Hospital Oakland Research Institute (CHORI).

2.3. Sample collection

Apheresis cone blood, umbilical cord blood and spleen samples were obtained through Health Sciences Authorities, Singapore Cord Blood Bank and Dr Jerry Chan of KK Women's and Children's Hospital, and Dr Tony Lim of Singapore General Hospital, respectively. Written informed consents were obtained from the donors according to the procedures approved by the National University Singapore Institutional Review Board and SingHealth Centralised Institutional Review Board. Bone marrow mononuclear cells (BM) were purchased from Lonza.

PBMC of SLE patients were obtained from Dr Anna-Marie Fairhurst of Singapore Immunology Network (SIgN).

2.4. Construction of Upk1b-cre targeting plasmid

2.4.1. Infusion cloning

Cloning was achieved by homologous recombination using In-Fusion® HD Cloning Kit (Clontech). Briefly, PCR products were treated with cloning enhancer and incubated at 37°C for 15 mins, followed by 80°C for 15 mins. The treated PCR products were incubated with linearized plasmid at 37°C for 15 mins, followed by 50°C for 15 mins. The reaction mix was diluted 10-fold with 1X TE buffer and 2.5 µl of reaction mix was transformed into XL-10 Gold competent *E. coli* cells. The transformed cells were plated on LB plates with the appropriate antibiotics and incubated overnight at 37°C. Individual colonies were picked and screened by colony PCR using primers listed in Table 1. Plasmid DNA was extracted using NucleoSpin® Plasmid Kit (Macherey-Nagel) following manufacturer's protocol and sent for DNA sequencing (Axil Scientific Pte Ltd).

2.4.2. Construction of mini-targeting and retrieval plasmids

To generate the mini-targeting plasmid pJET-Upk1b Cre (**Figure 5**), a 1,071 bp homology arm was PCR amplified from RP24-157N17 and inserted into pJET1.2/blunt plasmid as instructed in the manufacturer's instruction (CloneJET™ PCR Cloning Kit, Fermentas) to generate pJET-Upk1b 5'. Next, a 1,334 bp Cre fragment with *NdeI*, *AflII*, *NheI* and *EcoRV* restriction sites were PCR amplified from pPGK-Cre-bpA and inserted into *EcoRV* digested pJET-Upk1b 5' by Infusion cloning as described in Section 2.4.1, generating pJET-Upk1b 5' Cre. pTA-frt-neo-frt plasmid was then digested with *NdeI* and *AflII* to yield a 1,651 bp fragment, which was ligated into *NdeI*-*AflII* digested pJET-Upk1b 5'Cre to generate pJET-Upk1b 5' Cre Neo. Finally, a 734 bp downstream homology

arm was PCR amplified from RP24-157N17 and inserted into *AflI-NheI* digest pJET-Upk1b 5' Cre Neo by Infusion cloning to generate pJET-Upk1b Cre. The PCR conditions and primers used are listed in Table 1. To generate the retrieval plasmid, a 542 bp long arm and 526 bp short arm fragments were PCR amplified from RP24-157N17 using the primers and PCR conditions listed in Table 1. Next, the two fragments were PCR spliced together. Briefly, both PCR products were diluted 10-fold with 1X TE buffer and mixed in equal portion. 2 µl of the mixed PCR products were amplified with the primers and PCR conditions listed in Table 1. The spliced PCR fragment was inserted into *BamHI-SalI* digested pBlight plasmid by Infusion cloning as described in Section 2.4.1 to generate pBlight-Upk1b (**Figure 6**).

2.4.3. Transformation of BAC into SW102 *E. coli* cells

The transformation of BAC or plasmid DNA into SW102 *E. coli* cells were performed as described in (Liu et al. 2003). Briefly, DH10B electrocompetent cells containing the BAC clone RP24-157N17 were grown overnight in 5 ml of LB broth (Biopolis Shared Facilities (BSF), A*STAR) with chloramphenicol. BAC DNA was extracted using PureLink HiPure BAC Buffer Kit (Invitrogen) according to manufacturer's instructions. 1 µl of freshly prepared BAC DNA (100 ng) was used for electroporation. SW102 *E. coli* cells were grown overnight in 5 ml of LB broth at 32°C. The following day, 500 µl of overnight culture was transferred into 25 ml LB broth and grown at 32°C until the OD₆₀₀ is 0.5-0.6. Next, the cells were collected by centrifuging at 4000 rpm at 0°C for 5 mins. Cells were resuspended in ice-cold water, transferred to 1.5 ml eppendorf tubes and centrifuged at 4000 rpm at 0°C for 5 mins using a benchtop centrifuge. The process was repeated two more times. Finally, the cell pellet was resuspended in 80 µl of ice-cold water. 45 µl of cells were transferred to a pre-cooled electroporation cuvette with 0.1 cm gap (BIO-RAD). 1 µl of BAC was added to the cells and mixed. Electroporation was performed using a BIO-RAD electroporator

under the following condition: 1.75 kV, 25 μ F with the pulse controller set at 200 Ω and time constant set at 4.0. 1 ml of LB was added to each cuvette and the transformants were recovered at 32°C for an hour before plating onto LB plates with appropriate antibiotics.

Table 1. PCR conditions and primers used in generating Upk1b-Cre targeting plasmid.

Primer	Sequence (5' – 3')	PCR Conditions	
Upk1b 5' For	GCTGGATCCTTTTCGCACTA A	95 °C – 5 min 95 °C – 30s 55 °C – 30s	x 34 cycles
Upk1b 5' Rev	ATCCATCTTCAGGATTTTCT AAAAGCTG	72 °C – 1 min 72 °C – 7 min	
Cre For	ATCCTGAAGATGGATCCCA AGAAGAAGAGGAAGGTG	95 °C – 5 min 95 °C – 30s 55 °C – 30s	x 34 cycles
Cre Rev	ATCTTCTAGAAAGATATCG CTAGCCTTAAGCATATGCC ATAGAGCCCACCGCAT	72 °C – 2 min 72 °C – 7 min	
Upk1b 3' For	TCGTATTAAGCTTAAGGCC AAAGACGATTCCACTGT	95 °C – 5 min 95 °C – 30s 58 °C – 30s	x 34 cycles
Upk1b 3' Rev	GAAAGATATCGCTAGCTGA GTCTGTCAGGCTTGTGG	72 °C – 1 min 72 °C – 7 min	
Upk1b LA For	CTTATCGATGTCGACCCAG TATCCTCTGCCCGTAAG	95 °C – 5 min 95 °C – 30s 55 °C – 30s	x 34 cycles
Upk1b LA Rev	GTTCTGTACTGCCTCGAG CCCATCTCAGCTTCTCAAG G	72 °C – 1 min 72 °C – 7 min	
Upk1b SA For	AAGCTGAGATGGGCTCGA GGCAGTACAGGAACCTG GAA	95 °C – 5 min 95 °C – 30s 55 °C – 30s	x 34 cycles
Upk1b SA Rev	GACTCTAGAGGATCCTTGT GCTTTCACCTGCCTGAC	72 °C – 1 min 72 °C – 7 min	
Upk1b LA For	CTTATCGATGTCGACCCAG TATCCTCTGCCCGTAAG	95 °C – 5 min 95 °C – 30s 60 °C – 1 min	x34 cycles

Upk1b SA Rev	GACTCTAGAGGATCCTTGT GCTTTCACCTGCCTGAC	72 °C – 2 min 72 °C – 7 min	
-----------------	--	--------------------------------	--

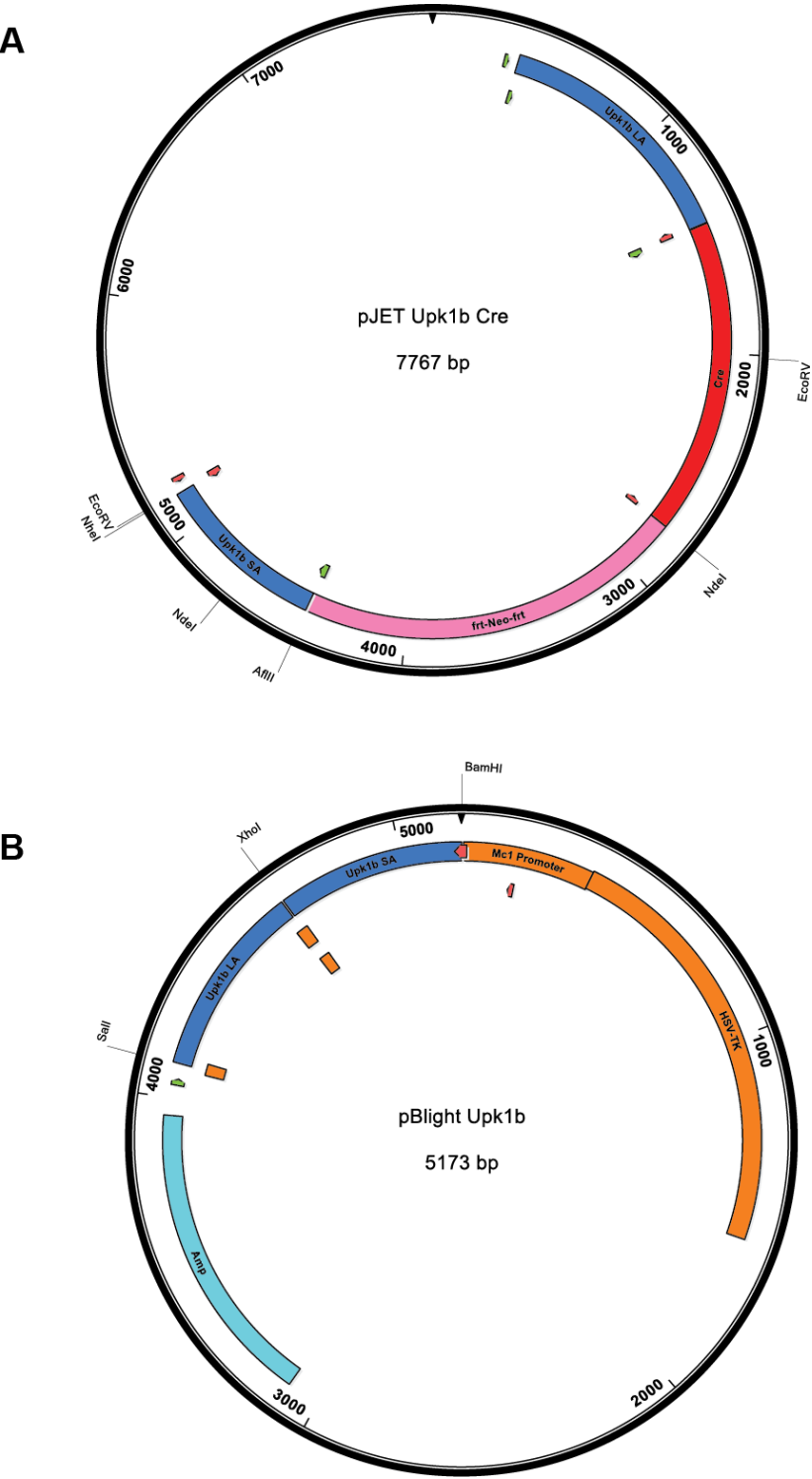


Figure 6. Plasmid map of mini-targeting and retrieval plasmid.

The mini-targeting vector, pJET-Upk1b Cre was constructed by sequential cloning of Upk1b 5', Cre-bpA, frt-Neo-frt and Upk1b 3'. (B) The retrieval

plasmid pBlight Upk1b was constructed by Infusion cloning of PCR-spliced Upk1b LA and SA fragments.

2.4.4. Retrieving

SW102 *E. coli* cells containing BAC clone RP24-157N17 were grown overnight in 5 ml of LB broth at 32°C. The following day, 500 µl of overnight culture was transferred into 25 ml LB broth and grown at 32°C until the OD₆₀₀ is 0.5-0.6. 10 ml of culture was transferred to a 50 ml conical flask and incubated in a shaking waterbath set at 42°C for 15 mins. Next, the flask was placed and shook on ice to cool the temperature rapidly, following that cells were collected by centrifuging at 4000 rpm at 0°C for 5 mins. Cells were resuspended in ice-cold water, transferred to 1.5 ml Eppendorf tubes and centrifuged at 4000 rpm at 0°C for 5 mins using a benchtop centrifuge. The process was repeated two more times. Finally, the cell pellet was resuspended in 80 µl of ice-cold water. 45 µl of cells were transferred to a pre-cooled electroporation cuvette with 0.1 cm gap (BIO-RAD). 1 µl of *Xho*I linearized pBlight-Upk1b (100 ng) was added to the cells and mixed. Electroporation was performed as described in Section 2.4.3. The transformants were recovered at 32°C for an hour before plating onto LB plates with appropriate antibiotics.

2.4.5. Targeting

The mini-targeting plasmid pJET-Upk1b Cre was linearized with *Nhe*I and resuspended to give a final concentration of 100 ng/ul. It was cotransformed with 10 ng/ul of pBlight-Upk1b generated from Section 2.4.4. SW102 *E. coli* cells were prepared as described in Section 2.4.3. Electroporation was performed as described in Section 2.4.3, and the transformants were recovered at 32°C for an hour before plating onto LB plates with appropriate antibiotics. The plasmid generated is denoted as pBlight-Upk1b-Cre targeting plasmid (**Figure 7**). The plasmid was sequenced with the primers listed in Table 1 to ensure that mutations were not found in the Cre

gene. The plasmid was also digested with *Nde*I to ensure that the Cre gene and Neo genes were present.

2.5. Gene targeting in mouse ES cells

The pBlight-Upk1b Cre targeting plasmid was linearized with *Sa*II and resuspended to a final concentration of 1 µg/µl. The linearized targeting plasmid was electroporation into JM8 and Bruce4 ES cells by Dr Esther Wong. Single ES clones were cultured onto 24-well plates. DNA was extraction from the individual clones using DNeasy Blood & Tissue Kit (QIAGEN), and screened using the primers and PCR conditions listed in Table 2. Targeted clones identified by PCR screening were expanded and confirmed by Southern blots with long arm and short arm probes.

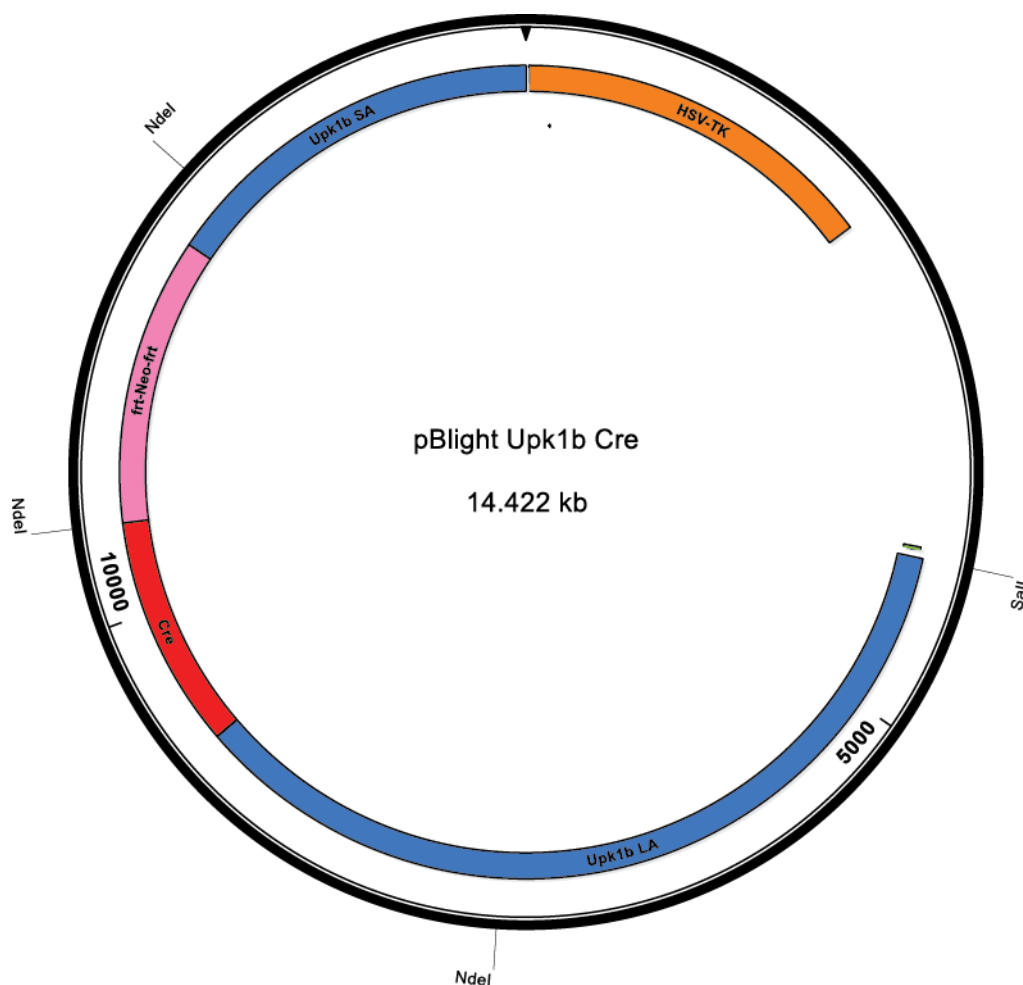


Figure 7. Plasmid map of pBlight-Upk1b Cre.

pBlight-Upk1b Cre was generated using homologous recombination. The linearized mini-targeting plasmid, pJET-Upk1b Cre and retrieval plasmid, pBlight-Upk1b Cre was co-transformed into SW102 E. coli.

Table 2. PCR conditions and primers used for ES clones and KI mice screening.

Primer	Sequence (5' – 3')	PCR Conditions	
Upk1b 421R	ACATAGATCCACAGAAGTC AGGAA	95 °C – 2 min 95 °C – 30s 58 °C – 30s	x 39 cycles
Neo 1487F	GACTCTGGGGTTCTGAATAA AGAC	68 °C – 4 min 68 °C – 10 min	

2.6. Southern blot analysis of targeted clones

Southern blot was performed using Digoxigenin (DIG) Nonradioactive Nucleic Acid Labelling and Detection System (Roche) according to manufacturer's instructions. The long arm and short arm probes were generated using Roche PCR DIG Probe Synthesis Kit using RP24-157N17 as the template and the primers and PCR conditions listed in Table 3. Genomic DNA of the ES clones were digested with either *HindIII* and *NotI* or *BamHI* overnight for detection with the DIG-labeled long arm probe or DIG-labeled short arm probe, respectively.

Table 3. PCR conditions and primers used to generate DIG-labeled probes.

Primer	Sequence (5' – 3')	PCR Conditions	
Upk1b LA probe_For	AGACAGCATGGTAGGGTCTCT	95 °C – 2 min 95 °C – 30s 55 °C – 1 min	X 30 cycles
Upk1b LA probe Rev	ATCAGGTACCAAGTTGCACGT	72 °C – 1 min 72 °C – 7 min	
Upk1b SA probe For	TGTTCAACTCTGTTCCAGCCA	95 °C – 2 min 95 °C – 30s 55 °C – 1 min	X 30 cycles
Upk1b SA probe Rev	TCAGCTGCTACTTGGAATGGG	72 °C – 1 min 72 °C – 7 min	

2.7. Establishment of Upk1b-Cre knock-in mouse strain

Microinjection of selected ES clones into blastocysts was performed by Dr Esther Wong. Chimeric mice generated via blastocyst microinjection were weaned 3 weeks after birth and mated with albino C57BL/6J mice when they were 6 weeks old. The founder mice were screened for targeted insertion via PCR on genomic DNA extracted from the tail tip using the primers listed in Table 2. The tail tip was digested overnight in tail lysis buffer (50mM Tris-HCl (Promega) pH 8.0, 100mM NaCl (Promega), 100mM EDTA (Promega), 1% SDS (1st Base)) supplemented with 0.2 mg/ml Proteinase K (Promega) at 55°C in a shaking eppendorf tube incubator. The digested tails were centrifuged at 12,000 rpm for 5 mins and the supernatant was pipetted into a new Eppendorf tube containing 500 µl of isopropanol. The Eppendorf tube was inverted a few times to precipitate the genomic DNA, centrifuged at 12,000 rpm for 5 mins, and the supernatant was removed. 300 µl of 70% ethanol was added to the Eppendorf tube, centrifuged at 12,000 rpm for 3 mins and the supernatant was removed. The genomic DNA was air dried for 5 mins, dissolved in 100 µl of nuclease free water, and placed in a shaking Eppendorf tube incubator at 55°C for an hour to fully dissolve the DNA. Correctly targeted founder mice were then crossed with either C57BL/6J mice to maintain the line or Rosa-LSL-YFP mice for experimentation.

2.8. Murine and human cell suspension preparation

Murine bone marrow cells were harvested from the femurs and tibias by flushing them with ice-cold PBS. The cells were centrifuged at 1,350 rpm for 5 mins, resuspended in blocking buffer (1X phosphate buffered saline (PBS) (BSF) supplemented with 0.5% bovine serum albumin (BSA) (GE Healthcare), 2mM EDTA, 1% mouse serum (Sigma), 1% rat serum (Sigma). Spleen was harvested and prepared as described previously (Ginhoux et al. 2009). Briefly, the spleen was minced and digested in RPMI1640 (GE Healthcare) with 10% foetal bovine serum (FBS) (Serana), 0.2 mg/ml collagenase Type IV (Sigma) and 5,000 U/ml DNase I (Roche) at 37°C for 1 hour. A homogenous cell

suspension was obtained by passing through a 19G syringe. Erythrocytes were lysed with red blood cell lysis buffer (155mM NH₄Cl (Sigma), 10mM KHCO₃ (Sigma), 0.1mM EDTA) for 5 minutes, washed with FACS buffer (1X PBS supplemented with 0.5% BSA, 2mM EDTA).

Human peripheral blood mononuclear cells (PBMC) and cord blood mononuclear cells (CB) were isolated by Ficoll-Paque (GE Healthcare) density gradient centrifugation. After density gradient centrifugation, aliquots of mononuclear cells were frozen and stored in liquid nitrogen for future analysis.

2.9. Antibodies and flow cytometry

Antibodies were purchased from Biolegend unless stated otherwise. **Appendix A and B** listed the antibodies used for mouse and human samples, respectively. Flow cytometry was performed on either a BD LSRII or BD LSRFortessa, while fluorescence-activated cell sorting (FACS) was performed using BD FACSAriaII. Software analysis was performed with FlowJo (TreeStar).

For sorting of murine DC progenitors in the BM, the cells were incubated with biotin-conjugated anti-mouse Flt3 monoclonal antibodies (eBioscience), followed by anti-biotin microbeads (Miltenyi Biotec) for 20 mins each. For sorting of murine DC subsets in the tissues, the cell suspension was incubated with anti-CD11c microbeads (Miltenyi Biotec) for 20 mins. The cell suspensions were filtered through a 70-µm strainer and the labeled cells were magnetically enriched using the autoMACS Pro Separator (Miltenyi Biotec) prior to staining for FACS.

To sort for pre-DCs in the human peripheral blood, PBMC were first depleted of T cells, monocytes and B cells with anti-CD3, anti-CD14 and anti-CD20 microbeads from Miltenyi Biotec using the AutoMACS Pro Separator (Miltenyi Biotec) according to manufacturer's protocol.

2.10. Immunofluorescence microscopy

Sorted bone marrow progenitors were spun onto glass slides, fixed with 4% paraformaldehyde and air dried prior to staining. The cells were blocked in 0.2% BSA for 15 mins, and stained with Goat anti-uroplakin (N-20, Santa Cruz) overnight before counterstaining with Donkey anti-Goat AF488 (Jackson Immuno Research). The cells were analyzed using Olympus FV-100 confocal system.

2.11. DC assay on MS5 stromal cells

MS5 stromal cells were a gift from Dr Muzlifah Haniffa (Newcastle University, Newcastle upon Tyne). MS5 stromal cells were maintained and passaged as described in (Lee et al. 2015a). MS5 stromal cells were seeded in 96-well round bottom plates (Corning) at a density of 3,000 cells per well in complete α -MEM (Life Technologies) supplemented with 10% FBS and 1% penicillin/streptomycin (Nacalai Tesque) 18-24 hours before addition of sorted purified populations. 5,000 sorted purified populations were seeded in medium containing 200 ng/ml of Flt3L (Miltenyi Biotec), 20 ng/ml SCF (Miltenyi Biotec) and 20 ng/ml GM-CSF (Miltenyi Biotec) and cultured for up to 5 days. Cells in wells were resuspended by physical dissociation, filtered into polystyrene FACS tube capped with a cell strainer

2.12. Stimulation with TLR ligands

5×10^6 frozen PBMCs or BM cells were cultured in complete RPMI-1640 Glutmax media (Life Technologies) supplemented with 10% FBS and 1% penicillin/streptomycin and stimulated with either 10 ng/ml lipopolysaccharide (LPS) (Sigma), 10 μ g/ml Imidazoquinoline (CL097) (InvivoGen), 1000 U/ml interferon gamma (IFN- γ) (R&D Systems) and 5 μ M CpG oligodeoxynucleotides (CpG ODN) 2216 (InvivoGen) for 3 hours, following which 10 μ g/ml of Brefeldin A solution (eBioscience) was added and the cells were further stimulated for an additional 11 hours. After the 14 hours stimulation, the cells were analysed by flow cytometry.

2.13. Mixed lymphocyte reaction (MLR)

Naïve T cells were isolated from PBMCs using Naïve Pan T Cell Isolation Kit (Miltenyi Biotec) according to manufacturer's instructions, and labelled with 0.2 μ M carboxyfluorescein succinimidyl ester (CFSE) (Life Technologies) for 5 min at 37 °C. 5,000 sorted DC populations were co-cultured with 100,000 CFSE labelled naïve T cells for 7 days in Iscove's Modified Dulbecco's Medium (iMDM) (Life Technologies) supplemented with 10% KnockOut™ Serum Replacement (Life Technologies). On day 7, T cells were re-stimulated with 10 μ g/ml phorbol myristate acetate (PMA) (InvivoGen) and 500 μ g/ml ionomycin (Sigma) for 1 hour at 37 °C. 10 μ g/ml Brefeldin A solution was added for 4 hours and the cells were analysed by flow cytometry.

2.14. Microarray analysis

For the mouse samples, total RNA was extracted using mirVana™ miRNA isolation kit (Ambion), and prepare for microarray using Illumina Mouse WG6 chips according to the manufacturer's instructions. For the human samples, total RNA was isolated Qiagen RNeasy Micro kit. Total RNA integrity was assessed using Agilent Bioanalyzer and the RNA Integrity Number (RIN) was calculated; all RNA samples had a RIN \geq 7.1. Biotinylated cRNA was prepared according to the protocol by Epicentre TargetAmp™ 2-Round Biotin-aRNA Amplification Kit 3.0 using 500pg of total RNA. Hybridization of cRNA was performed on Illumina Human-HT12 Version 4 chips. Microarray data was exported from GenomeStudio software without background subtraction. Probes with detection p-value of > 0.05 were considered as not detected in a sample and probes that were not detected in any of the samples were filtered out. Expression values of the remaining probes were log2 transformed and quantile normalized. For differentially expressed gene (DEG) analysis, comparison of one cell subset with another was carried out with limma R software package (Smyth 2004) with samples paired by donor identifiers. DEGs were selected with Benjamini-Hochberg (BH) multiple testing (Benjamini and Hochberg 1995) corrected p-value of < 0.05 . In this way, limma was used to select genes that were up- or

down-regulated in the pre-DC subsets by comparison of the pre-DC subset against each other as well as with defined DC subset (in-house microarray data).

2.15. Quantitative RT-PCR

RNA and cDNAs of FACS-sorted progenitors were prepared with RNeasy® Mini Kit (Qiagen) and Superscript™ First-strand Synthesis System for RT-PCR (Invitrogen). Briefly, the cells were lysed in RLT buffer, applied to RNeasy® spin column and extracted according to the manufacturer's instructions. cDNA was synthesized with oligo (dT) primers. Quantitative PCR was performed with LightCycler® 480 SYBR Green I Master Mix (Roche, Basel, Switzerland). PCR conditions were initial activation at 95°C for 10 mins, followed by 45 cycles of denaturation at 95°C for 10 s, primer annealing at 60°C for 10 s and elongation at 72°C for 20 s. The primers used for measurement of murine *Upk1b* expression were listed in Table 4.

Table 4. Primers used in qPCR.

Primer Name	Sequence (5' – 3')
Upk1b qPCR For	GACGATTCCACTGTTCGTTG
Upk1b qPCR Rev	GGGCGATGCCACACATAC
GAPDH qPCR For	TGCGACTTCAACAGCAACTC
GAPDH qPCR Rev	ATGTAGGCCATGAGGTCCAC

2.16. Statistical analysis

Mann-Whitney test was used to compare control and Systemic Lupus Erythematosus (SLE) patients. Pearson correlation was used to determine the immune cell population with respects to increasing SLE disease activity index (SLEDAI). Differences were defined as statistically significant when $p < 0.05$. All tests were performed using GraphPad Prism 6.

3. RESULTS

3.1. Generation of fate mapping model for DC ontogeny

3.1.1. Uroplakin (Upk) 1b is a potential candidate to map DCs derived from CDPs

Pure populations of monocyte, MDP, CDP and pre-cDC from murine BM, and DC subsets (cDC1, cDC2 and pDC) from murine spleen and lung were isolated and subjected to microarray analysis to obtain their whole gene transcriptomics. Next, we performed subtractive analysis whereby differentially expressed genes in DC-restricted progenitors, CDP and pre-cDCs were identified, while commonly expressed genes between all sorted populations were removed. 13 candidates were obtained, of which we focused on Uroplakin (Upk) -1b, a tetraspanin molecule (**Figure 8A**). We also checked the ImmGEN database (Miller et al. 2012), which contained the microarray data of all immune cells and identified that Upk1b was expressed on the CDP and microglia but not on other immune cells (**Appendix C**). We performed RT-qPCR on sorted DC progenitors and lung cDC subsets to validate *Upk1b* mRNA expression. Expression of *Upk1b* mRNA was higher in CDP and pre-cDC but low in MDP, pDC and lung DC subsets (**Figure 8B**). We also validated the protein expression of Upk1b in BM pre-cDCs and observed that the protein is located on the cell surface membrane (**Figure 8C**). We postulated that Upk1b could play a role in DC development. Hence we crossed Upk1b^{RFP/+} mice, whereby the red fluorescence protein (RFP) was inserted after the start codon of Upk1b promoter, to generate homozygous Upk1b^{RFP/RFP} mice where the endogenous Upk1b protein was knockout. In contrary to our expectations, the proportion of splenic DCs remained the same in littermate control and Upk1b^{RFP/RFP} mice (**Figure 8D**). Similar results were observed in NLT (Data not shown). We also did not observe RFP fluorescence in the DC-restricted progenitors or cDC subsets (**Figure 8D**).

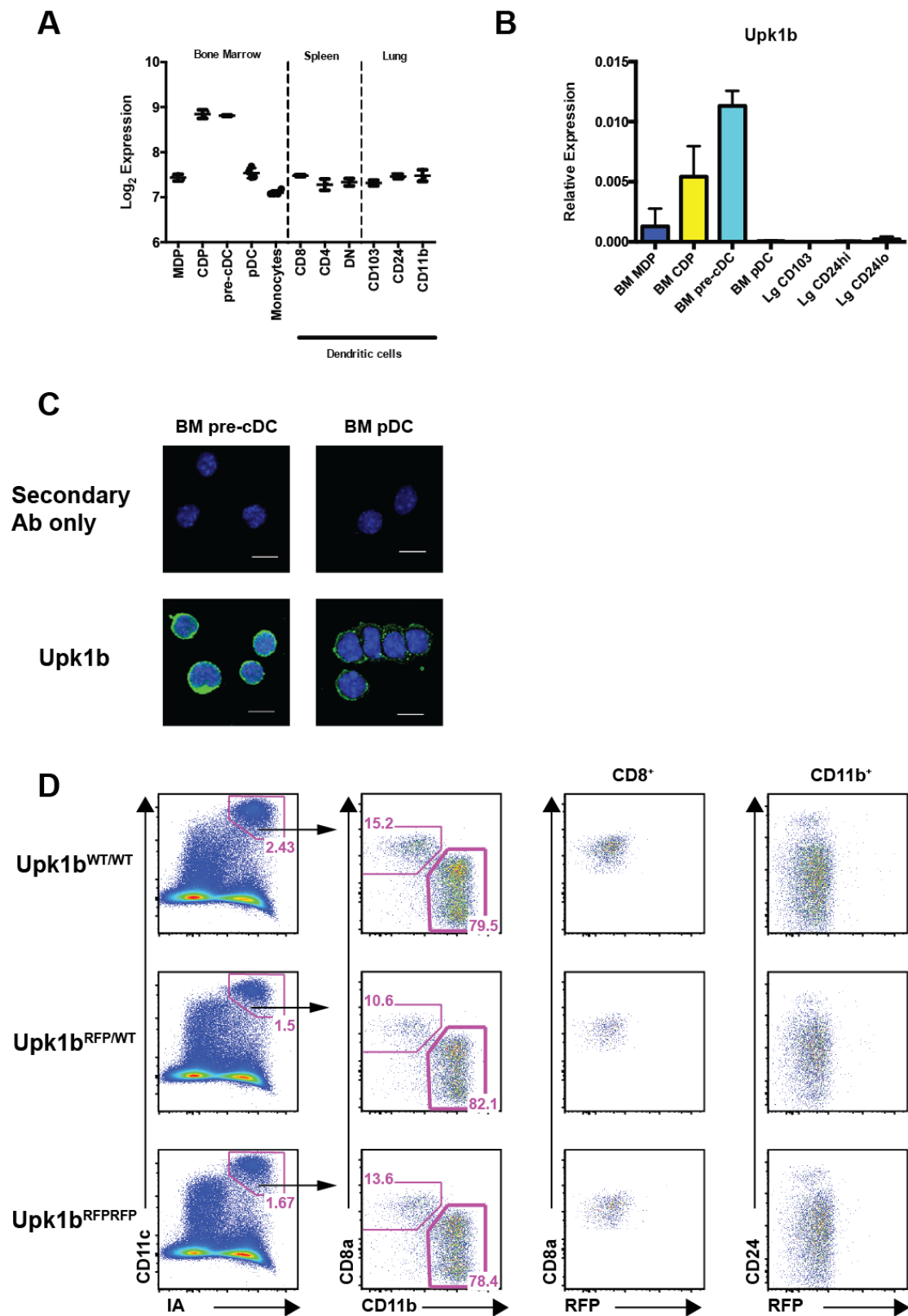


Figure 8. Upk1b is a uniquely expressed in CDP and pre-cDC.

DC-restricted progenitors, monocytes and pDCs from the bone marrow, as well as DC subsets in the spleen and lung were sorted for microarray

analysis. (A) A tetraspanin molecule *Upk1b* was identified as uniquely expressed in CDP and pre-cDC. (B) RNA expression of *Upk1b* was determined in DC progenitors and lung DC subsets by quantitative RT-PCR. The bar graph represented the relative expression of *Upk1b* in the various populations. (C) BM pre-cDC and pDC were sorted and spun onto cytopsin slides before staining with *Upk1b* antibody (green) to visualise its localisation in the cell. (D) Splenic DC subsets in littermate controls and *Upk1b*^{RFP/RFP} mice were analysed by flow cytometry. No reduction in splenic DC proportion was observed. For all experiments, *n*=3 and representative plots were shown. The error bar represented SEM.

3.1.2. Generation of knock-in *Upk1b*-cre mouse model

Since *Upk1b* is only expressed on DC-restricted progenitors (CDP and pre-cDC) and not on MDP, monocytes or DC subsets, it could be used as a marker to fate map DC subsets arising from DC-restricted progenitors. We constructed a mini-targeting vector where short fragments of *Upk1b* homology arms flanked the Cre recombinase gene (**Figure 6**). We also constructed a retrieval plasmid containing short fragments of *Upk1b* regions to retrieve a 7 kb genomic fragment from the BAC clone RP24-157N14 (**Figure 6**). Both plasmids were co-transformed into *E. coli* SW102 to generate a targeting vector via homologous recombination where the Cre recombinase gene was flanked by 5 kb and 2 kb homology arms upstream and downstream of *Upk1b* start codon (**Figure 9A**). The targeting vector was linearized and electroporated into JM8 and Bruce4 ES cells and correctly targeted clones were identified by PCR (**Figure 9B**) and Southern blot of both upstream and downstream regions flanking the *Upk1b* promoter (**Figure 9C**). A total of 6 ES clones (1 from JM8 and 5 from Bruce4 ES) were obtained. 3 of the clones, F5' (JM8), B1 and D5 (Bruce4) were expanded and microinjected into blastocysts to generate chimeric mice. Chimeric mouse from B1 clone did not yield any founder mice. Founder mice from F5' and D5 were obtained and crossed with

Rosa-LSL-YFP reporter mice to generate Upk1b-cre:Rosa-YFP mice, thereby allowing fate mapping of DC progenitors.

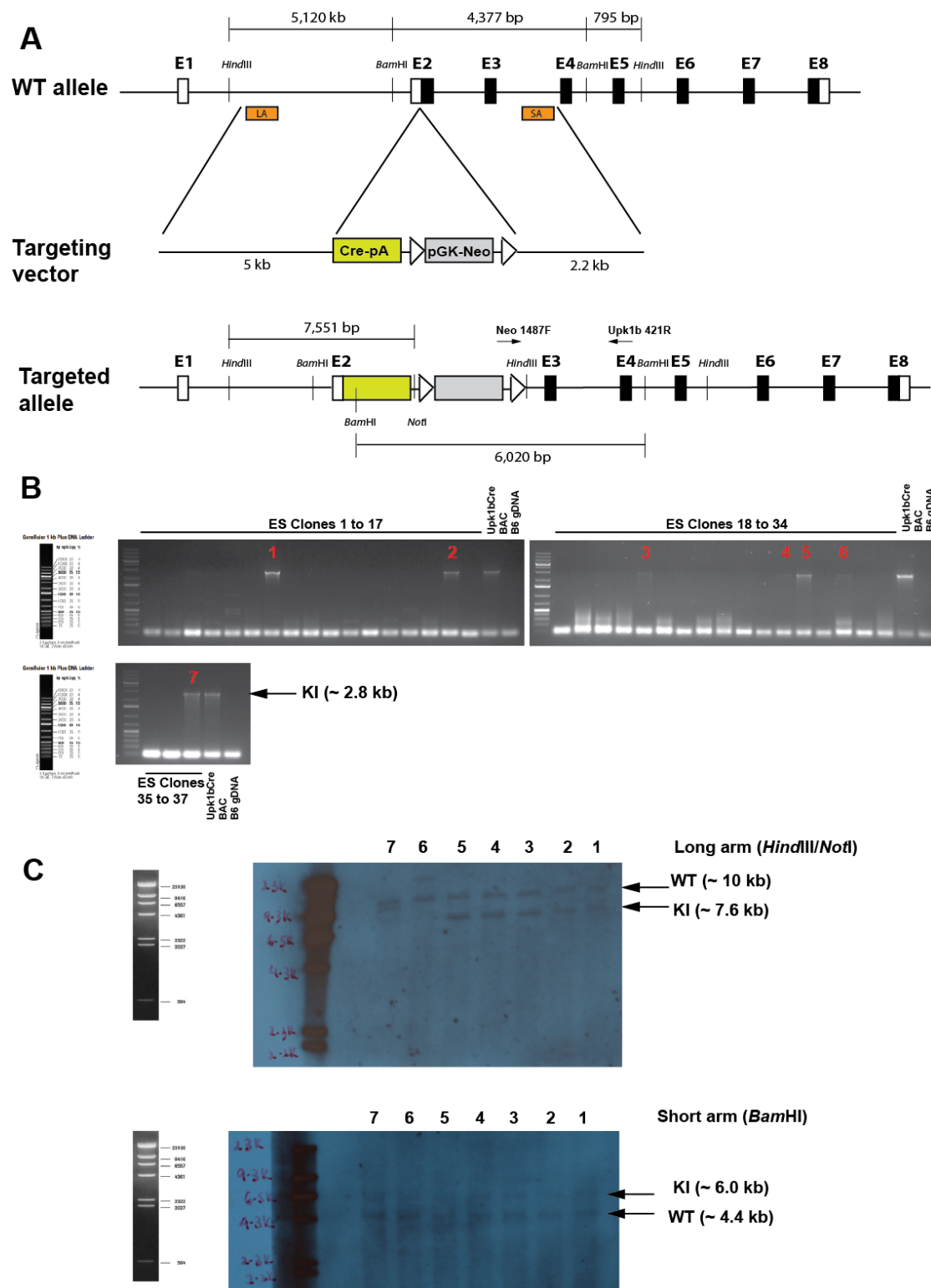


Figure 9. Generation of knock-in Upk1b-cre mice.

The Upk1b-cre targeting vector, where the Cre recombinase gene flanked by Upk1b homology arms, was generated via homologous recombination. It was electroporated into (A) JM8 and Bruce4 ES cells, and correctly targeted clones were identified by (B) PCR and (C) Southern blotting. Black boxes represented coding DNA sequence while white boxes represented non-coding DNA sequence. The orange box labelled LA and SA denoted the relative location of the DIG-labelled probes used in Southern blotting, while the 2 arrows (Neo 1428F and Upk1b 421R) represented the primers used to screen correctly targeted ES clones and founder mice.

3.1.3. Low expression of YFP protein in DCs but not in microglia of Upk1b-cre:Rosa-YFP mice

We analysed the brain, blood, BM and spleen from both founder strains to detect for fluorescence from yellow fluorescence protein (YFP). No YFP signal was detected in D5 founder (Data not shown), thus we focused our analysis on F5' founders. In the blood, the immune cells expressed low levels of YFP fluorescence with B cells and pDCs having the highest recombination levels at about 0.3% (**Figure 10A and 10C**). In the spleen, the cDC subsets were tagged at between 0.1% to 0.2% (**Figure 9B and 9C**). Interestingly, the YFP fluorescence in ESAM⁺CD11b⁺ DC (0.2%) was higher than the ESAM⁻CD11b⁺ DC (**Figure 9C**). The low recombination could be due to incomplete labelling at the progenitor level due to the low level of Upk1b mRNA expression (**Figure 8A and 8B**). Hence we examined the level of YFP fluorescence in the DC-restricted progenitors in the BM. The recombination at the CDPs were low as < 1% of the CDPs were tagged (**Figure 11**). Recently committed pre-cDC populations were identified (Grajales-Reyes et al. 2015; Schlitzer et al. 2015b), and we examined the tagging level at subset level. Low level of recombination between 0.1% to 1.5% was observed across all the pre-cDC populations (**Figure 11**). However, the Siglec-H⁺Ly6C⁻ pre-cDC population expressed the highest level of YFP expression (1.5%) among the different DC-restricted

progenitors (**Figure 11**). This population was demonstrated to differentiate mainly to pDC and both cDC subsets (Schlitzer et al. 2015b), which might explained why we observed tagging in pDCs in the blood and spleen (**Figure 10C**). In contrary, the microglia showed higher level of recombination (~80%) as compared to the DC progenitors and subsets (**Figure 21A**). Thus, this eliminated the possibility of either absence of Cre gene expression or production of a non-functional Cre protein (**Figure 12A**). Among the immune cells in the brain, only microglia was observed to express YFP fluorescence (**Figure 12B**).

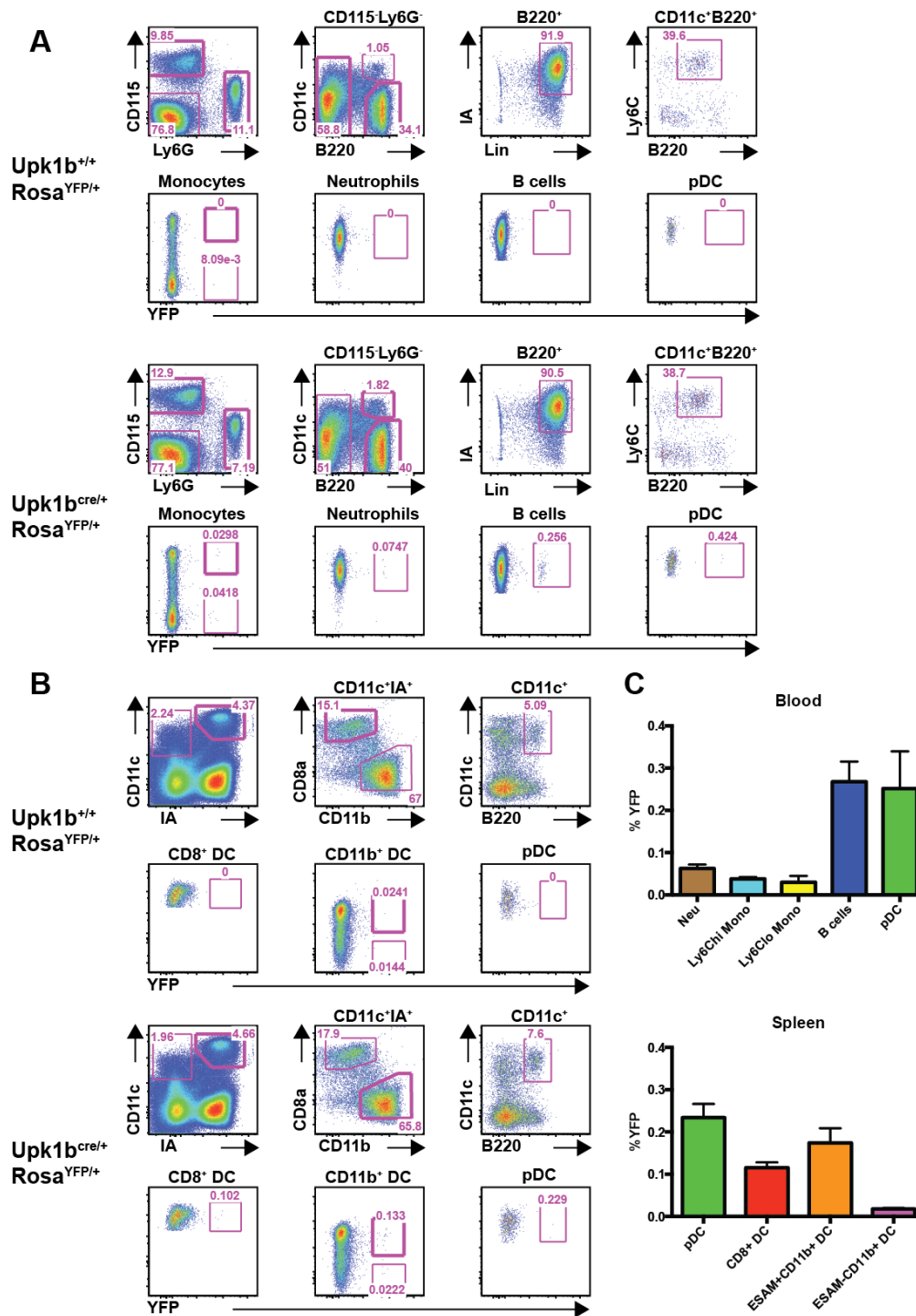


Figure 10. Low YFP fluorescence was detected in splenic DCs from the Upk1b-cre fate mapping model.

Upk1b-cre mice were crossed with Rosa-LSL-YFP reporter mouse to generate Upk1b-cre:Rosa-YFP. Upon induction of Upk1b gene in the cell, Cre protein would be expressed resulting in the excision of the stop codon preceding the YFP gene. This leads to YFP expression. We analysed the (A) blood and (B) spleen and observed low recombination in the splenic

DC compartment. (C) The level of recombinant was less than 1% as determined by the percentage of YFP⁺ cells. *n* = 4 mice and representative plots were shown. The error bar represented SEM.

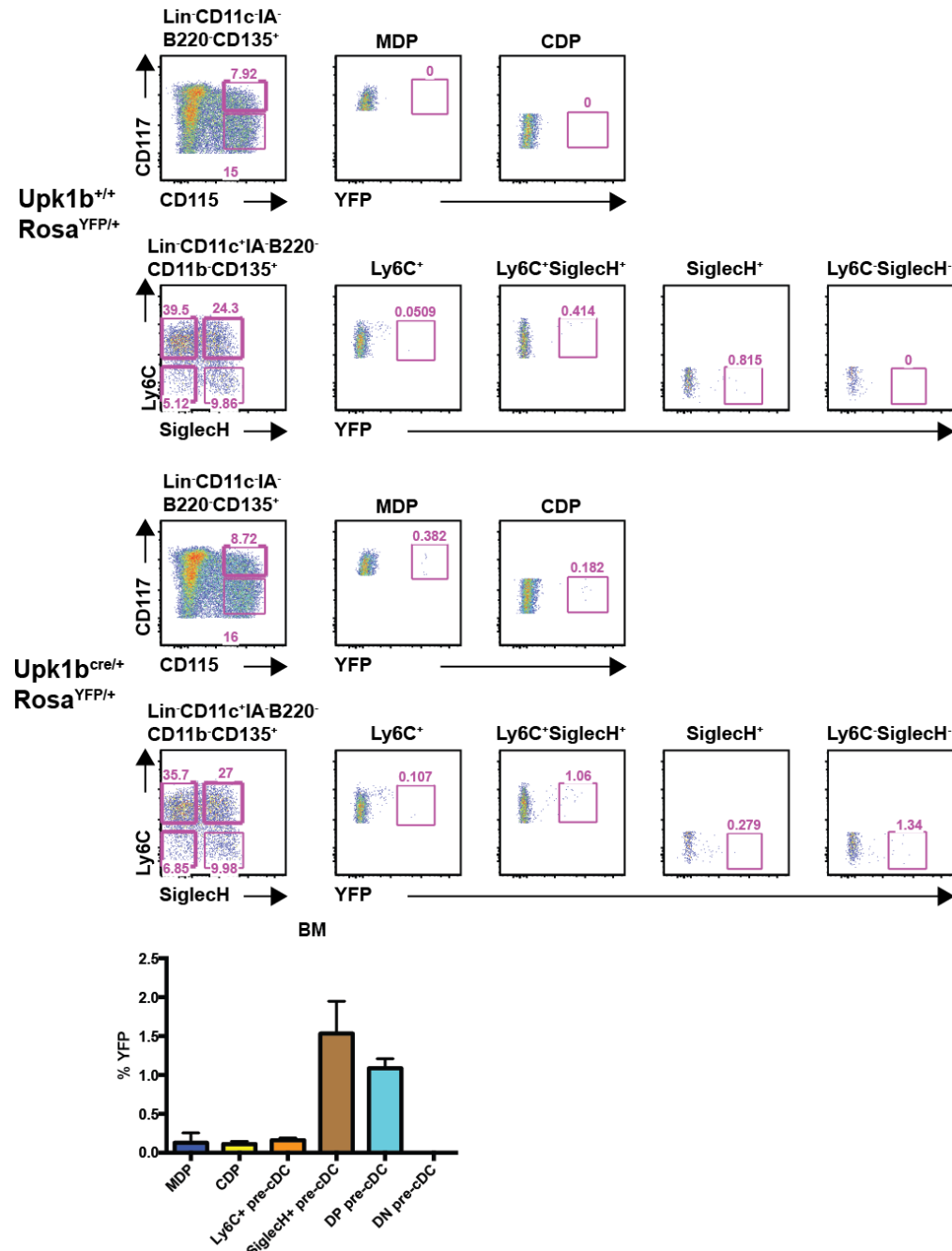
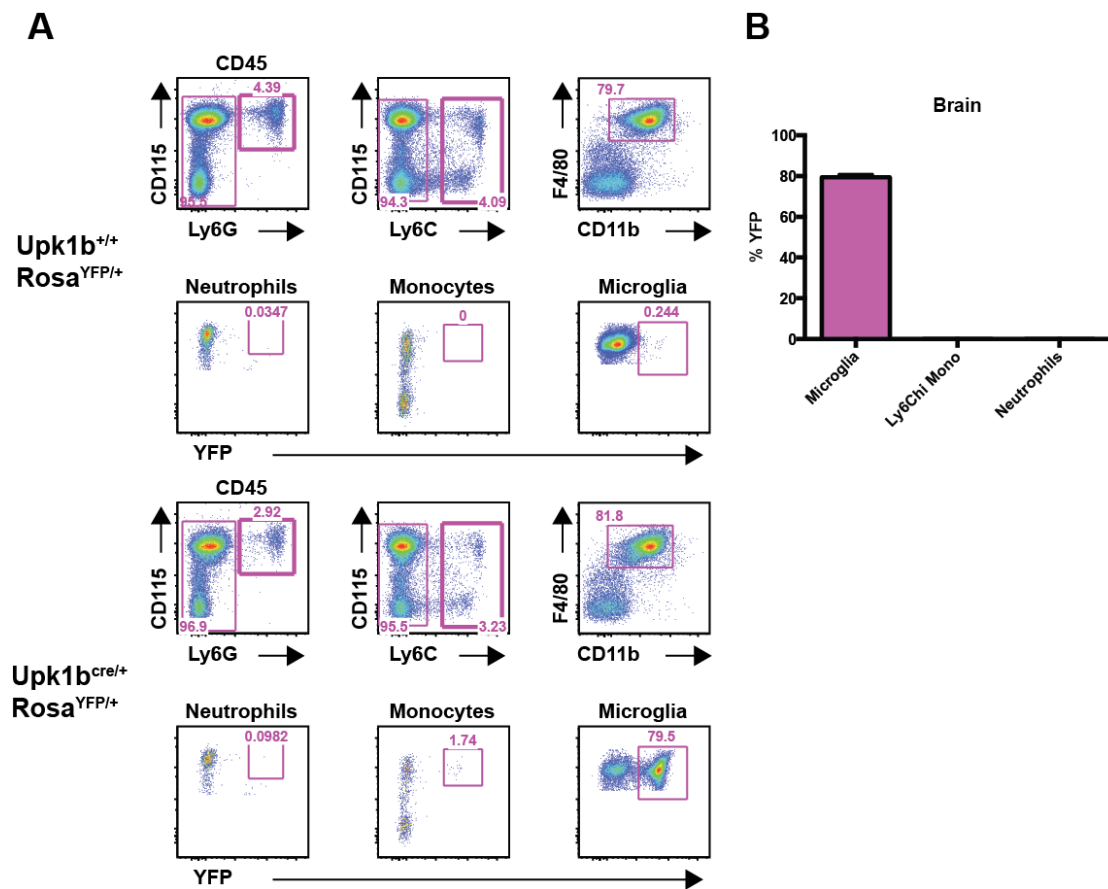


Figure 11. Low expression of YFP fluorescence in DC progenitors

In the BM compartment, low recombination was observed in MDP and CDP. The pre-cDC population was divided into 4 populations based on Ly6C and Siglec-H expression. Low recombination was also observed in all

4 pre-cDC populations. $n = 4$ mice and representative plots were shown. The error bar represented SEM.



(A) In the brain, YFP fluorescence was only detected in the microglia and not other immune cells. (B) The level of recombinant was around 80% as determined by the percentage of YFP⁺ cells. $n = 4$ mice and representative plots were shown. The error bar represented SEM.

3.1.4. Discussion

Lineage restricted reporter mice are widely used to map populations of distinct origins (Kretzschmar and Watt 2012; Jensen and Dymecki 2014). Reporter genes such as fluorescence proteins can be placed under a lineage-restricted promoter or it could be based on *Cre-loxP* technology. In this system, inducible reporter genes are placed under the control of constitutively promoters such as *Rosa26* locus. However, the reporter gene is flanked by a *loxP-STOP* cassette. Hence its expression is induced only after Cre recombinase (Cre) mediated excision of the stop codon. Such labelling is irreversible and is not affected by fluctuations in gene expression (Kretzschmar and Watt 2012). Regardless of which approach, the selected marker must faithfully mimic endogenous gene expression (On and Jung 2010; Kretzschmar and Watt 2012; Vorhagen et al. 2015).

Currently, there are limited mice models available to study the ontogeny of DCs. One model uses *Zbtb46*, a zinc finger BTB domain containing transcription factor, where green fluorescence protein (GFP) is placed under the control of *Zbtb46* promoter to trace the development of cDCs (Meredith et al. 2012a; Satpathy et al. 2012a). *Zbtb46* is expressed in pre-cDC and both cDC subsets but not in pDCs and monocytes. However, non-immune cells like endothelial cells, as well as monocytes stimulated with GM-CSF and IL-4 also expressed it (Satpathy et al. 2012a). *Zbtb46* is dispensable for cDC development as it is down regulated after DC stimulation (Satpathy et al. 2012a). Rather than control DC development, it may reinforce DC specific transcriptional program and suppress DC activation (Satpathy et al. 2012a; Meredith et al. 2012b). Hence, this marker may not be an indicator of cell ontogeny but of phenotype and function (Poltorak and Schraml 2015).

In another model, the Cre recombinase gene was placed under the promoter of DNGR-1 (Schraml et al. 2013). DNGR-1 is expressed at CDP, pre-cDC and cDC1 subset and at low levels in pDC. In this

model, the level of recombination in cDC2 is incomplete and uneven. In cDC1, the recombination is close to 100% as DNMF-1 expression is maintained in the mature cells, whereas in cDC2 subset, the level varies from 20% to 60% depending on the tissue analysed (Schlitzer and Ginhoux 2013). This could be due to incomplete labelling at the progenitors level (Schraml et al. 2013), but could also indicate a contribution from DNMF-1⁻ CDPs (Schlitzer and Ginhoux 2013; Schlitzer et al. 2015b).

Both models were useful in aiding the classification of myeloid cells with unclear origin and identify. For instance, DNMF-1 cre:Rosa-YFP and *Zbtb46* GFP reporter mice were infected with *Listeria monocytogenes* and the inflammatory monocyte-derived cells that appeared, were not labelled with YFP or GFP (Satpathy et al. 2012a; Schraml et al. 2013). Thus this indicated that these cells did not derive from CDP or the gene expression of DNMF1 or *Zbtb46* could be regulated during inflammation. Monocyte-derived cells share many similar phenotypic markers and functions as cDC (Schlitzer et al. 2015a). Hence, it is important to develop a genetic lineage fate mapping model specifically for DC. Here, we identified Upk1b, a tetraspanin molecule, as uniquely expressed in CDP and pre-cDC but not in MDP, monocytes and DC subsets (**Figure 8A**). Physiologically, this molecule is highly expressed in bladder tissue as it plays a role in maintaining bladder permeability (Wu et al. 1994; Yu et al. 1994). Interestingly, their levels are upregulated in tissues and blood of patients with transitional cell carcinoma (Yuasa et al. 1998; Olsburgh et al. 2003), suggesting their potential role as a cancer biomarker. Besides the bladder, it was documented to be expressed on the ocular surface epithelium (Adachi et al. 2000; Kinoshita et al. 2001). However, we also identified that it is expressed in microglia (Appendix C). It is unclear what roles Upk1b might play in DCs and microglia as knockout of Upk1b gene did not affect DC development (**Figure 8D**). Tetraspanin molecules are known to regulate cell morphology, motility, invasion, fusion and

immune signalling (Hemler 2005; Levy and Shoham 2005). Upk1b belongs to the same tetraspanin family as CD9, CD63, CD81 and CD151 (DeSalle et al. 2014). Some of these molecules have a role in immunity. For instance, CD9 and CD81 are found on the surfaces of T and B cells and mediate their activation and adherence (Tarrant et al. 2003; Levy and Shoham 2005). Hence, Upk1b may have a unique role in DC or microglial development and function.

We generated knock-in Upk1b-cre mice where the Cre recombinase gene was inserted after the start codon of Upk1b gene, thereby disrupting the endogenous gene (**Figure 9A**). Upk1b-cre mice were crossed with Rosa26-LSL-YFP reporter mice to generate Upk1b-cre:Rosa-YFP mice. Although we observed low recombination levels in CDPs, pre-cDCs and splenic DCs (**Figure 10C and 11**), but recombination in microglia was around 80% (**Figure 12B**). This suggested that functional Cre protein was produced. To induce a strong expression of Cre recombinase, the Cre recombinase gene should be placed under a constitutive active promoter (Kretzschmar and Watt 2012). Upk1b may not be constitutively expressed during DC development or could be expressed at low levels, resulting in low levels of Cre protein synthesis. Moreover, DC precursors are actively dividing (Onai et al. 2007; Liu et al. 2009) and there could be a lag time between Cre protein synthesis and DNA recombination. Hence, crossing the strain to homozygous may improve the recombination levels.

Alternatively, we could have chosen an inducible genetic fate mapping approach instead. The Cre recombinase gene is fused to an mutated oestrogen receptor (ER) ligand-binding domain (LBD), rendering it responsive to the synthetic ligand 4-hydroxytamoxifen (4-OHT) (Jensen and Dymecki 2014). Upon administration of 4-OHT, ER-LBD undergoes a conformational change, enters the nucleus and frees the Cre recombinase protein, thereby mediating site-specific recombination (Joyner and Zervas 2006). This approach is

widely used for cells with low gene expression to ensure a more robust tagging (Joyner and Zervas 2006)

Upk1b is conserved across species (DeSalle et al. 2014) and could be a potential marker to identify human DC-restricted progenitors. Currently, there is no suitable anti-human Upk1b antibody for flow cytometry. We have recently cloned and expressed the extracellular loops of Upk1b protein, which can be used to generate antibodies using phage display technology (Chan et al. 2014).

3.2. Identification and characterisation of human pre-cDC

3.2.1. Identification of human pre-cDC in cord blood, bone marrow and peripheral blood

We analysed cord blood, bone marrow and peripheral blood to identify human pre-cDC through exclusion of CD34⁺ HSCs, terminally differentiated lymphoid cells based on CD3, CD19 and CD20 expression, and monocytes based on CD14 and CD16 expression. Within the Lin⁻CD123⁺HLA-DR⁺ fraction that included mostly DCs, we excluded pDCs, which were defined as CD45RA⁺CD33⁻. From the remaining cells, we identified a minor CD45RA⁺CD123⁺ fraction and a major CD45RA^{+/}-CD123⁻ fraction. cDC1 and cDC2 subsets were contained within the major CD45RA^{+/}-CD123⁻ population (**Figure 13A**). The minor CD45RA⁺CD123⁺ population was positive for the markers CD2, Siglec-3 (CD33), CX3C chemokine receptor 1 (CX3CR1), Siglec-1 (CD169), CD303, FLT3 (CD135) and showed intermediate expression of CD11c and CD141 (**Figure 13B**). Interestingly, it shared similar markers with both cDCs and pDC. Back gating of this population showed that it falls close to the pDC fraction and appeared homologous to the recent population of pre-cDC described by Breton *et al.* (Breton *et al.* 2015). Hence, we named it pre-cDC (cyan population in **Figure 13**).

To test the differentiation potential of the newly identified population, we sorted pre-cDC, pDC and cDC subsets from the peripheral blood and cultured them in MS5 stromal culture supplemented with Flt3L, SCF and GM-CSF for 5 days. This stromal culture system supported the clonal analysis of DC progenitors (Lee *et al.* 2015a). Cells were analysed for cDC progenies on day 5. pDCs were not observed to differentiate into cDC subsets in this culture system (**Figure 14A**). There was a small population of cDC2 in the cDC1 fraction, however this could be a small fraction of cDC1 subset that expressed both

CD141 and CD1c. The pre-cDC population differentiated into both cDC subsets, with the majority being cDC2. (**Figure 14B**).

Recently, Breton *et al.* identified a similar human pre-cDCs in the cord blood and peripheral blood. However, their population appeared to be a rarity in adult peripheral blood. We compared both populations and observed that they shared similar phenotype (**Figure 15A&B**). However, the population defined by Breton *et al.*, was strictly negative for CD303 and CD141 expression and expressed higher levels of CD117 (**Figure 15A**). In contrary, our population was intermediate for CD303 and CD141, and expressed intermediate to low levels of CD117 (**Figure 15B**). Quantification of both pre-cDC populations showed that there was a 10-fold difference in terms of percentage of these cells (**Figure 15C**). In fact, most of the pre-cDCs were lost in the Breton *et al* strategy by the tight CD141 gate, as CD141 expression could be acquired upon pre-cDC maturation. Thus, this could suggest that their populations of pre-cDCs could be early pre-cDCs, while our population could comprise of both early pre-cDCs and committed pre-cDCs.

Seminal papers about pDCs have demonstrated that they were capable of differentiating into cells with cDC-like morphology in the presence of IL-3 and CD40 ligand (CD40L) (Grouard *et al.* 1997; Cella *et al.* 1999). We postulated that these pDCs, defined as either CD11c⁻CD4⁺ or ILT3⁺ILT1⁻, could contain a small population of contaminating pre-cDCs, as pre-cDCs largely overlap in phenotype with pDCs. We further characterised the pDC fraction and observed as expected that both populations contained a small pool of pre-cDCs (**Figure 16**). Interestingly, ILT3⁺ILT1⁻ pDCs were contaminated with a small population of cDC2 subset (**Figure 16**).

markers with pDC and DC subsets. Fluorescence-minus-one (FMO) control is indicated as grey. Representative plots were shown.

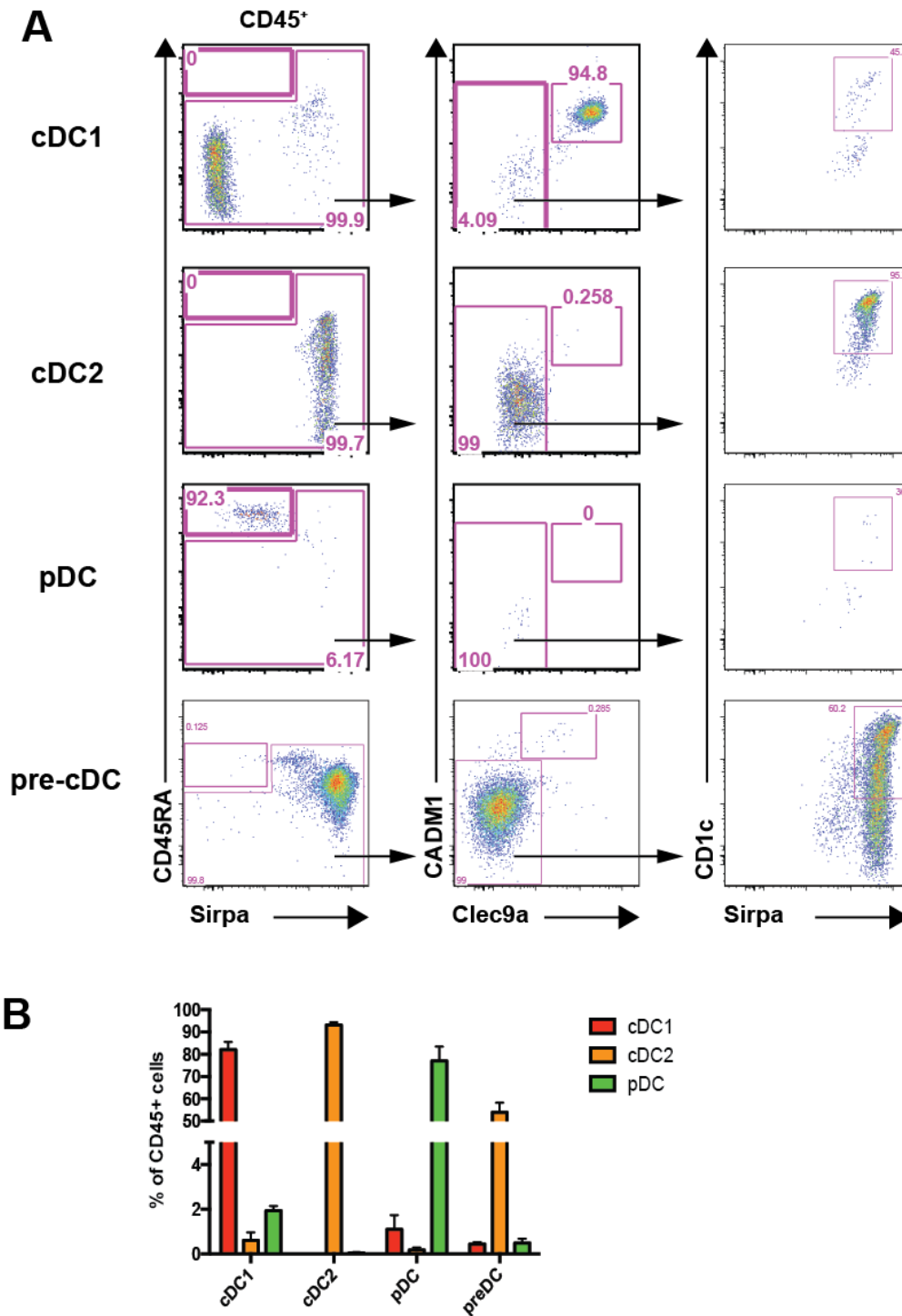


Figure 14. Pre-cDC is able to differentiate into cDC1 and cDC2 subsets.

Pure populations of pre-cDC and DC subsets were isolated from the peripheral blood and cultured on MS5 medium supplemented with Flt3L,

SCF and GM-CSF for 5 days. (A) Pre-cDC was capable of differentiating into both cDC1 and cDC2 subsets. (B) Proportion of DC subsets obtained from the *in vitro* differentiation assay (n=3). Representative plots were shown.

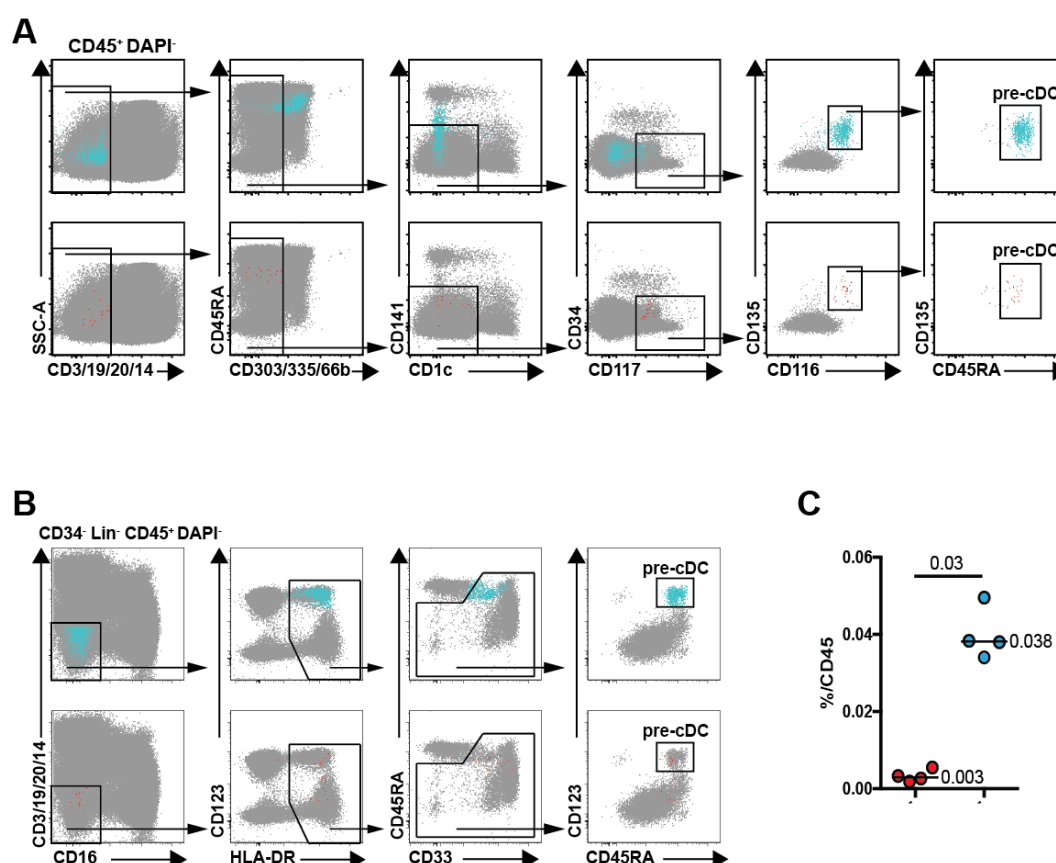


Figure 15. Comparison of pre-cDC population.

Pre-cDC was identified as described in Breton *et al.* (red) and according to our strategy (cyan). (A) Gating strategy as defined in Breton *et al.* (B) Gating strategy as described in Figure 13. (C) Percentage of pre-cDC among CD45⁺ cells defined using both gating strategies (n=4). Representative plots were shown. The error bars indicated SEM.

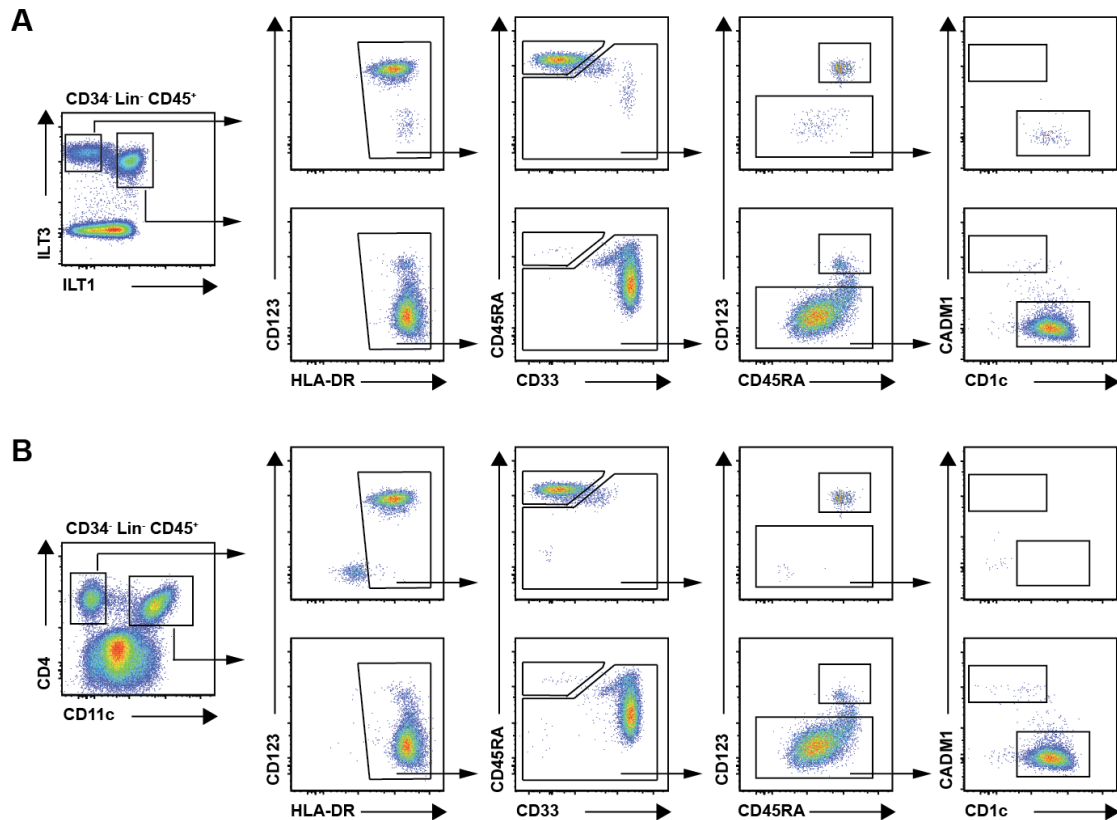


Figure 16. Characterisation of pDCs and pre-cDC using initial markers defining pDCs.

pDCs can be identified based on differential expression of either $ILT3$ and $ILT1$ or $CD4$ and $CD11c$. Both populations were demonstrated to differentiate into DC-like morphology in the presence of $IL-3$ and $CD40L$. We further characterised both pDC populations to determine if they were pure populations. (A) $ILT3^+ILT1^-$ pDCs and (B) $CD4^+CD11c^-$ pDCs are a heterogeneous population consisting of pDCs and pre-cDCs. $ILT3^+ILT1^-$ pDCs were also contaminated with a small population of cDC2 subset. Phenotyping was performed on blood from two different donors and representative plots were shown.

3.2.2. Identification of committed pre-DC subsets in peripheral blood

Recently our group has shown that in murine bone marrow, pre-cDCs are a heterogeneous population, and we identified pre-cDC1 and pre-cDC2 progenitors within the bulk pre-cDC population (Schlitzer et al. 2015b). We postulated that human pre-cDC population could be heterogeneous, and further interrogated the

bulk pre-DC population in the peripheral blood. Fully developed cDC subsets do not express CD45RA (Breton et al. 2015) (**Figure 13B**). Also, bulk pre-cDC was shown to express CD141 (**Figure 13B**), making it unsuitable to identify cDC1 subset. Instead, we used CADM1 to identify cDC1 subset. We postulated that the committed pre-cDC2 population would express low levels of CD1c, while early, uncommitted pre-cDC population would retain expression of CD123 (**Figure 13B**). Therefore, we refined our strategy and identified 3 novel populations of pre-cDC in the peripheral blood (**Figure 17A**). These populations were also observed in the spleen (**Figure 17A**) at a higher proportion as compared to the blood (**Figure 17B**), suggesting that circulating committed pre-cDCs, and not blood DCs, could seed the tissue and complete their differentiation in the tissues.

To substantiate our findings, we sorted pure populations of early pre-cDC and committed pre-cDC subsets from the peripheral blood and cultured them in MS5 stromal culture supplemented with Flt3L, SCF and GM-CSF for 5 days. None of the populations were capable of producing pDCs. Early pre-cDCs contained potential to differentiate to both cDC subsets while pre-cDC1 and pre-cDC2 differentiated exclusively into cDC1 and cDC2 subset, respectively (**Figure 17C**). As observed in the *in vitro* differentiation of bulk pre-cDC, majority of the differentiated cells were cDC2 subset (**Figure 17C**).

3.2.3. Gene expression analysis of pre-DC subsets

We sorted DC subsets and pre-cDC populations from peripheral blood and performed microarray analysis to determine their whole transcriptomics expression profile. The populations were clustered using hierarchical clustering. pDCs were grouped separately from the pre-cDCs and cDC subsets. Early pre-DCs were clustered together with committed pre-cDCs and cDC subsets, and the respective committed pre-cDCs clustered with its cDC subset (**Figure 18A**). Principal component analysis was also performed and

4 main clusters were identified from PC1 to PC3 (**Figure 18B**). pDCs (green) were clustered separately from pre-cDCs and DC populations (brown), while early pre-cDC (cyan), pre-cDC1/cDC1 (red) and pre-cDC2/cDC2 (orange) were individually grouped (**Figure 18B**). We measured the proportion of variance and approximately 40% of the cells in the first dimension of the PCA could be attributed to pDC (**Appendix D**).

Next, we compared the different populations to determine differentially expressed genes across cDC development (i.e. early pre-cDC to pre-cDC1 to cDC1 and early pre-cDC to pre-cDC2 to cDC2) (**Figure 18C**). CLEC4C (CD303), IL-3Ra (CD123) and LILRA4 (ILT7) were down regulated, while BTLA was upregulated when early pre-cDCs transited into committed pre-cDCs (**Figure 18C**). CADM1 and Clec9a were upregulated as the early pre-cDC commit towards cDC1 lineage, while CD1c was upregulated as early pre-cDC commit towards cDC2 lineage (**Figure 18C**). Transcription factor dependency is often used to define DC lineage. As early pre-cDC commits towards cDC1 lineage, we observed an increased in ID2, IRF8 and BATF3 expression, and a decreased in IRF4 expression (**Figure 18D**). However, the trend for cDC2 commitment was not as clear. Generally, we observed a decline in IRF8 and lower levels of ID2 and BATF3 while KLF4 expression was slightly higher (**Figure 18D**)

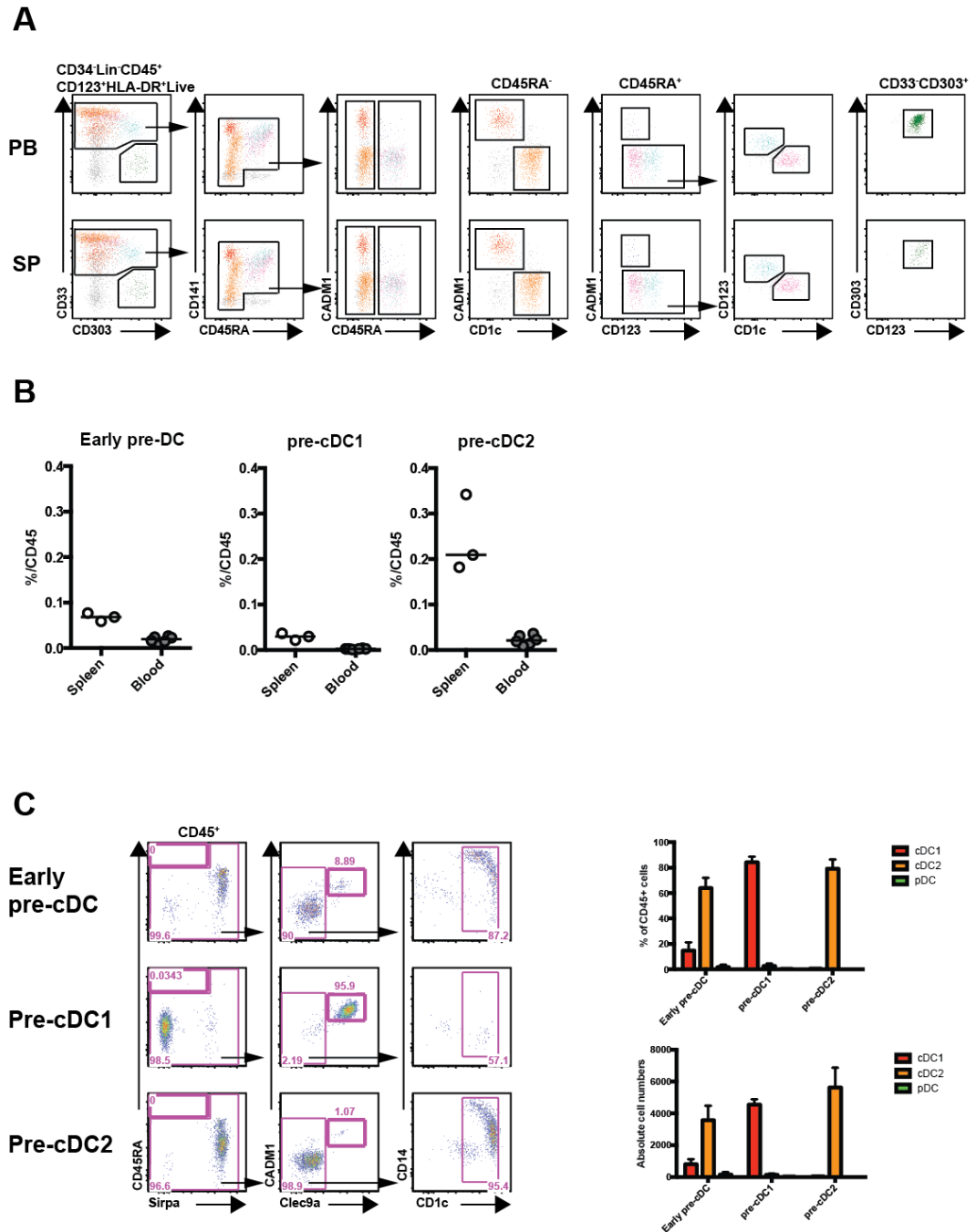


Figure 17. Identification of committed pre-cDC populations.

(A) Early and committed pre-cDCs subsets were identified in peripheral blood and spleen using a refined gating strategy in flow cytometry. (B) Proportion among CD45⁺ cells in spleen (n=3) or blood (n=6) of the pre-cDC subsets. (C) Early pre-cDC differentiated in vitro to both cDC subsets, while committed pre-cDCs differentiated in vitro to either lineage. (C) The absolute numbers and percentage of CD45⁺ cells obtained from the in vitro differentiation culture were calculated (n=3). Representative plots were shown. The error bars indicated SEM. (Green – pDC, Cyan – Early pre-

cDC, Purple – pre-cDC1, Red – cDC1, Dark pink – pre-cDC2, Orange – cDC2.)

We also confirmed some of the gene expression phenotypically using flow cytometry (**Figure 19**). As observed in the gene expression profiling, we observed a reduction in CD303, CD123 and ILT7 protein expression as the pre-cDCs commit towards DC lineage, and an increased in BTLA protein expression at the cDC1 lineage (**Figure 19**). Early pre-cDC was the only population that expressed CD169 (**Figure 19**). CXC chemokine receptor 3 (CXCR3), SLAM family member 7 (CD319) and Clec9a were either maintained or induced as early pre-cDCs differentiate into cDC1 subset (**Figure 19**). CD2, Siglec-6 (CD327) and Fc- ϵ receptor1 (Fc ϵ R1) were maintained as early pre-cDCs progressed towards cDC2 lineage but these markers were lost in cells committed towards cDC1 lineage (**Figure 19**). CD11c expression was also upregulated in cells committed towards cDC2 lineage (**Figure 19**). The pre-cDC populations also expressed low levels of CD80 and CD83 (**Figure 19**), suggesting that these cells were not mature, activated blood DCs.

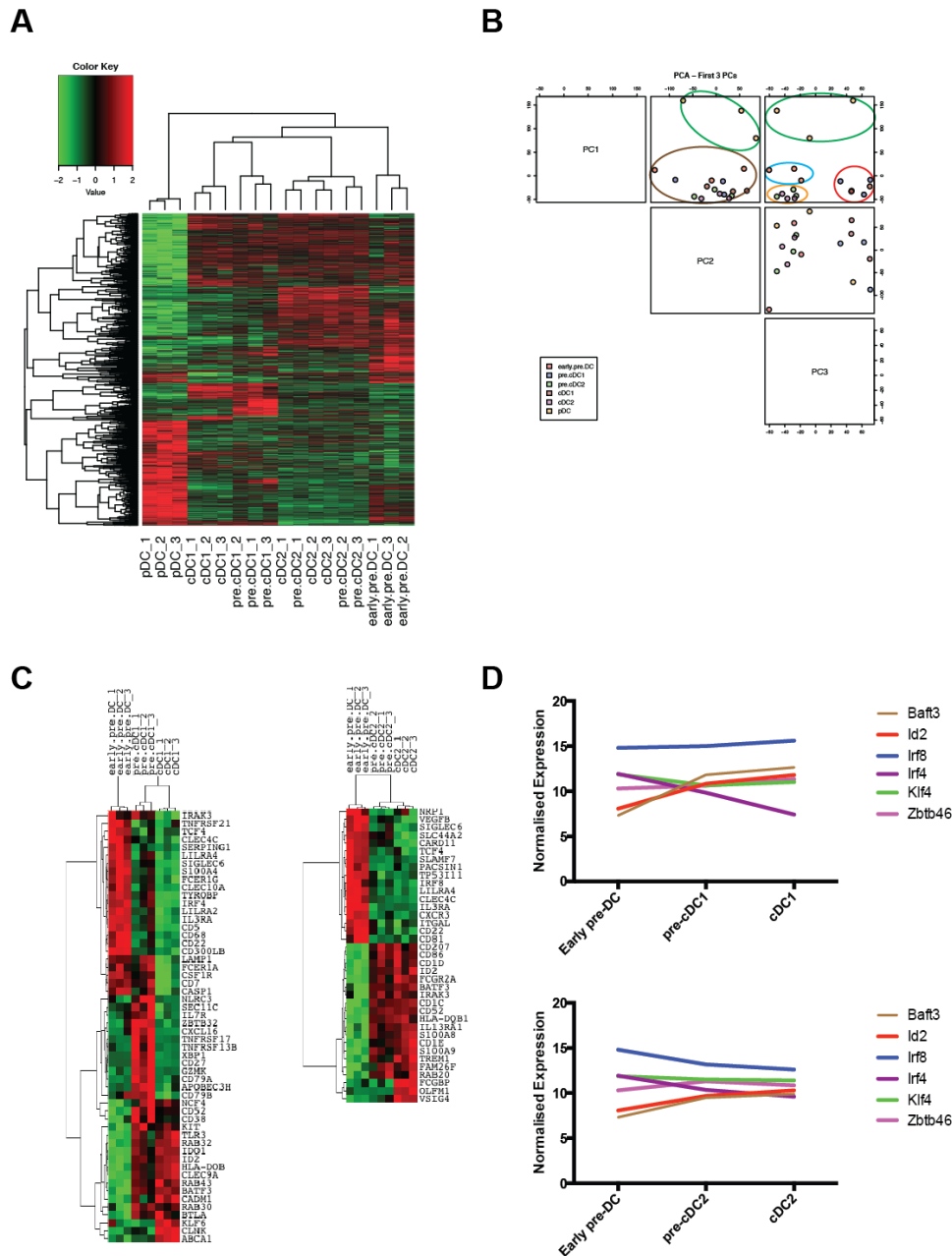


Figure 18. Microarray analysis of pre-cDC populations.

Pure populations of pre-cDCs and DCs were sorted from 3 different blood donors and microarray analysis was performed. (A) The populations were grouped together by hierarchical clustering. pDC was clustered separately from the DCs. Early pre-cDCs were clustered with committed pre-cDCs and their respective cDC subsets. (B) PCA analysis of the sorted populations. (C) List of differentially expressed genes during the commitment of early pre-cDC towards either cDC1 or cDC2 lineage. (D) Relative expression of known transcription factors that influence DC lineage. (Green – pDC; Brown – Mixture of pre-cDC and cDC; Cyan – pre-

cDC; Orange – Mixture of pre-cDC2/cDC2; Red – Mixture of pre-cDC1/cDC1.)

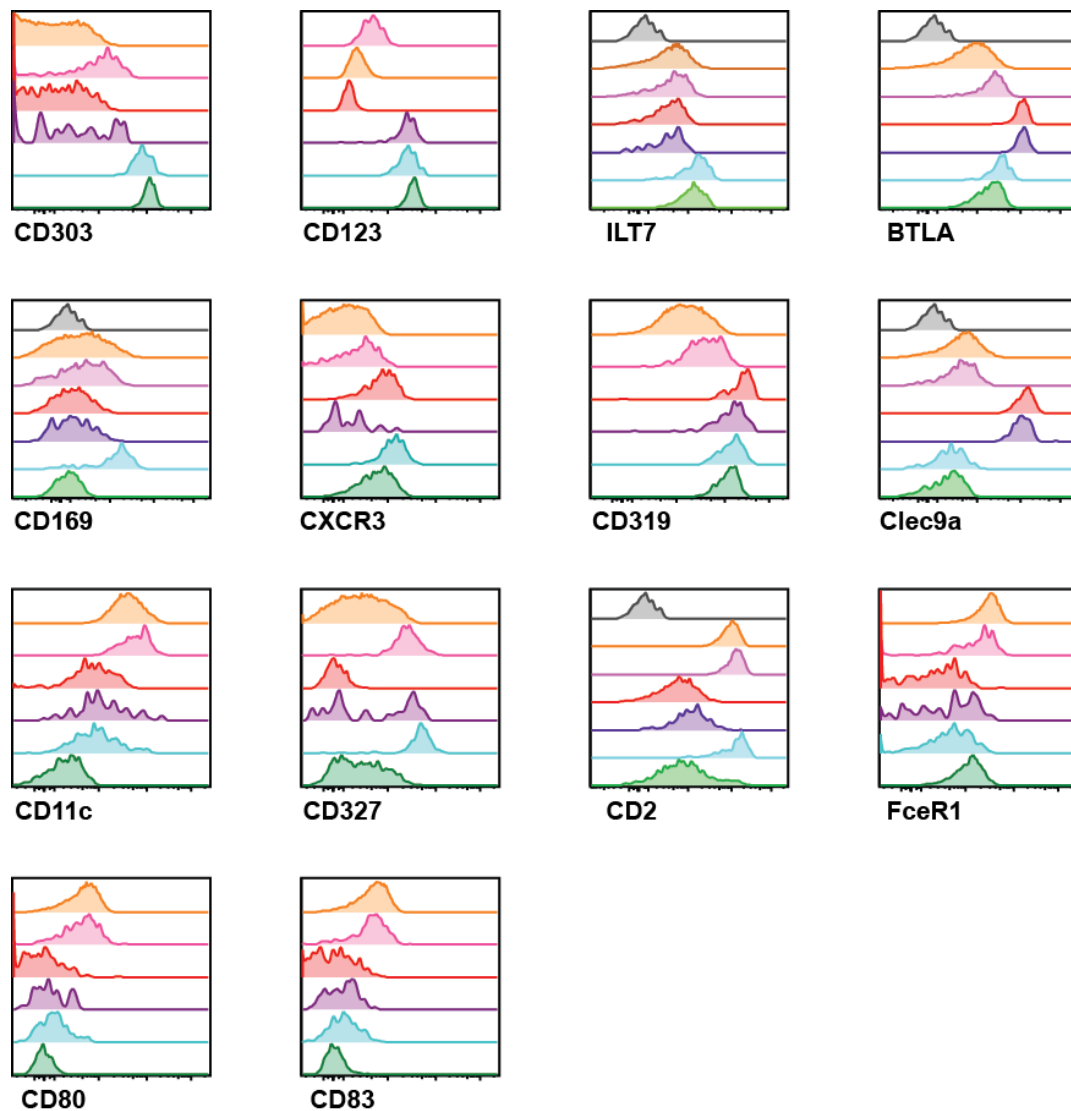


Figure 19. Phenotypic characterisation of pre-cDC and DC populations.

Pre-cDC and DC populations were characterised phenotypically with flow cytometry. CD303, CD123, ILT7 and CD169 were progressively lost as early pre-cDC differentiated into cDCs. CXCR3, CD319 and Clec9a were upregulated in cDC1 lineage but not in cDC2 lineage. CD327, CD2 and FcεR1 were upregulated in cDC2 lineage but not cDC1 lineage. CD80 and CD83 expression were relatively lower in the pre-cDC subsets as compared to the fully differentiated cDC subsets. (Green – pDC, Cyan –

Early pre-cDC, Purple – pre-cDC1, Red – cDC1, Dark pink – pre-cDC2, Orange – cDC2, FMO - grey). (n=2) Representative plots were shown.

3.2.4. Functional analysis of pre-DCs

Seminal reports of pDC have shown that pDCs were capable of secreting cytokines such as IFN- α and IL-12p40 upon stimulation with TLR agonists. This led us to question whether the cytokine secretion could be attributed to pre-cDCs present in the sorted pDC populations. We stimulated total PBMC *in vitro* with various TLR agonists for 3 hours. Stimulation of either TLR7/8 (CL097) or TLR9 (CpG ODN2216) resulted in the secretion of copious amount of IFN- α but not IL-12p40 in pure pDC populations. In contrast, early pre-cDC can produce low amounts of IFN- α and large amount of IL-12p40 (**Figure 20A**). Hence, pDCs are bona fide IFN- α producing cells.

pDCs were also shown to be capable of inducing T cell proliferation (Swiecki and Colonna 2015). To eliminate the possibility that the T cell proliferation and polarization was due to contaminating pre-cDCs, we performed allogeneic MLR with peripheral blood pre-cDC populations. We observed that pre-cDC subsets expressed lower levels of co-stimulatory molecules (**Figure 20B**) and they could induce proliferation of naïve CD4. However, pure pDC population was unable to induce proliferation and polarization of naïve T cells (**Figure 20C**).

3.2.5. Flt3L treatment of humanized mice expands DC-restricted progenitors

Flt3L is an important cytokine that regulated the development and survival of DC subsets. We injected humanized mice with 10 μ g of recombinant Flt3L per day for 6 consecutive days and analysed the mice at 12 hours, 2 days and 6 days post-injection. After 12 hours of Flt3L treatment, we observed an increased in proportion of total CD34⁺ HSCs, CDP and pre-cDC populations (**Figure 21A**). After

which, there was a sharp decline in proportion of all progenitors, but their numbers recovered and expanded over the remaining days (**Figure 21A**). Correspondingly in the spleen, there was a slight increase in proportion of circulating pre-cDC subsets, except for pre-cDC1 subset 12 hours post treatment (**Figure 21B**). Their proportion expanded and increased over the remaining days (**Figure 21B**). The proportion of splenic cDC subsets increased over the 6 days of treatment, but cDC2 subset expanded more than cDC1 subset (**Figure 21B**). pDCs in the BM and spleen also increased in proportion over the 6 days (**Figure 21B**).

3.2.6. Pre-cDC and its involvement in pathological diseases

Since pDCs and pre-cDCs are phenotypically similar, we speculated that some of the pDC-mediated diseases such as Systemic Lupus Erythematosus (SLE) could be mediated by pre-cDCs instead of pDCs. The SLE disease activity index (SLEDAI) is used to assess the disease progression of SLE with a high score indicating active disease that required therapy (Yee et al. 2011). The proportion of bulk pre-cDC in the peripheral blood was higher in SLE patients than in control patients ($p < 0.037$) (**Figure 22A**). We analysed the immune cell composition in the blood of SLE patients of varying SLEDAI score and observed a stronger positive correlation between pre-cDC across increasing SLEDAI score ($r = 0.75$, $p = 0.03$), as compared to pDC ($r = 0.48$, $p = 0.23$) (**Figure 22B**).

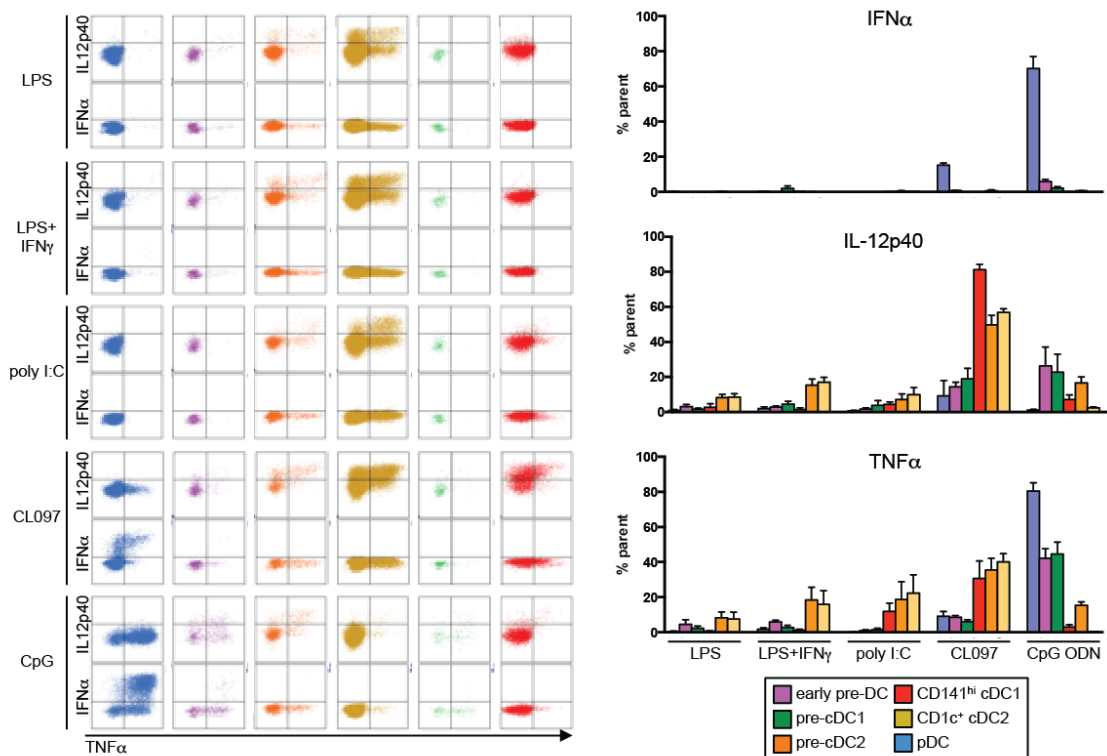
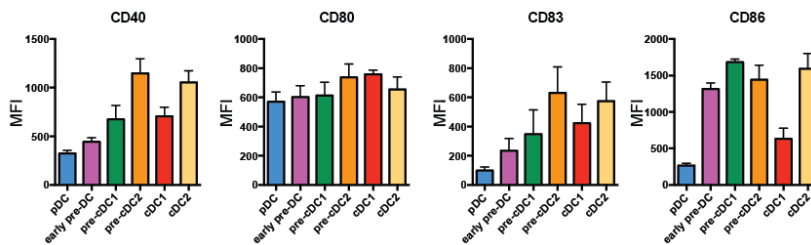
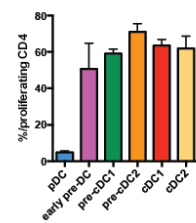
A**B****C**

Figure 20. Cytokine production by pre-cDC.

(A) Cytokine production by pre-DC and DC subsets upon TLR stimulation were evaluated by intracellular flow cytometry. Left panel showed the dot plots of IFN- α , IL12-p40 and TNF- α production by pDC (blue), early pre-cDC (purple), pre-cDC2 (orange), cDC2 (beige), pre-cDC1 (green) and cDC1 (red). Right panel displayed the mean production of cytokine production by the pre-cDC and DC subsets ($n=4$). (B) Expression level (MFI) of co-stimulatory molecules by blood pre-cDC and DC subsets ($n=4$). (C) Proliferation of naïve CD4⁺ T cells in an allogenic mixed lymphocyte reactions ($n=3$).

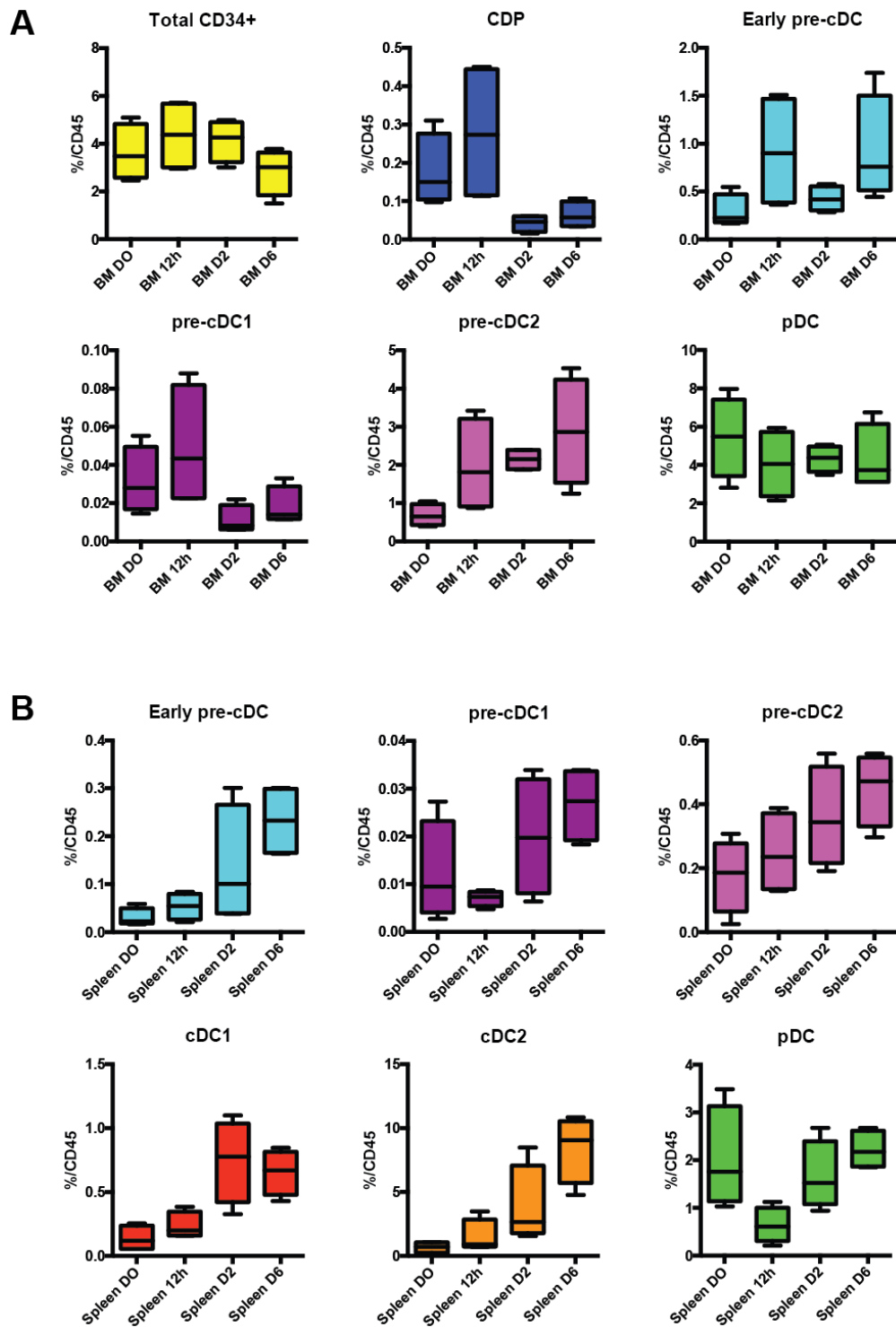


Figure 21. *Flt3L* expands the pre-cDC populations.

Humanized mice were injected with *Flt3L* over a course of 6 days and the BM and spleen were analysed. (A) DC-restricted progenitors in the BM expanded in proportion within 12 hours of *Flt3L* treatment, after which, there was a collapse in the system. However, the proportion of progenitors

recovered and increased over the remaining days of treatment. **(B)** Circulating pre-cDC as well as cDC subsets increased in proportion over the 6 days treatment. $n = 4$ mice and representative plots were shown. The error bar represented SEM.

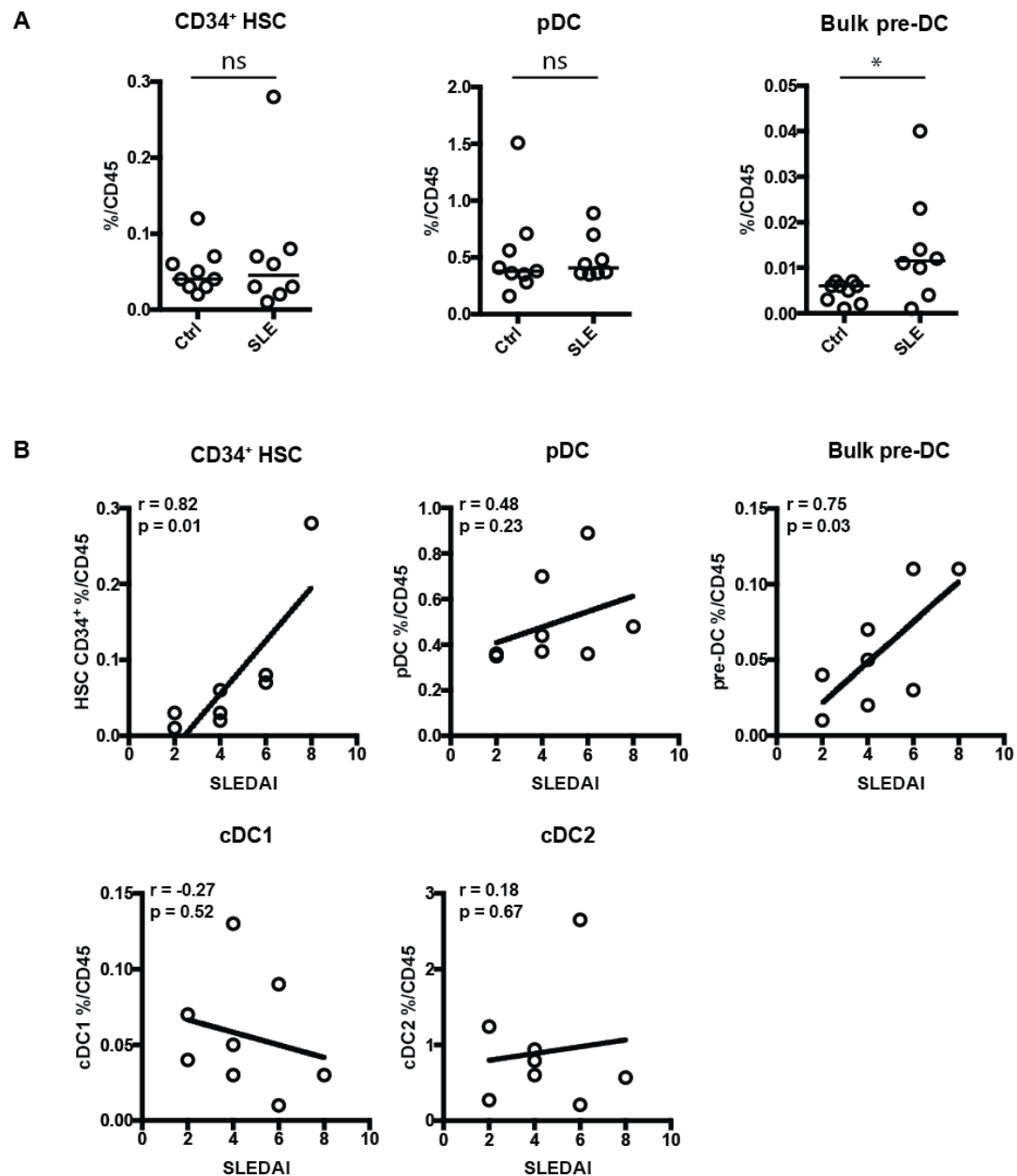


Figure 22. Bulk pre-cDC showed a positive correlation with SLEDAI score.

(A) Percentage of circulating CD34⁺ HSC, pDC and bulk pre-cDC in SLE patients ($n=9$ control; $n=8$ SLE patients). * denoted $p < 0.038$ (B) Correlation

of immune cells in the blood of SLE patients in relation to increasing SLEDAI scores. Mann-Whitney test was used for statistical analysis.

3.2.7. Discussion

The discovery of DC-restricted progenitors has been hampered due to a lack of suitable *in vitro* DC differentiation culture method to assay their potential. Human DCs can be derived *in vitro* from monocytes and CD34⁺ HSCs in the presence of GM-CSF but these cells resembled monocyte-derived DCs (Balan et al. 2014). In mouse, Flt3L is often used for differentiation of DC subsets from BM progenitors (Brasel et al. 2000; Naik et al. 2005), but in human it produced mainly cDCs and little pDCs (Doulatov et al. 2010; Poulin et al. 2010; Proietto et al. 2012). Recently, a stromal culture based differentiation protocol was developed, and it was shown to produce large amounts of both cDCs and pDCs, as well as promote the growth of other immune cells such as monocytes, granulocytes and B cells (Lee et al. 2015a). Unlike their mouse counterparts, the phenotypic expression of key markers used to identify murine DC-restricted progenitors could not be used in the same context to identify their human counterpart. For example, murine pre-cDCs are defined as CD11c⁺MHC II⁻Sirpα^{int}Flt3⁺, but human CD34⁺ cells express HLA-DR early in its development (Griffin et al. 1985). Despite the difficulties involved, two groups recently identified various DC-restricted progenitors in the BM, cord blood and peripheral blood (Breton et al. 2015; Lee et al. 2015b) during the course of this work.

We approached the identification of one of the DC-restricted progenitors, pre-cDC with a different methodology. Human pDC was shown to be heterogeneous as they were demonstrated to differentiate *in vitro* into cDC-like morphology in the presence of IL-3 and CD40L (Grouard et al. 1997; Cella et al. 1999) or monocyte-conditioned medium (O'Doherty et al. 1994). Furthermore, they can be divided into subsets with different function based on CD2

expression (Matsui et al. 2009). Although both subsets can produce IFN- α , CD2^{hi} pDCs produce lysozyme and large amounts of IL-12p40, as well as were better inducers of naïve allogeneic T cell proliferation (Matsui et al. 2009). It was also observed that within the CD123⁺ fraction in peripheral blood, 3 fractions based on CD7 and CD56 expression could be identified (Comeau et al. 2002). CD7⁻CD56⁺ exhibited pDC/cDC intermediate phenotype, produced proinflammatory cytokines, and differentiated into potent APC without stimulation (Comeau et al. 2002). Similarly in the mouse, Siglec-H⁺ pDCs are divided into 2 populations based on CCR9 expression. Both subsets were able to produce type I IFN but CCR9⁻ pDC-like common DC precursor showed DC potential as it was able to give rise to cDC2 subset (Schlitzer et al. 2011; 2012). It was recently clarified that this population was a pre-cDC population as bulk pre-cDC can be divided into 4 populations based on Ly6C and Siglec-H expression (Schlitzer et al. 2015b). Therefore, these data suggested that human pre-cDCs might lie within the pDC fraction as they share common phenotypic markers.

Herein, we identified a population of cells in BM, cord blood and peripheral blood that shared common phenotypic markers such as CD303, CD45RA and CD123 with pDC (**Figure 13A**). Back gating of the novel population showed that it laid close to both pDC and cDC subsets (**Figure 13A**). Unlike pDCs, this population expressed CD11c, CD33, CD2 and CX3CR1 (**Figure 13B**), which resembled the CD2^{hi} pDC (Matsui et al. 2009). We cultured the novel population in MS5 stromal culture supplemented with Flt3L, SCF and GM-CSF to investigate its DC differentiation potential (Lee et al. 2015a), and observed that the population could differentiate into both cDC subsets with some pDC potential (**Figure 14**). Therefore, this indicated that it could be the DC-restricted progenitor pre-cDC.

Our population and the newly defined circulating pre-cDC (Breton et al. 2015) shared similar phenotypic markers (**Figure 15A&B**). In

contrast with their population, our pre-cDCs were not a rarity in peripheral blood (**Figure 15C**). The low number of cells observed by them could be due to the strict use of CD303 and CD141 as lineage markers for pDC and cDC1 subset. Their pre-cDCs were negative with respect to both markers (**Figure 15**). However, we showed that our bulk pre-cDCs do express intermediate levels of both markers (**Figure 13B**). We also further examined the pDC fractions defined as CD4⁺CD11c⁻ or ILT3⁺ILT1⁻. These pDC fractions contained contaminating pre-cDCs, which might explain their differentiation ability as previously reported (**Figure 16**).

We further interrogated the bulk pre-cDC fraction in order to identify committed pre-cDC in the peripheral blood. Since differentiated cDCs do not express CD45RA (Breton et al. 2015), we postulated that committed pre-cDC would retain CD45RA expression. Moreover, bulk pre-cDC was negative for CADM1 and CD1c. Thus we speculated that CADM1 and CD1c expression could possibility marked lineage committed pre-cDCs. Hence, a population that is CD45RA⁺CADM1⁺ or CD45RA⁺CD1c^{low} might represent committed pre-cDC1 and pre-cDC2, respectively. We identified 3 new populations, namely early, uncommitted pre-cDC, committed pre-cDC1 and pre-cDC2 based on our refined gating strategy (**Figure 17A**). We tested their DC potential *in vitro* and observed that early, uncommitted pre-cDCs differentiated into both cDC subsets (**Figure 17C**). Committed pre-cDC1 and pre-cDC2 differentiated into cDC1 and cDC2 subsets, respectively (**Figure 17C**). The bulk of the differentiated cells in the early pre-cDC fraction were cDC2 subset. This could indicate that cDC2 lineage preceded cDC1 lineage. Alternatively, it could also imply that most of the uncommitted early pre-cDC is skewed towards cDC2 lineage and lesser towards pre-cDC1. A time course analysis of the differentiation or single cell colony culture would address this question. We also observed these circulating pre-cDCs in higher proportion in the spleen, suggesting that they, and not blood DCs, seed the tissues and complete their

differentiation in the tissue (**Figure 17B**). However, an *in vivo* transfer of the circulating pre-cDC populations into immunodeficiency mice would better address this question.

We also showed that the circulating pre-cDC populations have different transcriptomics profile (**Figure 18**). Further analysis such as pathway analysis is on going to better appreciate the data. pDCs were demonstrated to produce IFN- α and IL-12p40 in response to influenza virus or LPS stimulation {Cella:2000jj, Grouard:1997vz, Matsui:2009bj}. However, our data suggested that the production of IL-12p40 is due to the presence of contaminated pre-cDCs in the pDC fraction. In agreement with previous published reports, pDCs are still the major IFN- α producing cells (**Figure 20A**). We observed that pre-cDC subsets have a relatively lower level of expression for co-stimulatory molecules, were able to induce proliferation and differentiation of naïve CD4⁺ T cells in allogenic MLRs and can respond to TLR agonist stimulation through the secretion of IFN- α , TNF- α and IL-12p40 (**Figure 20**). Hence, they could potentially play a role in the context of disease, where dysregulation of their differentiation continuum may render them a potent source of inflammatory DC that is ready for rapid recruitment. How the tissue environment affects the role of pre-cDC subsets in inflammatory disease remains to be investigated.

The pre-cDC populations are also responsive to Flt3L treatment. The increase in CD34⁺ HSC and DC-restricted progenitors in the BM (**Figure 21A**) could be due to the local expansion and proliferation of the progenitors, as Flt3L was shown to instruct at the progenitor level (Karsunky et al. 2003). However, after 12 hours of Flt3L, the number of DC-restricted decreased as they would exit the bone marrow and entered circulation. This was reflected in the spleen where we observed an increase in circulating pre-cDCs and cDC subsets from day 2 onwards (**Figure 21B**). The decline in pre-cDC1 in the spleen after 12 hours of Flt3L treatment (**Figure 21B**) could

be due to a more sensitive response to Flt3 signaling, as the mRNA expression of FLT3 was shown to be higher in cDC1 subset than cDC2 subset (Haniffa et al. 2012).

Since pre-cDC share common phenotypic markers with pDC, there is a need to re-examine pDC associated diseases. We observed an increased correlation with the proportion of pre-cDC, but not pDC in the blood of SLE patients (**Figure 23**). We are currently investigating the role of pre-cDC in SLE. Nanostring analysis of the sorted pre-cDC and DC subsets would give a clearer indication of the cytokine production by each of the populations in a disease settings. The expansion of pre-cDC in disease setting would make them useful cellular biomarkers. Depending on the population of pre-cDC that is expanded, this could affect the polarization of the T cells and hence affect the type of immune response generation. Hence, this would affect the clinical outcome of the disease.

4. CONCLUSION AND FUTURE WORK

In this PhD, we have two major aims. Firstly, to develop a genetic lineage fate mapping mouse model, and secondly, to identify DC-restricted progenitors.

For the first aim, we have developed Upk1b-cre mice to trace the development of DCs derived from CDPs. Although we did not observed high levels of recombination in DC-restricted progenitors or at cDCs, this could be due to the rapid cycling of progenitors during their differentiation. Hence, there is a lag time between Cre protein synthesis and Cre mediated excision. Thus, an inducible Cre recombinase system might be a better model to tag DC-restricted progenitors due to the low expression of Upk1b in these cells. We observed around 80% recombinant in microglia. Thus, this model could be used to fate map microglia development during embryogenesis, infection or even depletion of microglia to observe the developmental, physiological or even neurological defects associated with the absence of microglia. Furthermore, the physiological functions of Upk1b in DC or microglia are still unknown. Overexpression of the gene or inducing inflammation in Upk1b knockout mice might provide more insights into its function.

For the second aim, we have identified novel circulating pre-cDCs in the peripheral blood. Although they share common phenotypic markers with pDC, pre-cDCs were able to differentiate into cDC subsets using the MS5 stromal culture system. They were also functionally different from pDCs. We have also demonstrated that they are expanded in SLE disease, however, its role in this disease is still further investigated. It is also necessary to re-examine other pDC-associated diseases such as psoriasis to determine if the pre-cDC is expanded in these diseases, as this would affect the clinical outcome and treatment of the disease. Knowledge of human DC development would also help to improve intervention and create new therapeutic treatments.

5. REFERENCES

1. Adachi, W, Okubo, K, Kinoshita, S (2000). Human uroplakin Ib in ocular surface epithelium. *Invest Ophthalmol Vis Sci* 41: 2900–5.
2. Aliberti, J, Schulz, O, Pennington, DJ, *et al.* (2003). Essential role for ICSBP in the in vivo development of murine CD8alpha + dendritic cells. *Blood* 101: 305–10.
3. Asselin-Paturel, C, Boonstra, A, Dalod, M, *et al.* (2001). Mouse type I IFN-producing cells are immature APCs with plasmacytoid morphology. *Nat Immunol* 2: 1144–50.
4. Bachem, A, GÜttler, S, Hartung, E, *et al.* (2010). Superior antigen cross-presentation and XCR1 expression define human CD11c+CD141+ cells as homologues of mouse CD8+ dendritic cells. *J Exp Med* 207: 1273–81.
5. Balan, S, Ollion, V, Colletti, N, *et al.* (2014). Human XCR1+ Dendritic Cells Derived In Vitro from CD34+ Progenitors Closely Resemble Blood Dendritic Cells, Including Their Adjuvant Responsiveness, Contrary to Monocyte-Derived Dendritic Cells. *J Immunol* 193: 1622–35.
6. Banchereau, J, Brière, F, Caux, C, *et al.* (2000). Immunobiology of dendritic cells. *Annu Rev Immunol* 18: 767–811.
7. Becker, AM, Michael, DG, Satpathy, AT, *et al.* (2012). IRF-8 extinguishes neutrophil production and promotes dendritic cell lineage commitment in both myeloid and lymphoid mouse progenitors. *Blood* 119: 2003–12.
8. Bedoui, S, Whitney, PG, Waithman, J, *et al.* (2009). Cross-

- presentation of viral and self antigens by skin-derived CD103⁺ dendritic cells. *Nat Immunol* 10: 488–95.
9. Belz, GT, Nutt, SL (2012). Transcriptional programming of the dendritic cell network. *Nat Rev Immunol* 12: 101–13.
 10. Benjamini, Y, Hochberg, Y (1995). Controlling the false discovery rate: a practical and powerful approach to multiple testing. *Journal of the Royal Statistical Society Series B ...* 57: 289–300.
 11. Björck, P (2001). Isolation and characterization of plasmacytoid dendritic cells from Flt3 ligand and granulocyte-macrophage colony-stimulating factor-treated mice. *Blood* 98: 3520–6.
 12. Bogunovic, M, Ginhoux, F, Helft, J, *et al.* (2009). Origin of the lamina propria dendritic cell network. *Immunity* 31: 513–25.
 13. Brasel, K, De Smedt, T, Smith, JL, *et al.* (2000). Generation of murine dendritic cells from flt3-ligand-supplemented bone marrow cultures. *Blood* 96: 3029–39.
 14. Breton, G, Lee, J, Zhou, YJ, *et al.* (2015). Circulating precursors of human CD1c⁺ and CD141⁺ dendritic cells. *J Exp Med* 212: 401–13.
 15. Caton, ML, Smith-Raska, MR, Reizis, B (2007). Notch-RBP-J signaling controls the homeostasis of CD8⁺ dendritic cells in the spleen. *Journal of Experimental Medicine* 204: 1653–64.
 16. Caux, C, Vanbervliet, B, Massacrier, C (1996). CD34⁺ hematopoietic progenitors from human cord blood differentiate along two independent dendritic cell pathways in response to GM-CSF+ TNF alpha. *The Journal of*

17. Cella, M, Facchetti, F, Lanzavecchia, A, *et al.* (2000). Plasmacytoid dendritic cells activated by influenza virus and CD40L drive a potent TH1 polarization. *Nat Immunol* 1: 305–10.
18. Cella, M, Jarrossay, D, Facchetti, F, *et al.* (1999). Plasmacytoid monocytes migrate to inflamed lymph nodes and produce large amounts of type I interferon. *Nat Med* 5: 919–23.
19. Chan, CEZ, Lim, APC, MacAry, PA, *et al.* (2014). The role of phage display in therapeutic antibody discovery. *Int Immunol* 26: 649–57.
20. Chen, Q, Khoury, M, Chen, J (2009). Expression of human cytokines dramatically improves reconstitution of specific human-blood lineage cells in humanized mice. *Proceedings of the National Academy of Sciences* 106: 21783–8.
21. Chen, W, Antonenko, S, Sederstrom, JM, *et al.* (2004). Thrombopoietin cooperates with FLT3-ligand in the generation of plasmacytoid dendritic cell precursors from human hematopoietic progenitors. *Blood* 103: 2547–53.
22. Cisse, B, Caton, ML, Lehner, M, *et al.* (2008). Transcription factor E2-2 is an essential and specific regulator of plasmacytoid dendritic cell development. *Cell* 135: 37–48.
23. Collin, M, Bigley, V, Haniffa, M, *et al.* (2011). Human dendritic cell deficiency: the missing ID? *Nat Rev Immunol* 11: 575–83.
24. Colonna, M, Trinchieri, G, Liu, Y-J (2004). Plasmacytoid dendritic cells in immunity. *Nat Immunol* 5:

1219–26.

25. Comeau, MR, Van der Vuurst de Vries, A-R, Maliszewski, CR, *et al.* (2002). CD123bright plasmacytoid predendritic cells: progenitors undergoing cell fate conversion? *The Journal of Immunology* 169: 75–83.
26. Coombes, JL, Siddiqui, KRR, Arancibia-Cárcamo, CV, *et al.* (2007). A functionally specialized population of mucosal CD103+ DCs induces Foxp3+ regulatory T cells via a TGF-beta and retinoic acid-dependent mechanism. *Journal of Experimental Medicine* 204: 1757–64.
27. Crowley, M, Inaba, K, Witmer-Pack, M, *et al.* (1989). The cell surface of mouse dendritic cells: FACS analyses of dendritic cells from different tissues including thymus. *Cell Immunol* 118: 108–25.
28. Crozat, K, Guiton, R, Contreras, V, *et al.* (2010a). The XC chemokine receptor 1 is a conserved selective marker of mammalian cells homologous to mouse CD8alpha+ dendritic cells. *J Exp Med* 207: 1283–92.
29. Crozat, K, Guiton, R, Guilliams, M, *et al.* (2010b). Comparative genomics as a tool to reveal functional equivalences between human and mouse dendritic cell subsets. *Immunol Rev* 234: 177–98.
30. DeSalle, R, Chicote, JU, Sun, T-T, *et al.* (2014). Generation of divergent uroplakin tetraspanins and their partners during vertebrate evolution: identification of novel uroplakins. *BMC Evol Biol* 14: 13.
31. Desch, AN, Randolph, GJ, Murphy, K, *et al.* (2011). CD103+ pulmonary dendritic cells preferentially acquire and present apoptotic cell-associated antigen. *J Exp Med*

208: 1789–97.

32. Ding, Y, Wilkinson, A, Idris, A, *et al.* (2014). FLT3-ligand treatment of humanized mice results in the generation of large numbers of CD141⁺ and CD1c⁺ dendritic cells in vivo. *J Immunol* 192: 1982–9.
33. Doulatov, S, Notta, F, Eppert, K, *et al.* (2010). Revised map of the human progenitor hierarchy shows the origin of macrophages and dendritic cells in early lymphoid development. *Nat Immunol* 11: 585–93.
34. Dutertre, C-A, Wang, L-F, Ginhoux, F (2014). Aligning bona fide dendritic cell populations across species. *Cell Immunol* 291: 3–10.
35. Dzionek, A, Fuchs, A, Schmidt, P, *et al.* (2000). BDCA-2, BDCA-3, and BDCA-4: three markers for distinct subsets of dendritic cells in human peripheral blood. *The Journal of Immunology* 165: 6037–46.
36. Dzionek, A, Inagaki, Y, Okawa, K, *et al.* (2002). Plasmacytoid dendritic cells: from specific surface markers to specific cellular functions. *Hum Immunol* 63: 1133–48.
37. D’Agostino, PM, Gottfried-Blackmore, A, Anandasabapathy, N, *et al.* (2012). Brain dendritic cells: biology and pathology. *Acta Neuropathologica* 124: 599–614.
38. Edelson, BT, Bradstreet, TR, KC, W, *et al.* (2011). Batf3-dependent CD11b(low/-) peripheral dendritic cells are GM-CSF-independent and are not required for Th cell priming after subcutaneous immunization. *PLoS ONE* 6: e25660.
39. Edelson, BT, KC, W, Juang, R, *et al.* (2010). Peripheral

- CD103⁺ dendritic cells form a unified subset developmentally related to CD8α⁺ conventional dendritic cells. *J Exp Med* 207: 823–36.
40. Feinberg, MW, Wara, AK, Cao, Z, *et al.* (2007). The Kruppel-like factor KLF4 is a critical regulator of monocyte differentiation. *The EMBO Journal* 26: 4138–48.
 41. Fogg, DK, Sibon, C, Miled, C, *et al.* (2006). A clonogenic bone marrow progenitor specific for macrophages and dendritic cells. *Science* 311: 83–7.
 42. Förster, R, Davalos-Misslitz, AC, Rot, A (2008). CCR7 and its ligands: balancing immunity and tolerance. *Nat Rev Immunol* 8: 362–71.
 43. Geiger, TL, Abt, MC, Gasteiger, G, *et al.* (2014). Nfil3 is crucial for development of innate lymphoid cells and host protection against intestinal pathogens. *J Exp Med* 211: 1723–31.
 44. Geissmann, F, Jung, S, Littman, DR (2003). Blood monocytes consist of two principal subsets with distinct migratory properties. *Immunity* 19: 71–82.
 45. Ghosh, HS, Cisse, B, Bunin, A, *et al.* (2010). Continuous expression of the transcription factor e2-2 maintains the cell fate of mature plasmacytoid dendritic cells. *Immunity* 33: 905–16.
 46. Ginhoux, F, Jung, S (2014). Monocytes and macrophages: developmental pathways and tissue homeostasis. *Nat Rev Immunol* 14: 392–404.
 47. Ginhoux, F, Liu, K, Helft, J, *et al.* (2009). The origin and development of nonlymphoid tissue CD103⁺ DCs. *J Exp Med* 206: 3115–30.

48. Ginhoux, F, Merad, M (2010). Ontogeny and homeostasis of Langerhans cells. *Immunol Cell Biol* 88: 387–92.
49. Grajales-Reyes, GE, Iwata, A, Albring, J, *et al.* (2015). Batf3 maintains autoactivation of Irf8 for commitment of a CD8 α (+) conventional DC clonogenic progenitor. *Nat Immunol* 16: 708–17.
50. Greter, M, Helft, J, Chow, A, *et al.* (2012). GM-CSF controls nonlymphoid tissue dendritic cell homeostasis but is dispensable for the differentiation of inflammatory dendritic cells. *Immunity* 36: 1031–46.
51. Griffin, JD, Sabbath, KD, Herrmann, F (1985). Differential expression of HLA-DR antigens in subsets of human CFU-GM.
52. Grouard, G, Rissoan, MC, Filgueira, L, *et al.* (1997). The enigmatic plasmacytoid T cells develop into dendritic cells with interleukin (IL)-3 and CD40-ligand. *Journal of Experimental Medicine* 185: 1101–11.
53. Guilliams, M, Crozat, K, Henri, S, *et al.* (2010). Skin-draining lymph nodes contain dermis-derived CD103(-) dendritic cells that constitutively produce retinoic acid and induce Foxp3(+) regulatory T cells. *Blood* 115: 1958–68.
54. Guilliams, M, Ginhoux, F, Jakubzick, C, *et al.* (2014). Dendritic cells, monocytes and macrophages: a unified nomenclature based on ontogeny. *Nat Rev Immunol* 14: 571–8.
55. Haan, den, JM, Lehar, SM, Bevan, MJ (2000). CD8(+) but not CD8(-) dendritic cells cross-prime cytotoxic T cells in vivo. *Journal of Experimental Medicine* 192: 1685–96.

56. Hacker, C, Kirsch, RD, Ju, X-S, *et al.* (2003). Transcriptional profiling identifies Id2 function in dendritic cell development. *Nat Immunol* 4: 380–6.
57. Hambleton, S, Salem, S, Bustamante, J, *et al.* (2011). IRF8 mutations and human dendritic-cell immunodeficiency. *N Engl J Med* 365: 127–38.
58. Haniffa, M, Bigley, V, Collin, M (2015). Human mononuclear phagocyte system reunited. *Semin Cell Dev Biol* 41: 59–69.
59. Haniffa, M, Shin, A, Bigley, V, *et al.* (2012). Human tissues contain CD141^{hi} cross-presenting dendritic cells with functional homology to mouse CD103⁺ nonlymphoid dendritic cells. *Immunity* 37: 60–73.
60. Harman, AN, Bye, CR, Nasr, N, *et al.* (2013). Identification of lineage relationships and novel markers of blood and skin human dendritic cells. *J Immunol* 190: 66–79.
61. Hart, DN, Fabre, JW (1981). Demonstration and characterization of Ia-positive dendritic cells in the interstitial connective tissues of rat heart and other tissues, but not brain. *Journal of Experimental Medicine* 154: 347–61.
62. Helft, J, Ginhoux, F, Bogunovic, M, *et al.* (2010). Origin and functional heterogeneity of non-lymphoid tissue dendritic cells in mice. *Immunol Rev* 234: 55–75.
63. Hemler, ME (2005). Tetraspanin functions and associated microdomains. *Nat Rev Mol Cell Biol* 6: 801–11.
64. Henri, S, Poulin, LF, Tamoutounour, S, *et al.* (2010).

- CD207+ CD103+ dermal dendritic cells cross-present keratinocyte-derived antigens irrespective of the presence of Langerhans cells. *J Exp Med* 207: 189–206.
65. Hettinger, J, Richards, DM, Hansson, J, *et al.* (2013). Origin of monocytes and macrophages in a committed progenitor. *Nat Immunol* 14: 821–30.
 66. Hémond, C, Neel, A, Heslan, M, *et al.* (2013). Human blood mDC subsets exhibit distinct TLR repertoire and responsiveness. *J Leukoc Biol* 93: 599–609.
 67. Hildner, K, Edelson, BT, Purtha, WE, *et al.* (2008). Batf3 deficiency reveals a critical role for CD8alpha+ dendritic cells in cytotoxic T cell immunity. *Science* 322: 1097–100.
 68. Hoeffel, G, Ripoche, A-C, Matheoud, D, *et al.* (2007). Antigen crosspresentation by human plasmacytoid dendritic cells. *Immunity* 27: 481–92.
 69. Hoeffel, G, Wang, Y, Greter, M, *et al.* (2012). Adult Langerhans cells derive predominantly from embryonic fetal liver monocytes with a minor contribution of yolk sac-derived macrophages. *J Exp Med* 209: 1167–81.
 70. Hohl, TM, Rivera, A, Lipuma, L, *et al.* (2009). Inflammatory monocytes facilitate adaptive CD4 T cell responses during respiratory fungal infection. *Cell Host Microbe* 6: 470–81.
 71. Holtschke, T, Löhler, J, Kanno, Y, *et al.* (1996). Immunodeficiency and chronic myelogenous leukemia-like syndrome in mice with a targeted mutation of the ICSBP gene. *Cell* 87: 307–17.
 72. Honda, K, Mizutani, T, Taniguchi, T (2004). Negative

- regulation of IFN- α / β signaling by IFN regulatory factor 2 for homeostatic development of dendritic cells. *PNAS* 101: 2416–21.
73. Ichikawa, E, Hida, S, Omatsu, Y, *et al.* (2004). Defective development of splenic and epidermal CD4⁺ dendritic cells in mice deficient for IFN regulatory factor-2. *Proc Natl Acad Sci USA* 101: 3909–14.
 74. Inaba, K, Inaba, M, Romani, N, *et al.* (1992). Generation of large numbers of dendritic cells from mouse bone marrow cultures supplemented with granulocyte/macrophage colony-stimulating factor. *Journal of Experimental Medicine* 176: 1693–702.
 75. Ippolito, GC, Dekker, JD, Wang, Y-H, *et al.* (2014). Dendritic cell fate is determined by BCL11A. *Proc Natl Acad Sci USA* 111: E998–1006.
 76. Ito, T, Amakawa, R, Inaba, M, *et al.* (2004). Plasmacytoid dendritic cells regulate Th cell responses through OX40 ligand and type I IFNs. *The Journal of Immunology* 172: 4253–9.
 77. Ito, T, Yang, M, Wang, Y-H, *et al.* (2007). Plasmacytoid dendritic cells prime IL-10-producing T regulatory cells by inducible costimulator ligand. *Journal of Experimental Medicine* 204: 105–15.
 78. Iwasaki, A, Medzhitov, R (2015). Control of adaptive immunity by the innate immune system. *Nat Immunol* 16: 343–53.
 79. Jackson, JT, Hu, Y, Liu, R, *et al.* (2011). Id2 expression delineates differential checkpoints in the genetic program of CD8 α ⁺ and CD103⁺ dendritic cell lineages. *The EMBO*

Journal 30: 2690–704.

80. Jakubzick, C, Tacke, F, Ginhoux, F, *et al.* (2008). Blood monocyte subsets differentially give rise to CD103⁺ and CD103⁻ pulmonary dendritic cell populations. *J Immunol* 180: 3019–27.
81. Jensen, P, Dymecki, SM (2014). Essentials of recombinase-based genetic fate mapping in mice. *Methods Mol Biol* 1092: 437–54.
82. Joffre, OP, Segura, E, Savina, A, *et al.* (2012). Cross-presentation by dendritic cells. *Nat Rev Immunol* 12: 557–69.
83. Joyner, AL, Zervas, M (2006). Genetic inducible fate mapping in mouse: establishing genetic lineages and defining genetic neuroanatomy in the nervous system. *Dev Dyn* 235: 2376–85.
84. Kabashima, K, Banks, TA, Ansel, KM, *et al.* (2005). Intrinsic lymphotoxin-beta receptor requirement for homeostasis of lymphoid tissue dendritic cells. *Immunity* 22: 439–50.
85. Kadowaki, N, Antonenko, S, Lau, JY, *et al.* (2000). Natural interferon alpha/beta-producing cells link innate and adaptive immunity. *Journal of Experimental Medicine* 192: 219–26.
86. Kapsenberg, ML (2003). Dendritic-cell control of pathogen-driven T-cell polarization. *Nat Rev Immunol* 3: 984–93.
87. Karrich, JJ, Balzarolo, M, Schmidlin, H, *et al.* (2012). The transcription factor Spi-B regulates human plasmacytoid dendritic cell survival through direct induction

- of the antiapoptotic gene BCL2-A1. *Blood* 119: 5191–200.
88. Karsunky, H, Merad, M, Cozzio, A, *et al.* (2003). Flt3 ligand regulates dendritic cell development from Flt3+ lymphoid and myeloid-committed progenitors to Flt3+ dendritic cells in vivo. *Journal of Experimental Medicine* 198: 305–13.
89. Kashiwada, M, Pham, N, Pewe, LL, *et al.* (2011). NFIL3/E4BP4 is a key transcription factor for CD8 α + dendritic cell development. *Blood* 117: 6193–7.
90. Kawai, T, Akira, S (2011). Toll-like receptors and their crosstalk with other innate receptors in infection and immunity. *Immunity* 34: 637–50.
91. Kinoshita, S, Adachi, W, Sotozono, C, *et al.* (2001). Characteristics of the human ocular surface epithelium. *Prog Retin Eye Res* 20: 639–73.
92. Kobayashi, T, Walsh, PT, Walsh, MC, *et al.* (2003). TRAF6 is a critical factor for dendritic cell maturation and development. *Immunity* 19: 353–63.
93. Kretzschmar, K, Watt, FM (2012). Lineage tracing. *Cell* 148: 33–45.
94. Kumamoto, Y, Linehan, M, Weinstein, JS, *et al.* (2013). CD301b⁺ dermal dendritic cells drive T helper 2 cell-mediated immunity. *Immunity* 39: 733–43.
95. Kurotaki, D, Osato, N, Nishiyama, A, *et al.* (2013). Essential role of the IRF8-KLF4 transcription factor cascade in murine monocyte differentiation. *Blood* 121: 1839–49.
96. Langlet, C, Tamoutounour, S, Henri, S, *et al.* (2012). CD64 expression distinguishes monocyte-derived and

- conventional dendritic cells and reveals their distinct role during intramuscular immunization. *J Immunol* 188: 1751–60.
97. Lauterbach, H, Bathke, B, Gilles, S, *et al.* (2010). Mouse CD8alpha⁺ DCs and human BDCA3⁺ DCs are major producers of IFN-lambda in response to poly IC. *J Exp Med* 207: 2703–17.
98. Lee, J, Breton, G, Aljoufi, A, *et al.* (2015a). Clonal analysis of human dendritic cell progenitor using a stromal cell culture. *J Immunol Methods*.
99. Lee, J, Breton, G, Oliveira, TYK, *et al.* (2015b). Restricted dendritic cell and monocyte progenitors in human cord blood and bone marrow. *J Exp Med* 212: 385–99.
100. León, B, López-Bravo, M, Ardavín, C (2007). Monocyte-derived dendritic cells formed at the infection site control the induction of protective T helper 1 responses against Leishmania. *Immunity* 26: 519–31.
101. Levy, S, Shoham, T (2005). The tetraspanin web modulates immune-signalling complexes. *Nat Rev Immunol* 5: 136–48.
102. Lewis, KL, Caton, ML, Bogunovic, M, *et al.* (2011). Notch2 receptor signaling controls functional differentiation of dendritic cells in the spleen and intestine. *Immunity* 35: 780–91.
103. Li, L, Jin, H, Xu, J, *et al.* (2011). Irf8 regulates macrophage versus neutrophil fate during zebrafish primitive myelopoiesis. *Blood* 117: 1359–69.
104. Liu, K, Vitoria, GD, Schwickert, TA, *et al.* (2009). In

- vivo analysis of dendritic cell development and homeostasis. *Science* 324: 392–7.
105. Liu, P, Jenkins, NA, Copeland, NG (2003). A highly efficient recombineering-based method for generating conditional knockout mutations. *Genome Res* 13: 476–84.
 106. Lubber, CA, Cox, J, Lauterbach, H, *et al.* (2010). Quantitative proteomics reveals subset-specific viral recognition in dendritic cells. *Immunity* 32: 279–89.
 107. MacDonald, KPA, Munster, DJ, Clark, GJ, *et al.* (2002). Characterization of human blood dendritic cell subsets. *Blood* 100: 4512–20.
 108. Matsui, T, Connolly, JE, Michnevitz, M, *et al.* (2009). CD2 distinguishes two subsets of human plasmacytoid dendritic cells with distinct phenotype and functions. *J Immunol* 182: 6815–23.
 109. McKenna, HJ, Stocking, KL, Miller, RE, *et al.* (2000). Mice lacking flt3 ligand have deficient hematopoiesis affecting hematopoietic progenitor cells, dendritic cells, and natural killer cells. *Blood* 95: 3489–97.
 110. Merad, M, Sathe, P, Helft, J, *et al.* (2013). The dendritic cell lineage: ontogeny and function of dendritic cells and their subsets in the steady state and the inflamed setting. *Annu Rev Immunol* 31: 563–604.
 111. Meredith, MM, Liu, K, Darrasse-Jèze, G, *et al.* (2012a). Expression of the zinc finger transcription factor zDC (Zbtb46, Btbd4) defines the classical dendritic cell lineage. *J Exp Med* 209: 1153–65.
 112. Meredith, MM, Liu, K, Kamphorst, AO, *et al.* (2012b). Zinc finger transcription factor zDC is a negative regulator

- required to prevent activation of classical dendritic cells in the steady state. *J Exp Med* 209: 1583–93.
113. Mildner, A, Yona, S, Jung, S (2013). A close encounter of the third kind: monocyte-derived cells. *Adv Immunol* 120: 69–103.
 114. Miller, JC, Brown, BD, Shay, T, *et al.* (2012). Deciphering the transcriptional network of the dendritic cell lineage. *Nat Immunol* 13: 888–99.
 115. Mintern, JD, Macri, C, Villadangos, JA (2015). Modulation of antigen presentation by intracellular trafficking. *Curr Opin Immunol* 34: 16–21.
 116. Moseman, EA, Liang, X, Dawson, AJ, *et al.* (2004). Human plasmacytoid dendritic cells activated by CpG oligodeoxynucleotides induce the generation of CD4⁺CD25⁺ regulatory T cells. *The Journal of Immunology* 173: 4433–42.
 117. Mouriès, J, Moron, G, Schlecht, G, *et al.* (2008). Plasmacytoid dendritic cells efficiently cross-prime naive T cells in vivo after TLR activation. *Blood* 112: 3713–22.
 118. Murphy, KM (2013). Transcriptional control of dendritic cell development. *Adv Immunol* 120: 239–67.
 119. Muzaki, ARBM, Tetlak, P, Sheng, J, *et al.* (2015). Intestinal CD103(+)CD11b(-) dendritic cells restrain colitis via IFN- γ -induced anti-inflammatory response in epithelial cells. *Mucosal Immunol*.
 120. Münz, C (2012). Antigen processing for MHC class II presentation via autophagy. *Front Immunol* 3.
 121. Naik, SH, Proietto, AI, Wilson, NS, *et al.* (2005). Cutting Edge: Generation of Splenic CD8⁺ and CD8⁻ Dendritic Cell

- Equivalents in Fms-Like Tyrosine Kinase 3 Ligand Bone Marrow Cultures. *The Journal of Immunology* 174: 6592–7.
122. Naik, SH, Sathe, P, Park, H-Y, *et al.* (2007). Development of plasmacytoid and conventional dendritic cell subtypes from single precursor cells derived in vitro and in vivo. *Nat Immunol* 8: 1217–26.
 123. Nakano, H, Free, ME, Whitehead, GS, *et al.* (2012). Pulmonary CD103(+) dendritic cells prime Th2 responses to inhaled allergens. *Mucosal Immunol* 5: 53–65.
 124. Nakano, H, Yanagita, M, Gunn, MD (2001). CD11c+ B220+ Gr-1+ cells in mouse lymph nodes and spleen display characteristics of plasmacytoid dendritic cells. *Journal of Experimental Medicine* 194: 1171–8.
 125. Nussenzweig, MC, Steinman, RM (1980). Dendritic cells are accessory cells for the development of anti-trinitrophenyl cytotoxic T lymphocytes. *Journal of Experimental Medicine* 152: 1070–84.
 126. O'Doherty, U, Peng, M, Gezelter, S, *et al.* (1994). Human blood contains two subsets of dendritic cells, one immunologically mature and the other immature. *Immunology* 82: 487–93.
 127. Ohl, L, Mohaupt, M, Czeloth, N, *et al.* (2004). CCR7 governs skin dendritic cell migration under inflammatory and steady-state conditions. *Immunity* 21: 279–88.
 128. Olsburgh, J, Harnden, P, Weeks, R, *et al.* (2003). Uroplakin gene expression in normal human tissues and locally advanced bladder cancer. *J Pathol* 199: 41–9.
 129. Olweus, J, BitMansour, A, Warnke, R, *et al.* (1997).

- Dendritic cell ontogeny: a human dendritic cell lineage of myeloid origin. *Proc Natl Acad Sci USA* 94: 12551–6.
130. On, LB, Jung, S (2010). Defining dendritic cells by conditional and constitutive cell ablation. *Immunol Rev* 234: 76–89.
131. Onai, N, Kurabayashi, K, Hosoi-Amaiike, M, *et al.* (2013). A clonogenic progenitor with prominent plasmacytoid dendritic cell developmental potential. *Immunity* 38: 943–57.
132. Onai, N, Obata-Onai, A, Schmid, MA, *et al.* (2007). Identification of clonogenic common Flt3+M-CSFR+ plasmacytoid and conventional dendritic cell progenitors in mouse bone marrow. *Nat Immunol* 8: 1207–16.
133. Persson, EK, Uronen-Hansson, H, Semmrich, M, *et al.* (2013). IRF4 transcription-factor-dependent CD103(+)CD11b(+) dendritic cells drive mucosal T helper 17 cell differentiation. *Immunity* 38: 958–69.
134. Plantinga, M, Guillems, M, Vanheerswynghe, M, *et al.* (2013). Conventional and monocyte-derived CD11b(+) dendritic cells initiate and maintain T helper 2 cell-mediated immunity to house dust mite allergen. *Immunity* 38: 322–35.
135. Poltorak, MP, Schraml, BU (2015). Fate mapping of dendritic cells. *Front Immunol* 6: 199.
136. Poulin, LF, Rey, Y, Uronen-Hansson, H, *et al.* (2012). DNGR-1 is a specific and universal marker of mouse and human Batf3-dependent dendritic cells in lymphoid and nonlymphoid tissues. *Blood* 119: 6052–62.
137. Poulin, LF, Salio, M, Griessinger, E, *et al.* (2010).

- Characterization of human DNGR-1+ BDCA3+ leukocytes as putative equivalents of mouse CD8alpha+ dendritic cells. *J Exp Med* 207: 1261–71.
138. Proietto, AI, Mittag, D, Roberts, AW, *et al.* (2012). The equivalents of human blood and spleen dendritic cell subtypes can be generated in vitro from human CD34(+) stem cells in the presence of fms-like tyrosine kinase 3 ligand and thrombopoietin. *Cell Mol Immunol* 9: 446–54.
 139. Pulendran, B, Banchereau, J, Burkeholder, S, *et al.* (2000). Flt3-Ligand and Granulocyte Colony-Stimulating Factor Mobilize Distinct Human Dendritic Cell Subsets In Vivo. *The Journal of Immunology* 165: 566–72.
 140. Qiu, C-H, Miyake, Y, Kaise, H, *et al.* (2009). Novel subset of CD8{alpha}+ dendritic cells localized in the marginal zone is responsible for tolerance to cell-associated antigens. *J Immunol* 182: 4127–36.
 141. Randolph, GJ, Angeli, V, Swartz, MA (2005). Dendritic-cell trafficking to lymph nodes through lymphatic vessels. *Nat Rev Immunol* 5: 617–28.
 142. Raphael, I, Nalawade, S, Eagar, TN, *et al.* (2015). T cell subsets and their signature cytokines in autoimmune and inflammatory diseases. *Cytokine* 74: 5–17.
 143. Reis e Sousa, C, Hieny, S, Scharon-Kersten, T, *et al.* (1997). In vivo microbial stimulation induces rapid CD40 ligand-independent production of interleukin 12 by dendritic cells and their redistribution to T cell areas. *Journal of Experimental Medicine* 186: 1819–29.
 144. Reizis, B, Bunin, A, Ghosh, HS, *et al.* (2011). Plasmacytoid dendritic cells: recent progress and open

- questions. *Annu Rev Immunol* 29: 163–83.
145. Rissoan, M (1999). Reciprocal Control of T Helper Cell and Dendritic Cell Differentiation. *Science* 283: 1183–6.
146. Robbins, SH, Walzer, T, Dembélé, D, *et al.* (2008). Novel insights into the relationships between dendritic cell subsets in human and mouse revealed by genome-wide expression profiling. *Genome Biol* 9: R17.
147. Romao, S, Gasser, N, Becker, AC, *et al.* (2013). Autophagy proteins stabilize pathogen-containing phagosomes for prolonged MHC II antigen processing. *J Cell Biol* 203: 757–66.
148. Salio, M (2004). CpG-matured Murine Plasmacytoid Dendritic Cells Are Capable of In Vivo Priming of Functional CD8 T Cell Responses to Endogenous but Not Exogenous Antigens. *Journal of Experimental Medicine* 199: 567–79.
149. Sallusto, F, Lanzavecchia, A (2009). Heterogeneity of CD4+ memory T cells: functional modules for tailored immunity. *Eur J Immunol* 39: 2076–82.
150. Sasaki, I, Hoshino, K, Sugiyama, T, *et al.* (2012). Spi-B is critical for plasmacytoid dendritic cell function and development. *Blood* 120: 4733–43.
151. Satpathy, AT, Briseño, CG, Lee, JS, *et al.* (2013). Notch2-dependent classical dendritic cells orchestrate intestinal immunity to attaching-and-effacing bacterial pathogens. *Nat Immunol* 14: 937–48.
152. Satpathy, AT, KC, W, Albring, JC, *et al.* (2012a). Zbtb46 expression distinguishes classical dendritic cells and their committed progenitors from other immune

- lineages. *J Exp Med* 209: 1135–52.
153. Satpathy, AT, Wu, X, Albring, JC, *et al.* (2012b). Re(de)fining the dendritic cell lineage. *Nat Immunol* 13: 1145–54.
 154. Schiavoni, G, Mattei, F, Sestili, P, *et al.* (2002). ICSBP Is Essential for the Development of Mouse Type I Interferon-producing Cells and for the Generation and Activation of CD8 Dendritic Cells. *Journal of Experimental Medicine* 196: 1415–25.
 155. Schlitzer, A, Ginhoux, F (2013). DNNGR-ing the dendritic cell lineage. *EMBO Rep* 14: 850–1.
 156. Schlitzer, A, Ginhoux, F (2014). Organization of the mouse and human DC network. *Curr Opin Immunol* 26: 90–9.
 157. Schlitzer, A, Heiseke, AF, Einwächter, H, *et al.* (2012). Tissue-specific differentiation of a circulating CCR9- pDC-like common dendritic cell precursor. *Blood* 119: 6063–71.
 158. Schlitzer, A, Loschko, J, Mair, K, *et al.* (2011). Identification of CCR9- murine plasmacytoid DC precursors with plasticity to differentiate into conventional DCs. *Blood* 117: 6562–70.
 159. Schlitzer, A, McGovern, N, Ginhoux, F (2015a). Dendritic cells and monocyte-derived cells: Two complementary and integrated functional systems. *Semin Cell Dev Biol* 41: 9–22.
 160. Schlitzer, A, McGovern, N, Teo, P, *et al.* (2013). IRF4 transcription factor-dependent CD11b⁺ dendritic cells in human and mouse control mucosal IL-17 cytokine responses. *Immunity* 38: 970–83.

161. Schlitzer, A, Sivakamasundari, V, Chen, J, *et al.* (2015b). Identification of cDC1- and cDC2-committed DC progenitors reveals early lineage priming at the common DC progenitor stage in the bone marrow. *Nat Immunol* 16: 718–28.
162. Schmid, D, Pypaert, M, Münz, C (2007). Antigen-loading compartments for major histocompatibility complex class II molecules continuously receive input from autophagosomes. *Immunity* 26: 79–92.
163. Schotte, R, Nagasawa, M, Weijer, K, *et al.* (2004). The ETS transcription factor Spi-B is required for human plasmacytoid dendritic cell development. *Journal of Experimental Medicine* 200: 1503–9.
164. Schraml, BU, van Blijswijk, J, Zelenay, S, *et al.* (2013). Genetic tracing via DNNGR-1 expression history defines dendritic cells as a hematopoietic lineage. *Cell* 154: 843–58.
165. Segura, E, Amigorena, S (2015). Cross-Presentation in Mouse and Human Dendritic Cells. *Adv Immunol* 127: 1–31.
166. Segura, E, Valladeau-Guilemond, J, Donnadieu, M-H, *et al.* (2012). Characterization of resident and migratory dendritic cells in human lymph nodes. *J Exp Med* 209: 653–60.
167. Seillet, C, Rankin, LC, Groom, JR, *et al.* (2014). Nfil3 is required for the development of all innate lymphoid cell subsets. *J Exp Med* 211: 1733–40.
168. Serbina, NV, Salazar-Mather, TP, Biron, CA, *et al.* (2003). TNF/iNOS-producing dendritic cells mediate innate

- immune defense against bacterial infection. *Immunity* 19: 59–70.
169. Sertl, K, Takemura, T, Tschachler, E, *et al.* (1986). Dendritic cells with antigen-presenting capability reside in airway epithelium, lung parenchyma, and visceral pleura. *Journal of Experimental Medicine* 163: 436–51.
 170. Sharpe, AH, Freeman, GJ (2002). The B7-CD28 superfamily. *Nat Rev Immunol* 2: 116–26.
 171. Shortman, K, Heath, WR (2010). The CD8⁺ dendritic cell subset. *Immunol Rev* 234: 18–31.
 172. Siegal, FP, Kadowaki, N, Shodell, M, *et al.* (1999). The Nature of the Principal Type 1 Interferon-Producing Cells in Human Blood. *Science* 284: 1835–7.
 173. Smyth, GK (2004). Linear models and empirical bayes methods for assessing differential expression in microarray experiments. *Stat Appl Genet Mol Biol* 3: Article3.
 174. Steinman, RM (2012). Decisions about dendritic cells: past, present, and future. *Annu Rev Immunol* 30: 1–22.
 175. Steinman, RM, Cohn, ZA (1973). Identification of a novel cell type in peripheral lymphoid organs of mice I. Morphology, quantitation, tissue distribution. *J Exp Med* 137: 1142–62.
 176. Steinman, RM, Witmer, MD (1978). Lymphoid dendritic cells are potent stimulators of the primary mixed leukocyte reaction in mice. *Proc Natl Acad Sci USA* 75: 5132–6.
 177. Summers deLuca, L, Gommerman, JL (2012). Fine-tuning of dendritic cell biology by the TNF superfamily. *Nat Rev Immunol* 12: 339–51.

178. Suzuki, S, Honma, K, Matsuyama, T, *et al.* (2004). Critical roles of interferon regulatory factor 4 in CD11b^{high}CD8 - dendritic cell development. *Proceedings of the National Academy of Sciences* 101: 8981–6.
179. Swiecki, M, Colonna, M (2015). The multifaceted biology of plasmacytoid dendritic cells. *Nat Rev Immunol* 15: 471–85.
180. Tailor, P, Tamura, T, Morse, HC, *et al.* (2008). The BXH2 mutation in IRF8 differentially impairs dendritic cell subset development in the mouse. *Blood* 111: 1942–5.
181. Tamoutounour, S, Henri, S, Lelouard, H, *et al.* (2012). CD64 distinguishes macrophages from dendritic cells in the gut and reveals the Th1-inducing role of mesenteric lymph node macrophages during colitis. *Eur J Immunol* 42: 3150–66.
182. Tamura, T, Tailor, P, Yamaoka, K, *et al.* (2005). IFN regulatory factor-4 and-8 govern dendritic cell subset development and their functional diversity. *The Journal of Immunology* 174: 2573–81.
183. Tarrant, JM, Robb, L, van Spriel, AB, *et al.* (2003). Tetraspanins: molecular organisers of the leukocyte surface. *Trends Immunol* 24: 610–7.
184. Tsujimura, H, Tamura, T, Ozato, K (2003). Cutting edge: IFN consensus sequence binding protein/IFN regulatory factor 8 drives the development of type I IFN-producing plasmacytoid dendritic cells. *The Journal of Immunology* 170: 1131–5.
185. Turcotte, K, Gauthier, S, Tuite, A, *et al.* (2005). A mutation in the *Icsbp1* gene causes susceptibility to

- infection and a chronic myeloid leukemia-like syndrome in BXH-2 mice. *Journal of Experimental Medicine* 201: 881–90.
186. Tussiwand, R, Everts, B, Grajales-Reyes, GE, *et al.* (2015). Klf4 expression in conventional dendritic cells is required for T helper 2 cell responses. *Immunity* 42: 916–28.
 187. Tussiwand, R, Lee, W-L, Murphy, TL, *et al.* (2012). Compensatory dendritic cell development mediated by BATF-IRF interactions. *Nature* 490: 502–7.
 188. Valladeau, J, Clair-Moninot, V (2002). Identification of mouse langerin/CD207 in Langerhans cells and some dendritic cells of lymphoid tissues. *The Journal of Immunology* 168: 782–92.
 189. Valladeau, J, Ravel, O, Dezutter-Dambuyant, C, *et al.* (2000). Langerin, a novel C-type lectin specific to Langerhans cells, is an endocytic receptor that induces the formation of Birbeck granules. *Immunity* 12: 71–81.
 190. Varol, C, Vallon-Eberhard, A, Elinav, E, *et al.* (2009). Intestinal lamina propria dendritic cell subsets have different origin and functions. *Immunity* 31: 502–12.
 191. Villadangos, JA, Schnorrer, P (2007). Intrinsic and cooperative antigen-presenting functions of dendritic-cell subsets in vivo. *Nat Rev Immunol* 7: 543–55.
 192. Villadangos, JA, Young, L (2008). Antigen-presentation properties of plasmacytoid dendritic cells. *Immunity* 29: 352–61.
 193. Vorhagen, S, Jackow, J, Mohor, SG, *et al.* (2015). Lineage Tracing Mediated by Cre-Recombinase Activity.

Journal of Investigative Dermatology 135: e28.

194. Vremec, D, Lieschke, GJ, Dunn, AR, *et al.* (1997). The influence of granulocyte/macrophage colony-stimulating factor on dendritic cell levels in mouse lymphoid organs. *Eur J Immunol* 27: 40–4.
195. Vremec, D, Pooley, J, Hochrein, H, *et al.* (2000). CD4 and CD8 expression by dendritic cell subtypes in mouse thymus and spleen. *J Immunol* 164: 2978–86.
196. Waskow, C, Liu, K, Darrasse-Jèze, G, *et al.* (2008). The receptor tyrosine kinase Flt3 is required for dendritic cell development in peripheral lymphoid tissues. *Nat Immunol* 9: 676–83.
197. Watchmaker, PB, Lahl, K, Lee, M, *et al.* (2014). Comparative transcriptional and functional profiling defines conserved programs of intestinal DC differentiation in humans and mice. *Nat Immunol* 15: 98–108.
198. Wilson, NS, Villadangos, JA (2005). Regulation of antigen presentation and cross-presentation in the dendritic cell network: facts, hypothesis, and immunological implications. *Adv Immunol*.
199. Wu, L, D'Amico, A, Winkel, KD, *et al.* (1998). RelB is essential for the development of myeloid-related CD8alpha- dendritic cells but not of lymphoid-related CD8alpha+ dendritic cells. *Immunity* 9: 839–47.
200. Wu, X, Satpathy, AT, KC, W, *et al.* (2013). Bcl11a controls Flt3 expression in early hematopoietic progenitors and is required for pDC development in vivo. *PLoS ONE* 8: e64800.
201. Wu, XR, Lin, JH, Walz, T, *et al.* (1994). Mammalian

- uroplakins. A group of highly conserved urothelial differentiation-related membrane proteins. *J Biol Chem* 269: 13716–24.
202. Yamane, H, Paul, WE (2012). Cytokines of the $\gamma(c)$ family control CD4⁺ T cell differentiation and function. *Nat Immunol* 13: 1037–44.
203. Yee, C-S, Farewell, VT, Isenberg, DA, *et al.* (2011). The use of Systemic Lupus Erythematosus Disease Activity Index-2000 to define active disease and minimal clinically meaningful change based on data from a large cohort of systemic lupus erythematosus patients. *Rheumatology (Oxford)* 50: 982–8.
204. Yu, C-I, Becker, C, Metang, P, *et al.* (2014). Human CD141⁺ dendritic cells induce CD4⁺ T cells to produce type 2 cytokines. *J Immunol* 193: 4335–43.
205. Yu, J, Lin, JH, Wu, XR, *et al.* (1994). Uroplakins Ia and Ib, two major differentiation products of bladder epithelium, belong to a family of four transmembrane domain (4TM) proteins. *J Cell Biol* 125: 171–82.
206. Yuasa, T, Yoshiki, T, Tanaka, T, *et al.* (1998). Expression of uroplakin Ib and uroplakin III genes in tissues and peripheral blood of patients with transitional cell carcinoma. *Jpn J Cancer Res* 89: 879–82.
207. Zhou, Q, Ho, AWS, Schlitzer, A, *et al.* (2014). GM-CSF-licensed CD11b⁺ lung dendritic cells orchestrate Th2 immunity to *Blomia tropicalis*. *J Immunol* 193: 496–509.

APPENDIX A

List of anti-human antibodies used for flow cytometry

Name	Clone	Fluorophore	Source
CD1c	L161	PerCP5.5	Biolegend
CD2	TS1/8	BV421	Biolegend
CD3	OKT3	BV650	Biolegend
CD4	OKT4	PE	Biolegend
CD11c	B-ly6	V450	BD Pharmingen
CD14	M5E2	BV650	Biolegend
CD14	RMO52	ECD	Beckman Coulter
CD16	3G8	APC-Cy7	Biolegend
CD19	HIB19	BV650	Biolegend
CD20	2H7	BV650	Biolegend
CD33	WM53	PE-CF594	BD Biosciences
CD34	581	A700	Biolegend
CD45	HI30	FITC	Biolegend
CD45	HI30	A700	Biolegend
CD45	HI30	V500	BD Horizon
CD45RA	HI100	BV605	Biolegend
CD66b	G10F5	PerCP5.5	Biolegend
CD80	ASL24	PE	Biolegend
CD83	HB15e	PE	Biolegend
CD116	4H1	Biotin	Biolegend
CD117	104D2	BV421	Biolegend
CD123	7G3	BUV395	BD Horizon
CD135	4G8	PE	BD Pharmigen
CD141	AD5-14H12	PE-VIVO770	Miltenyi Biotec
CD169	7-239	PE	Biolegend
CD172	SE5a5	PECy7	Biolegend
CD272	MIH26	PE	Biolegend
CD303	AC144	Biotin	Miltenyi Biotec
CD319	162.1	PE	Biolegend
CD327	767329	APC	R&D Systems
CD335	9E2	PerCP5.5	Biolegend
CADM1	3E1	Purified	MBL
Clec9a	8F9	PE	Biolegend
CX3CR1	2A9-1	PE	Biolegend
CXCR3	G025H7	PE	Biolegend
FcεR1	AER-37	PE	Biolegend
HLA-DR	G46-4	V500	BD Horizon
ILT1	REA219	Biotin	Miltenyi Biotec
ILT3	ZM4.1	PE	Biolegend
ILT7	REA100	Biotin	Miltenyi Biotec
A649 Anti-IgY			Jackson Immunoresearch
BUV737 Strep			BD Horizon

APPENDIX B

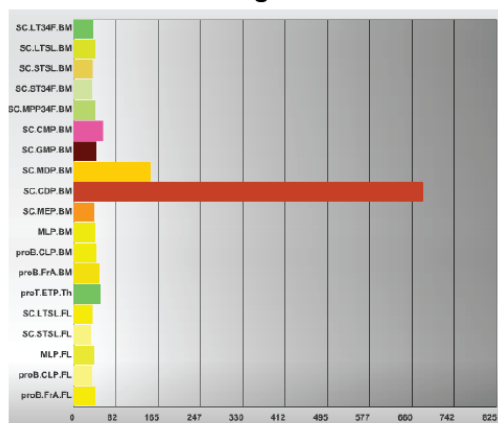
List of anti-mouse antibodies used for flow cytometry

Name	Clone	Fluorophore	Source
CD3e	145-2C11	APC	eBioscience
CD8a	53-6.7	APC	eBioscience
CD11b	M1/70	BV650	Biolegend
CD11c	N418	PECy7	Biolegend
CD19	6D5	APC	eBioscience
CD45	30-F11	BUV395	BD Horizon
CD115	AFS98	PE	eBioscience
CD117	2B8	PE-CF594	BD Horizon
CD135	A2F10	Biotin	eBioscience
ESAM	1G8	PE	Biolegend
F4/80	BM8	Biotin	Biolegend
IA/IE	M5/114.152	A700	Biolegend
Ly6C	HK1.4	APCCy7	Biolegend
Ly6G	1A8	PE-CF594	BD Horizon
NK1.1	PK136	APC	eBioscience
Siglec-H	551	PerCP5.5	Biolegend
Ter119	Ter119	APC	eBioscience
PECy7 Strep			Biolegend

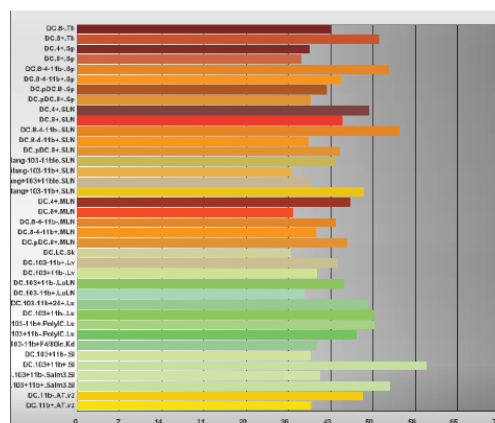
APPENDIX C

UPK1b expression in various immune cells in the ImmGEN database

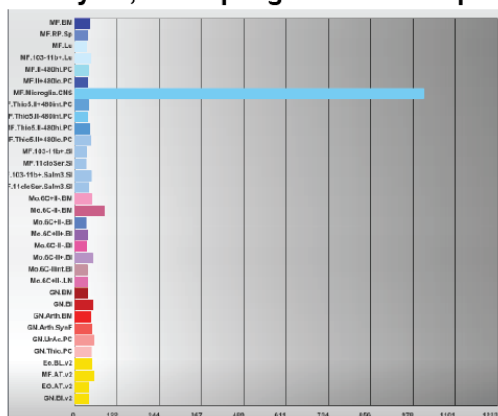
Stem and Progenitors Cells



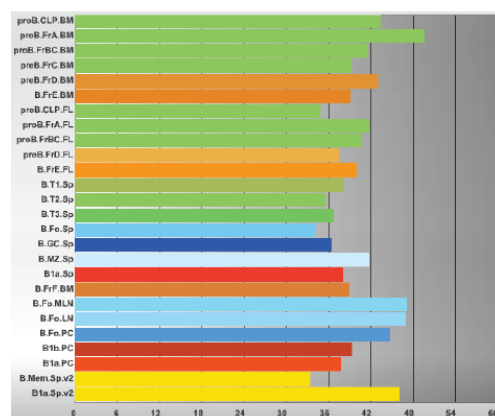
DC subsets



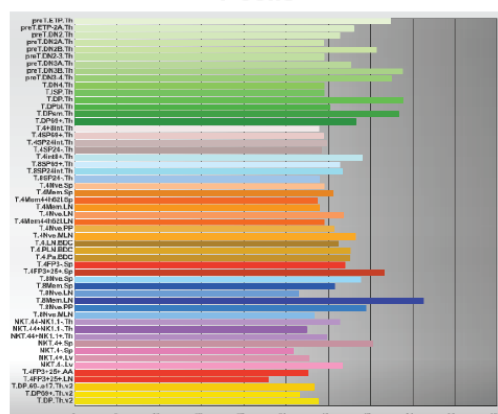
Monocytes, Macrophages and Neutrophils



B cells



T cells



APPENDIX D

Proportion of variance (%) of sorted pre-cDC and cDC populations in PCA.

